

**Alma Mater Studiorum-University of Bologna**

---

---

**PhD in  
Pharmaceutical Sciences  
Ciclo XXV  
Settore Concorsuale: 03/A1  
SSD: Analytical Chemistry CHIM/01**

**New synthetic bile acid analogue agonists of  
FXR and TGR5 receptors:  
Analytical methodologies for the study of  
their physico-chemical properties,  
pharmacokinetic activity and metabolism.**

**PhD candidate: CAROLINA COLLIVA**

**Supervisor  
Prof. Aldo Roda**

**PhD coordinator  
Prof. Maurizio Recanatini**

**Co-supervisor  
Prof. Roberto Pellicciari**

---

---

**Final examination year 2013**

*“Ai miei genitori”*

## ABSTRACT

This thesis reports an integrated analytical approach for the study of physicochemical and biological properties of new synthetic bile acid (BA) analogues agonists of FXR and TGR5 receptors. Structure-activity data were compared with those previously obtained using the same experimental protocols on a large series of synthetic and natural occurring BA.

The new synthetic BA analogues are classified in different groups according also to their potency as a FXR and TGR5 agonists: unconjugated and steroid modified BA and side chain modified BA including taurine or glycine conjugates and pseudo-conjugates (sulphonate and sulphate analogues).

In order to investigate the relationship between structure and activity the synthetic analogues were admitted to a physicochemical characterization and to a preliminary screening for their pharmacokinetic and metabolism using a bile fistula rat model. Sensitive and accurate analytical methods have been developed for the quantitative analysis of BA in biological fluids and sample used for physicochemical studies.

Combined High Performance Liquid Chromatography – Electrospray – tandem mass spectrometry (HPLC-ESI-MS/MS) with efficient chromatographic separation of all studied BA and their metabolites have been optimized and validated. Analytical strategies for the identification of the BA and their minor metabolites have been developed. Taurine and glycine conjugates were identified in MS/MS by monitoring the specific ion transitions in multiple reaction monitoring (MRM) mode while all other metabolites (sulphate, glucuronic acid, dehydroxylated, decarboxylated or oxo) were monitored in a selected-ion reaction (SIR) mode with a negative ESI interface by the following ions.

Accurate and precise data were achieved regarding the main physicochemical properties including solubility, detergency, lipophilicity and albumin binding. These studies have shown that minor structural modification greatly affect the pharmacokinetics and metabolism of the new analogues in respect to the natural BA and on turn their site of action, particularly where their receptor are located in the enterohepatic circulation.

# INDEX

1.1. PHYSIOLOGY OF BILE ACIDS.....	4
1.1.1. The structure of natural bile acids .....	4
1.1.2. Hepatic metabolism of bile acids.....	7
1.1.3. Intestinal metabolism of bile acids .....	8
1.1.4. Enterohepatic circulation of bile acids .....	9
1.2. BILE ACIDS A ANALOGUE SIGNALING PATHWAYS AS THERAPEUTIC TARGETS .....	12
1.2.1. FXR $\alpha$ agonists .....	13
1.2.2. FXR antagonists and modulators.....	15
1.2.3. TGR5 agonists .....	16
1.2.4. Dual Farnesoid X Receptor and TGR5 Agonist.....	19
1.3. PHYSICO-CHEMICAL PROPERTIES OF BILE ACIDS .....	21
1.3.1. Critical Micellar Concentration .....	21
1.3.2. Water solubility .....	22
1.3.3. Lipophilicity of the molecule: the value of LogP <sub>O/W</sub> .....	23
1.3.4. Affinity binding to serum albumin .....	24
1.4. AIM AND RATIONALE .....	26
2. METHOD HPLC-ESI-MS/MS .....	31
2.1. Material and methods .....	32
2.1.1. Chemicals .....	32
2.1.2. Calibration curve .....	34

2.1.3. Sample preparation .....	35
2.1.4. Quantification .....	36
2.1.5. Instrumentation: HPLC-ES-MS/MS analysis.....	36
2.1.6. Identification of the metabolites .....	38
2.1.7. Method validation.....	40
2.2. Results and Discussion .....	41
2.2.1. Optimization of chromatographic conditions .....	41
2.2.2. Optimization of mass spectrometry conditions .....	45
2.2.3. Method validation.....	48
2.2.4. Pharmacokinetics (biliary secretion) and hepatic metabolism of the administered analogues: iv and id infusion. ....	51
2.3. Conclusions .....	58
3. PHYSICO-CHEMICAL PROPERTIES .....	59
3.1. Material and Methods .....	59
3.1.1. Chemicals .....	59
3.1.2. Critical Micellar Concentration .....	62
3.1.3. Water Solubility.....	63
3.1.4. Octanol/Water Partition Coefficient.....	63
3.1.5. Albumin Binding .....	64
3.1.6. Critical micellar pH .....	64
3.2. Results and Discussion .....	65
3.2.1. Critical Micellar Concentration .....	65
3.2.2. Water Solubility.....	68
3.2.3. Octanol/Water Partition Coefficient.....	71

3.2.4. Albumin Binding .....	73
3.2.5. Critical micellar pH .....	75
3.3. Conclusions .....	76
4. PHARMACOKINETICS AND METABOLISM OF THE BA ANALOGUES: IV and ID single –dose administration to bile-fistula rat model.....	79
4.1. Material and methods .....	81
4.1.1. Chemicals .....	81
4.1.2. Duodenal infusion.....	82
4.1.3. Intravenous infusion .....	82
4.2. Results and discussion .....	83
4.2.1. Choleric effect after id and iv administration .....	83
4.2.2. BA secretion rates and hepatic metabolism after id and iv administration ..	87
4.3. Conclusions .....	100
5. REFERENCES .....	102

# **1. INTRODUCTION**

## **1.1. PHYSIOLOGY OF BILE ACIDS**

### **1.1.1. The structure of natural bile acids**

In vertebrates, cholesterol, a major lipid constituent of all biological membranes, is converted into amphipathic derivatives soluble in water that are secreted into the bile. As a family, these molecules are called bile acids (BA) or cholanooids. Unconjugated BA once synthesized are mainly conjugated BA with taurine and glycine, but also sulphates and other conjugates of bile alcohols, as well as glucuronides and N-acetylglucosamidates.

The first mechanism of BA biosynthesis is de novo synthesis from cholesterol in the epathocyte (primary BA); the second is the modification of the hydroxyl substituents by of the enzymes of the intestinal bacterial flora, with formation of secondary BA. Figure 1.1 shows a schematic representation of BA biosynthesis pathways. In the classic pathway, cholic acid and chenodeoxycholic acid, two primary BA in humans, are formed. In the alternative pathway, mainly chenodeoxycholic acid is formed.

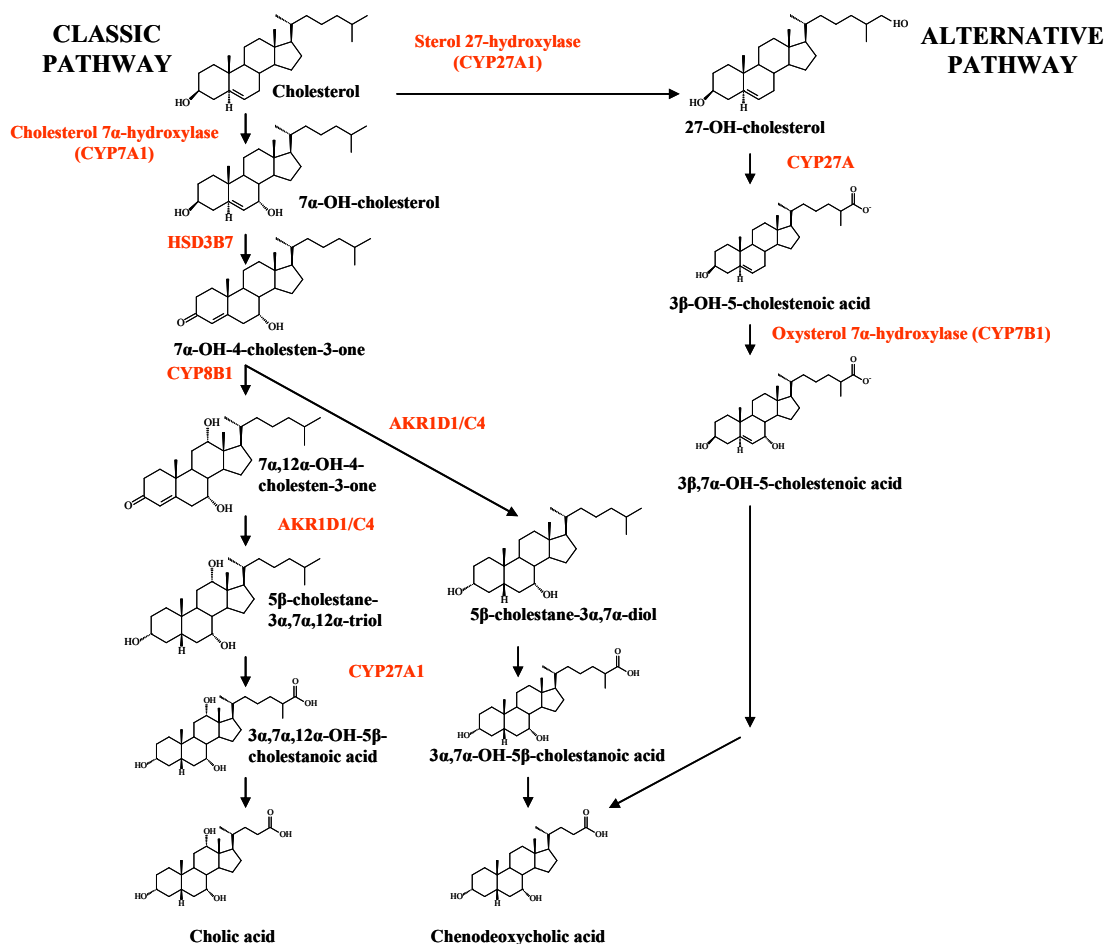


Figure 1.1: Schematic representation of BA biosynthesis pathways.

The BA molecule can be considered as consisting of two parts: the steroidal ring and the side chain.

➤ **Side Chain:** The structure of the side chain determines the main BA classes. The side chain of cholesterol contains eight carbon atoms, with ramifications in C<sub>20</sub> and C<sub>25</sub>; if the terminal carbon (C<sub>27</sub>) is hydroxylated, bile C<sub>27</sub> alcohols are formed, if oxidized to carboxyl, BA C<sub>27</sub> are formed (cholestanoic acids). If the side chain undergoes oxidative carboxylation with formation of a chain C<sub>5</sub>, the result is BA C<sub>24</sub> (cholanoic acids). There are also naturally occurring bile alcohols C<sub>26</sub>, C<sub>25</sub> and C<sub>24</sub>.

In many mammals and in most vertebrates, BA C<sub>27</sub> or C<sub>24</sub> predominate (Haslewood et al. 1978). Bile alcohols, such as sulphates, are present in appreciable quantities only in the most primitive species (elephant, hyrax, rhinoceros, walrus) (Hagey et al. 1992). In birds, BA C<sub>27</sub> and C<sub>24</sub> predominate, while bile alcohols (sulphate) are present in



primitive fish (e.g. sharks) and reptiles and may be the main constituent of bile. Alligators, crocodiles and turtles produce mainly BA C<sub>27</sub> (Hagey et al. 1992). The presence of a hydroxyl in position C<sub>23</sub> or C<sub>22</sub> is also possible; in the first case we speak of  $\alpha$ -hydroxy BA (some marine mammals), in the second of  $\beta$ -hydroxy BA (some fish).

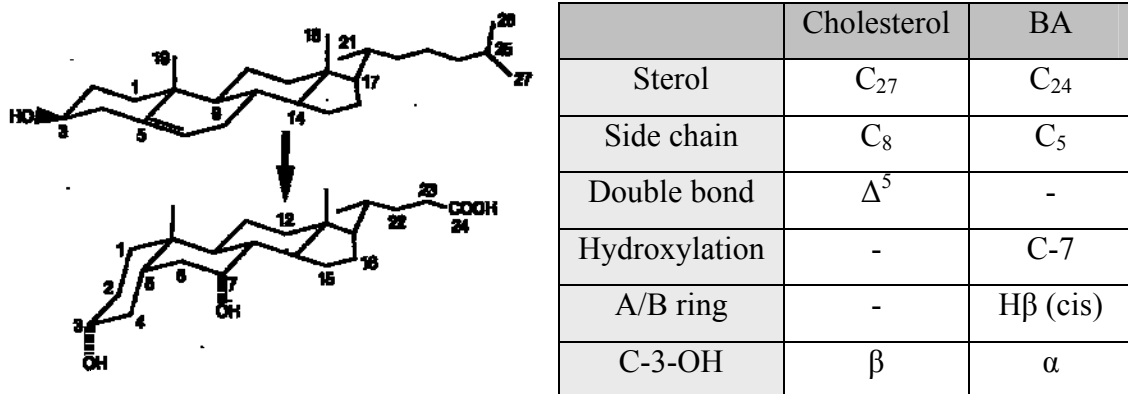


Figure 1.2: Differences between cholesterol and BA C<sub>24</sub>

➤ Steroidal ring: In higher vertebrates, the rings A and B have the cis configuration, giving a bent structure to the nucleus; since the hydrogen in position 5 is in the configuration  $\beta$ , these compounds are called 5  $\beta$ -BA. In lower vertebrates, some BA and alcohols are flat because of the trans junction of rings A and B (Hagey et al. 1992, 1995); the 5  $\alpha$ -BA are also called *Allo*-BA. In some genetic diseases of the metabolism of BA and conditions of cholestasis, BA whose nucleus still contains  $\Delta^{5,6}$  (the double bond between the carbons 5 and 6), typical of cholesterol, can be synthesized. The pattern of substitutions in the ring of the hydroxylic BA (and alcohols) derives from site-specific hydroxylations. Since cholesterol has a hydroxyl in C<sub>3</sub>, all natural BA must have a hydroxyl C<sub>3</sub>. Also, since the 7  $\alpha$ -hydroxylation of cholesterol is the limiting step in the biosynthesis of the speed of BA in all vertebrates (Russell et al. 1992), all the BA must have a primary hydroxyl C<sub>7</sub>. The 3 $\alpha$ ,7 $\alpha$ -dihydroxy-5  $\beta$ -cholan-24-oic acid (chenodeoxycholic acid, CDCA) can thus be considered the starting point for all “modern” (C<sub>24</sub>) BA. In many vertebrates, there is a further step of hydroxylation in the ring, with the result that the most important BA formats in the liver are CDCA (3 $\alpha$ , 7 $\alpha$ -dihydroxy) and CA (3 $\alpha$ ,7 $\alpha$ ,12 $\alpha$ -trihydroxy-5 $\beta$ -cholan-24-oic acid). In non-mammals, there are other possible positions: 3,7,16-trihydroxy BA are extremely common in birds (Hagey et al. 1992) and 1,3,7 trihydroxy BA have recently been

identified as the main BA of some vertebrates (Hagey et al. 1994). The BA in which the hydroxyl is in configuration rather than in  $\alpha$  (or  $\alpha$  instead of  $\beta$ ) are defined as epimers. In rats and mice there are significant quantities of  $3\alpha,6\beta,7\alpha$ - and  $3\alpha,6\beta,7\beta$ -trihydroxy AB, called muricholic acids, synthesized in the hepatocyte for  $6\beta$ -hydroxylation and possible epimerization of hydroxyl  $7\alpha$  (Waxman et al. 1991).

### 1.1.2. Hepatic metabolism of bile acids

In the hepatocyte, both the neo synthesized BA and those captured by the blood can undergo a series of biotransformation, in particular conjugations with glycine and taurine, and to a much less extent esterifications with glucuronides, sulphates, glucose and N-acetylglucosamine. The glucuronidation can take place in the hydroxyls on the side chain or the nucleus (ethers glucuronides) or on the carboxyl side chain (ester glucuronide). The esterification with sulphates, glucose and N-acetylglucosamine, instead, takes place only on the hydroxyls.

The amidation occurs in two steps: a first cytosol enzyme (coenzyme A ligase) reversibly transforms the BA into its CoA derivative (Killenberg et al. 1978; Vessey et al. 1977), which is irreversibly converted by a second microsomal enzyme (colil-CoA transferase amino acid) to BA tauro or glyco conjugate (Czuba et al. 1986; Vessey et al. 1979), which is then secreted into the bile. The rate of conjugation is strongly influenced by the structure of the side chain of the BA;  $C_{23}$  *nor*-BA in fact do not form amidated derivatives (Czuba et al. 1982). The second enzyme preferentially uses taurine rather than glycine. Taurine in humans is synthesized only in limited quantities, and consequently the main source of taurine available for the conjugation of BA is the diet and consequently the main amidation is with glycine.. Even conjugations with glucuronides (Takikawa et al. 1985), glucose (Matern et al. 1987) and N-acetylglucosamine (Marschall et al. 1989) are minor metabolic pathways for natural BA in healthy humans, except in the case of the hyodeoxycholic acid, massively glucuronidated in position 6 (Radomska-Pyrek et al. 1987).

The BA amidated are actively absorbed by the intestine even if highly hydrophilic while the conjugation with glucuronide and sulfate leads to a rapid elimination of the BA with stool or urine.

### 1.1.3. Intestinal metabolism of bile acids

When the BA reaches the intestinal regions rich in bacteria, they undergo a series of biotransformations (Mac Donald et al. 1983). In humans, the bacterial flora begins to increase in number and diversity in the terminal ileum, with a marked increase in the cecum. The changes that occur in the ileum of BA are due to aerobic or facultative anaerobic, while in the cecum are probably due to strictly anaerobic bacteria.

The main biotransformation i.e. their side-chain deconjugation is catalyzed by a large number of bacteria (Bacteroides, Clostridium, Lactobacillus, Bifidobacterium, Eubacterium and Escherichia); the enzyme involved is called cholyglycine hydrolase and that isolated from Clostridium perfringens has been characterized in detail with regard to its activity against structurally different BA

The second major metabolic pathway is the oxidation, of the hydroxyl groups in positions 3, 7 and 12 to form oxo derivatives by different bacterial dehydrogenases

The most relevant biotransformation, due to anaerobic bacteria in the cecum, is the 7-dehydroxylation of primary BA, CA and CDCA, with the formation of respectively, deoxycholic acid (DCA) and lithocholic acid (LCA), the two major secondary BA in the human bile. The amount of 7-dehydroxylation varies considerably between different species of animals; in rabbits the 7-dehydroxylation of CA is so massive that DCA is up to 95% of the pool of BA.. Generally the enzyme is less active against BA 7 $\beta$ -hydroxylated (White et al. 1982) and does not act on BA glycine/taurine conjugates (Batta et al. 1990).

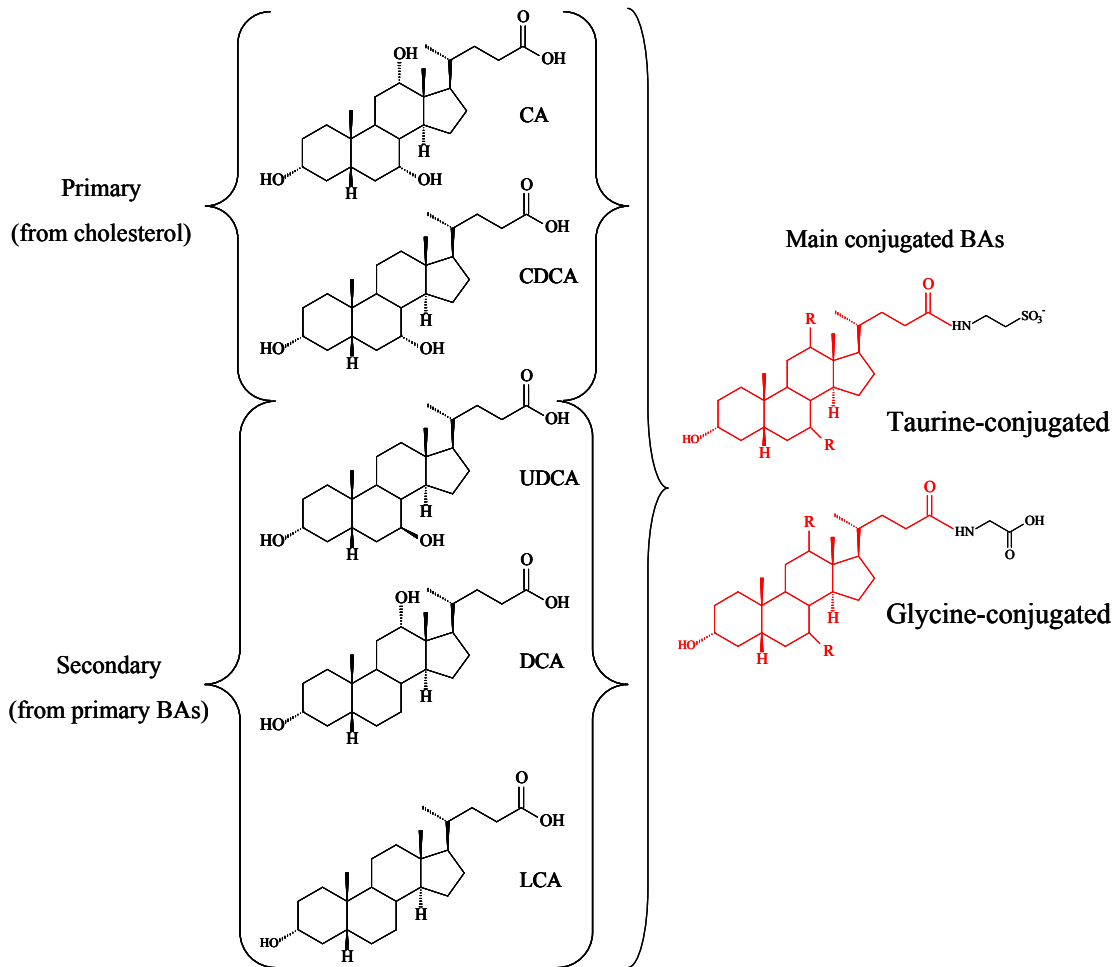


Figure 1.3: Structure of the major BA in man.

#### 1.1.4. Enterohepatic circulation of bile acids

The distribution of BA is essentially limited to the liver, bile ducts, intestines and circulatory system. The enterohepatic circulation of BA is a dynamic entity in which the BA "pool" (i.e. their mass) recirculates constantly but mainly after meals, carrying out its physiological functions and undergoing the processes of synthesis as well as hepatic and intestinal biotransformations (Hofmann et al. 1989; Vlahceovich et al. 1990). A representation schematic is shown in the Figure 1.4 below.

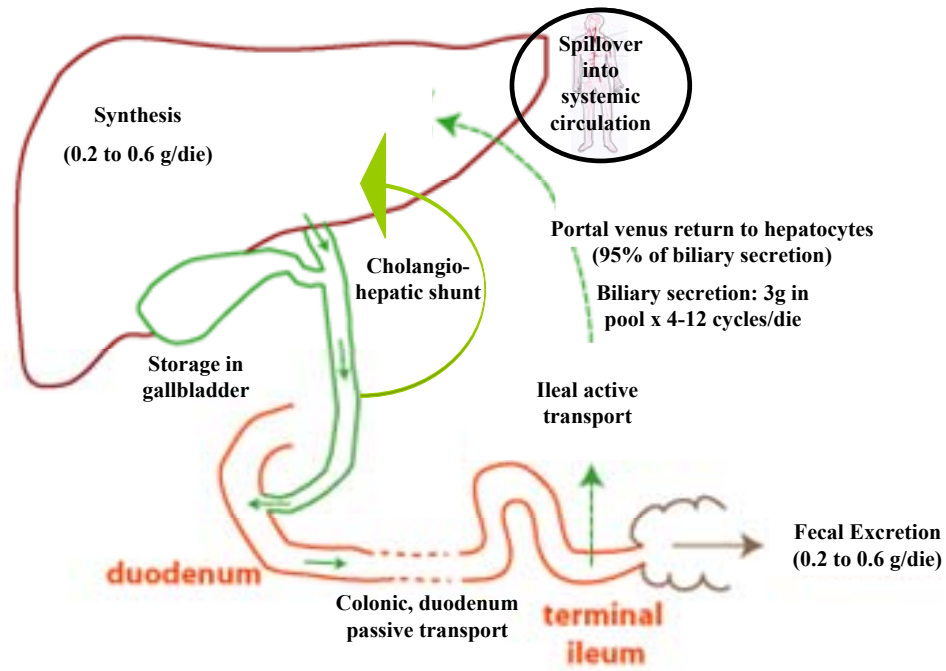


Figure 1.4: Schematic of the enterohepatic circulation

The total pool of BA is 4-6 gr; this remarkable mass recirculates in the enterohepatic circulation (EHC) at least 5-9 times a day, depending on the contraction of the gallbladder and intestinal motility.

The EHC of BA is made possible by the existence in the enterocytes two mechanisms passive and active of BA absorption and transport : passive absorption can occur along the entire intestinal tract and depends on the pH of the intestine and the pKa and the lipophilicity of the BA (Dietschy et al. 1968; Angelin et al. 1976; Schiff et al. 1972). A greater lipophilicity increases the probability that the molecule will cross the cell membrane (Cabral et al. 1987). The absorption is much greater for non-ionized molecules compared to ionized ones; since the pKa of the free BA, and tauro and glyco conjugates is respectively about 5, 3.9 and 1, and the pH of the jejunum, ileum and colon approximately 6, 8 and less than 7, only in the jejunum and colon will the BA be protonated in appreciable amounts free and to a lesser extent the glyco conjugates. In reality, only the colon is important in the absorption of passive free BA, as in all natural BA physiological conditions in the fasting conjugates.

The active absorption of BA occurs in the distal ileum and is due to a transport system coupled to the sodium localized in the apical membrane of ileocyte (Lin et al. 1988 ; Lin et al. 1993). This active transport takes place according to the kinetics typical Michaelis

Menten, described by a maximum speed of transport ( $V_{max}$ ) and a rate constant ( $K_m$ ), Only taurine and glycine conjugated BA are absorbed thanks to this active transport system.

➤ Hepatic uptake: The BA reach the liver by the intestine via portal vein. The BA are present in the serum bound to albumin, a proportion that varies from approximately 80% for the less hydrophobic compounds (e.g. TCA) to 95-99% for the mono and dehydroxylated free and conjugated BA (Roda et al. 1982). A small fraction of the BA (<10%) is bound to lipoproteins (Hedenborg et al. 1988). Uptake is due to two transport systems, a sodium dependent system and a sodium-independent system (Von Dyppe et al. 1983; Ananthanarayanan et al. 1988; Hagenbuch et al. 1991; Aldini et al. 1982, 1986).

## 1.2. BILE ACIDS AND ANALOGUE SIGNALING PATHWAYS AS THERAPEUTIC TARGETS

Bile acids (BA) are signaling molecules that exert genomic and non-genomic effects by activating the farnesoid X receptor (FXR, Figure 1.5), a member of the nuclear hormone receptor superfamily and also TGR5 (M-BAR, GP-BAR1 or BG37) a G-protein-coupled receptor. It has been previously found that some BA analogues act only on FXR receptors but others are specific for both FXR and TGR5, opening unexpected therapeutic opportunities not only for the treatment of cholestatic liver diseases like in primary biliary cirrhosis (PBC) but also in metabolic disorders of lipid and glucose homeostasis including diabetes and the metabolic syndrome (Fiorucci et al. 2009).

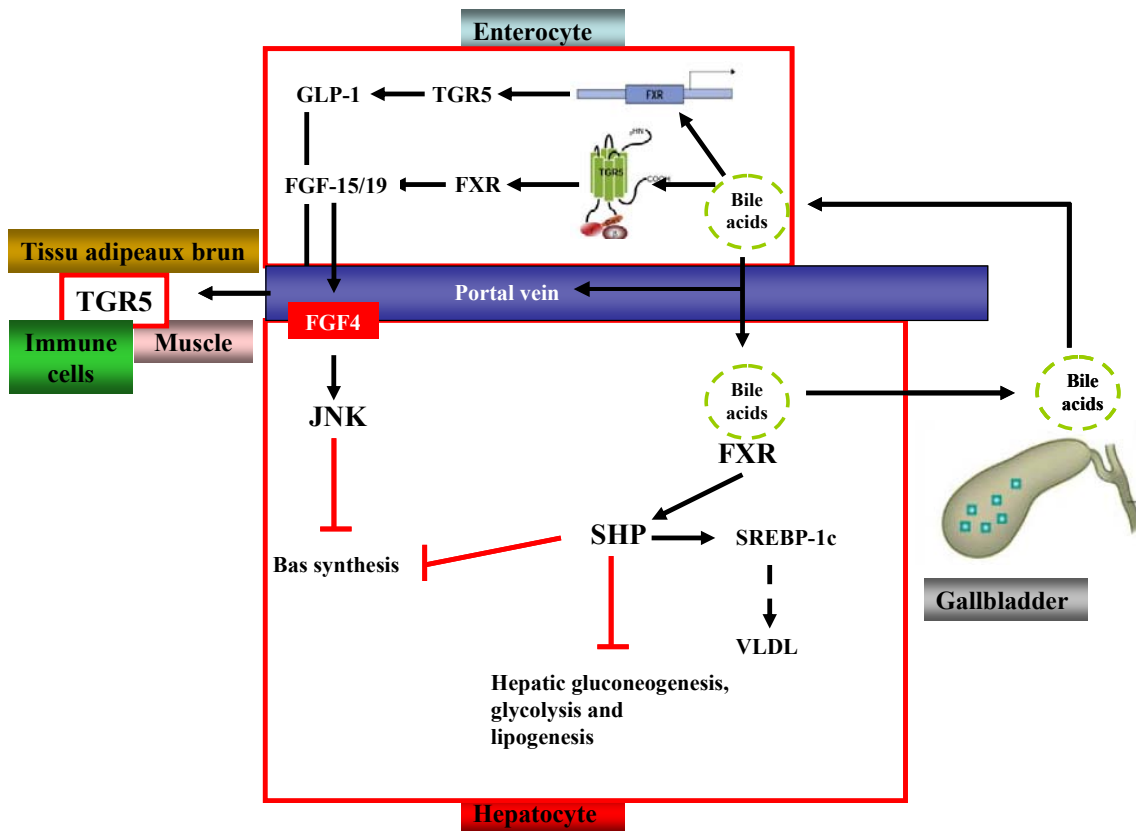


Figure 1.5.: FXR- and TGR5-mediated regulation of BA

### 1.2.1. FXR $\alpha$ agonists

FXR was shown to respond to physiological concentration of the primary BA chenodeoxycholic acid (CDCA) (Pellicciari et al. 2004a), as well as to lithocholic acid (LCA) and deoxycholic acid (DCA), but not to ursodeoxycholic acid (UDCA) and to regulate the expression of several genes controlling BA disposal through modulation of the cholesterol metabolism (Fitzgerald et al. 2002; Chawla et al. 2001). It has been demonstrated that FXR is involved in cholesterol catabolism, feedback inhibition of BA synthesis by repressing the expression of the CYP7A and CYP8B genes (Chen et al. 2001) through increase in the level of the nuclear receptor SHP (Costantino et al. 2003; Lu et al. 2000) and by activating gene expression of the BA transporters I-BABP, BSEP, and MAOT (Willson et al. 2001). All this information about FXR makes it a particularly attractive target for the discovery of drugs for the treatment of cholestasis or hyperlipidemia (Francis et al. 2003).

In 2003, Pellicciari et al (Costantino et al. 2003) reported the synthesis and the preliminary evaluation of a series of 6 $\alpha$ -alkyl-substituted analogues of chenodeoxycholic acid (CDCA), among which 6 $\alpha$ -ethyl-chenodeoxycholic acid (6 $\alpha$ -ECDCA called INT-747) turned out to be the most potent steroid agonist so far reported for the Farnesoid X Receptor (FXR) (Pellicciari et al. 2002).

The relationship between structure and activity showed the existence of a small hydrophobic pocket in the receptor that can accommodate small alkyl groups at position 6 of the ring steroid CDCA (in order of activity: ethyl 3> n-Propyl 4> Benzyl 5). The portion of ethyl in position 6 is stabilized in its hydrophobic pocket, consisting of Phe284, Thr288, Leu451 and Phe 461(Figure 1.6). On the other hand, the largest pocket (163 Å (Evans et al. 1988)) near the carboxylic group could easily guest the glycine (42 Å (Evans et al. 1988)) and taurine (69 Å (Evans et al. 1988)) moieties of the glycol- and tauro- conjugates of CDCA. Indeed, it has been reported that the glycine and taurine conjugates of CDCA activate FXR in tissues that express BA transporters (IBAT) (Parks et al. 1999).



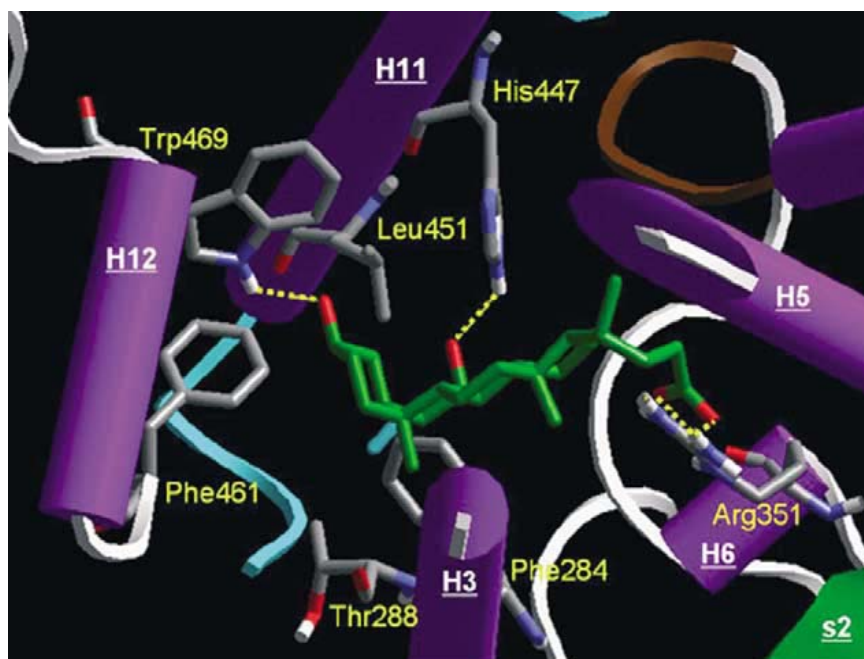


Figure 1.6: Docking result of 6-ECDC. (From Costantino et al. 2003)

In the past decade (Fiorucci et al. 2009), many synthetic FXR agonists (summary in table 1.1) have been generated. GW4064, 6-ECDC and fexaramine are synthetic FXR ligands with nanomolar potency (Maloney et al. 2000; Pellicciari et al. 2002; Downes et al. 2003; Mi et al. 2003).

Table 1.1: FXR agonists

NATURAL	Biological effects
CDCA	Decreases the plasma levels of TG and HDL but increases those of LDL (Porez et al. 2012).
LCA, DCA	Decreases the plasma levels of HDL. (Porez et al. 2012).
CA	Decreases the plasma levels of TG (Porez et al. 2012).
SYNTHETIC	Biological effects
Fexaramine (5)	In vitro assays have established that fexaramine induces recruitment of the coactivator SRC-1 to FXR in a manner comparable to that observed for GW4064 (Downes et al. 2003).
GW4064 (6)	A non-steroidal ligand; its potential cell toxicity and uncertain bioavailability prevent its development for clinical studies. Decreases plasma TG and insulin resistance in ob/ob mice.
6-ECDC (1)	Active in primary biliary cirrhosis. Decreases the plasma levels of TG and HDL but increases those of

	LDL. (Porez et al. 2012)
T0901317	It is a weak FXR ligand that induces BSEP and SHP expression and is a potent LXR agonist (Houck et al. 2004).
AGN43	Reduces cholesterol plasma levels in animals (Dussault et al. 2003).
MeCA	Activate FXR responsive genes in vitro but have not been tested in preclinical models (Suzuki et al. 2008).
MeDCA	
NIHS700	
MFA-1 (7)	It is nearly 500-fold more potent than CDCA and its activity on the receptor is comparable to that of GW4064. Binding to FXR is similar to that for steroid hormones (estrogens and glucocorticoids) (Soisson et al. 2008).
XL335 ( or FXR450 or WAY-362450) (8)	Decreases serum triglyceride and cholesterol levels (Evans et al. 2009).

1) Intercept Pharmaceuticals<sup>®</sup>; 5) Amgen<sup>®</sup>; 6) GSK<sup>®</sup>; 7) Merck<sup>®</sup>; 8) Wyeth Research (Fiorucci et al. 2009).

The first synthetic BA analogue 6-ECDCA (INT-747) is now in the clinical phase 3 trial for the treatment of PBC and its trivial name is Obetic cholic acid (OCA).

### 1.2.2. FXR antagonists and modulators

The activation of FXR leads to a complex response that integrates beneficial actions and potentially undesirable side-effects (Fiorucci et al. 2009; Kast et al. 2001).

The most important side effects that occurred with FXR agonists are:

1) The inhibition of BA synthesis which might reduce cholesterol excretion (Fiorucci et al. 2009b); 2) The repression of ApoAI leading to a decrease in circulating levels of HDL (Sinal et al. 2000). Thus, identification of gene-selective FXR modulators (selective BA receptor modulators, SBARMS) might be required for the development of compounds targeting specific clusters of genes avoiding the above mentioned side effects (Pellicciari et al. 2005a).

Some examples (Houten et al. 2006) are Guggulsterone (induces BSEP but exerts antagonistic effects on FXR-induced recruitment of SRC-1 (Urizar et al. 2002)), fexaramine and AGN34 that are gene-selective FXR $\alpha$  modulators, which means that

they can affect the expression of various FXR $\alpha$  target genes in different ways (antagonists or agonists) (Cui et al, 2003; Downes et al, 2003; Dussault et al, 2003).

### **1.2.3. TGR5 agonists**

Modern drug discovery has focused its efforts towards the development of potent and selective TGR5 agonists belonging to BA or non-BA classes due to the emerging roles of BA in the regulation of energy and glucose homeostasis as a ligand of TGR5 (Tiwari et al. 2009). The metabolic syndrome and related diseases including diabetes are in continuous growth in western countries and this stimulates research in this area (Pols et al. 2011).

The key amino acids implicated in the binding of BA in the binding pocket of the two receptors (TGR5 and FXR) are not entirely conserved, which allows the development of different BA derivatives with differing degrees of selectivity.

Screening of various modulators has allowed the development of a structure–activity relationship (SAR), indicating that these positions are important for potency and selectivity of BA at the TGR5 receptor (Sato et al. 2008):

- 1) Chain length of the carboxylic acid head (shortening the chain length of BA derivatives reduces their potency on TGR).
- 2) Substitution at the alpha position of the carboxylic acid (introduction of the S methyl group at the 23(S)-position of carboxylic acid increases potency and provides higher selectivity over FXR).
- 3) Rigidity of the cyclic system (introduction of a double bond to the cyclic systems of BA provides rigidity to the molecular system and, therefore reduces binding to TGR5, suggesting a flexible and spacious binding pocket).
- 4) The TGR5 receptor exhibits a highly conserved binding pocket with three hydrogen bond acceptors to anchor three hydroxyl groups of BA and a charged surface to bind with carboxylic acid groups.

The unique structural features of BA, which provide potency and selectivity towards TGR5, can be divided into four parts (Figure 1.7 below).

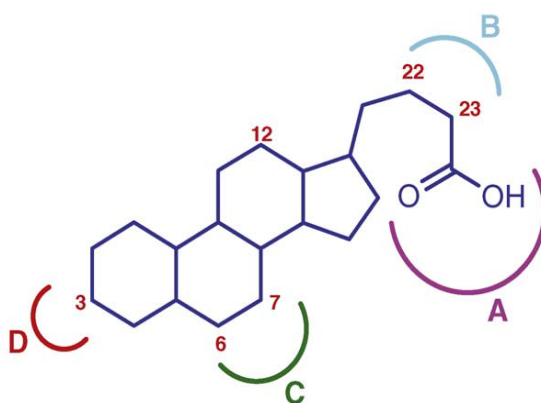


Figure 1.7: TGR5 receptor interaction sites for binding of BA. (From Tiwari et al. 2009)

Region	TGR5 receptor interaction sites for binding of BA
A	A large pocket, which consists of negatively charged residues to accommodate oppositely charged functional groups of the BA. Neutral groups like alcohols decrease the potency of BA binding to the TGR5 receptor.
B	A binding pocket large in size for TGR5 receptor (spans over C-22 and C-23) compared with FXR may be a reason why it is possible to achieve good selectivity. Pellicciari et al. have shown that the introduction of a small alkyl group at the C-23 position can be tolerated by TGR5 and provides selectivity against FXR (Pellicciari et al. 2007a). The pocket is enantiomerically specific for the S-isomer over the R-isomer.
C	This region is a large hydrophobic pocket, spanning C-6 and C-7 of the BA and hence tolerates alkyl (e.g. methyl, isopropyl) and fluoro substitution at C-7.
D	This is a narrow pocket with hydrogen bond acceptor groups, spanning the C-3 region. A hydroxyl (or ketone) group at C-3 anchors BA to the receptor through hydrogen bonds; removing these groups therefore decreases potency at TGR5.
Others	(i) hydrogen bonding at C-12 (ii) an electrostatic interaction at the terminal of the carboxylic acid group of BA (Macchiarulo et al. 2008).

(Fiorucci et al. 2009) The development of TGR5 ligands has been so far BAed on exploitation of the structure of natural ligands (LCA, TLCA and oleanolic acid) (Maruyama et al. 2002; Kawamata et al. 2003; Pellicciari et al. , 2007; Katsuma et al. 2005; Macchiarulo et al. 2008, Tiwari et al. 2009). The 23-alkyl-substituted and 6,23-alkyl-disubstituted derivatives of CDCA, such as the 6 $\alpha$ -ethyl-23(S)-methyl-CDCA (called INT-777), are potent and selective agonists of TGR5 (Pellicciari et al. 2007a; Macchiarulo et al. 2008) and methylation at the C23-(S) position of natural BA confers marked selectivity to TGR5 over FXR activation, whereas 6 $\alpha$ -alkyl substitution increases the potency at both receptors (Pellicciari et al. 2007a; Macchiarulo et al. 2008). In addition to these semi-synthetic steroidal TGR5 agonists, several synthetic non-steroidal TGR5 agonists are being developed (Table 1.2).

Table 1.2: TGR5 agonists

NATURAL	Biological effects
TLCA > LCA	Decrease the cytokine production in macrophages <i>in vitro</i> and increase the energy expenditure in mice (Porez et al. 2012).
DCA	
CDCA	
CA	
Oleanolic acid (4)	Decreases the insulin resistance in DIO mice. Decreases colitis in mice (Porez et al. 2012).
SYNTHETIC	Biological effects
6 $\alpha$ -ethyl-23(S)-methyl-CA (1)	Increases the energy expenditure and GLP-1 release. Decreases the glucose intolerance in mice and atherosclerosis in LDLR-KO mice and choleric action in mice (Porez et al. 2012).
Quinazolinones (2)	Induce GLP-1 secretion from GLUTag cells and increase insulin secretion and decrease glucose levels in mice ( Pinkerton et al.).
Imidazol[1,2- $\alpha$ ] [1,2]diazepin (2)	Modulators of TGR5 ( Pinkerton et al.).
Quinolines (2)	Increase GLP-1 release and OGTT in DIO mice.
BR27 (3)	Decreases the Cytokine production in mouse

	Kupffer cells (Porez et al. 2012).
6-methyl-2-oxo-4-thiophen-2-yl-1,2,3,4- tetrahydropyrimidine-5-carboxylic acid-benzeyl ester (4)	Improves metabolic homeostasis, pancreatic insulin secretion and inflammation (Sato et al. 2008.).

1) *Intercept Pharmaceuticals*; 2) *Kalypsys*; 3) *Bayer AG*; 4) *Takeda Chemical Industries LTD*; 5) *Amgen*; 6) *GSK*; 7) *Merck*; 8) *Wyeth Research*

There are several limitations of currently available steroidal TGR5 ligands because LCA is a toxic BA (Tan et al. 2007) and steroidal ligands have therefore been developed using the CA scaffold (i.e. the same strategy used to generate steroidal FXR ligands with CDCA). However, CDCA is not totally safe when administered to animals, and doses > 5 mg/kg increase AST and ALT in patients (Fiorucci et al. 2009a) but CA does not show this problem.

Non-steroidal compounds have been poorly described and information regarding their efficacy is not conclusive. The main indication for the development of TGR5 agonists is for treatment of obesity to exploit the effect of the receptor in regulating energy expenditure. The mechanisms involved in regulation of energy expenditure in man, however, are likely to be more complex than those described in mice, even though human fat contains a significant amount of brown adipose tissue, the thermogenically active tissue preferentially targeted by TGR5 in the mouse (Kirsi et al. 2009).

#### **1.2.4. Dual Farnesoid X Receptor and TGR5 Agonist**

In the previous paragraphs it was reported that 6E-CDCA (INT-747) is a potent and selective FXR agonist, while 6Ethyl, 23Methyl(S)-CA (INT-777) is a potent and selective TGR5 agonist (Rizzo et al. 2010).

During the development of these analogues it was found that other BA analogues exhibit a dual activity toward these two receptors.

It was previously found that 6-ethyl-3,7,23-trihydroxy-24-nor-5-cholan-23-sulfate sodium salt (INT-767) a synthetic 23-sulfate derivative of INT-747 developed by Pellicciari's group is a potent agonist for both FXR (EC<sub>50</sub>, 30 nM) and TGR5 (EC<sub>50</sub>,

630 nM), the first compound described so far to potently and selectively activate both BA receptors.

To summarize, the BA analogues acting as a ligand of FXR or TGR5 or for both of them can be interesting tools to develop future candidates for the therapy of different diseases. These analogues must, however, have the necessary physico-chemical properties and pharmacokinetics to deliver the molecules in the target organ.

The main therapeutic perspective are summarized below:

BA analogues are promising targets for:	Treatment of dyslipidemia (Fiorucci et al. 2009). Cholesterol-related disorders. Obesity. Type 2 diabetes.
Steroidal FXR ligands	Being tested against Nonalcoholic steatohepatitis NASH.
	Cholestasis, hyperlipidemia and primary biliary cirrhosis. Decreases the plasma levels of TG and HDL but increases those of LDL.
Steroidal TGR5 ligands	Stimulate incretin (GLP-1) release and decrease blood glucose levels in vivo and thus hold promise for the treatment of obesity and type 2 diabetes.
Dual TGR5/FXR ligands	Could provide new opportunities in the treatment of complex metabolic disorders in which several target pathways are involved.

Additional studies are required to better define suitable animal models or cell-based systems to better predict these effects in humans.

## **1.3. PHYSICO-CHEMICAL PROPERTIES OF BILE ACIDS**

The experimental evaluation of physico-chemical properties of BA analogues is particularly important since their pharmacokinetics and in general their biodistribution and metabolism are strongly related to their structure (Carey et al. 1981; Gurantz et al. 1984; Carey et al. 1983).

In previous papers it's been demonstrated that minor structural modifications such as the number of hydroxyls, their position and orientation modify the physico-chemical properties and, as a consequence, many biological properties such as intestinal absorption, albumin binding and the interaction with other lipids such as cholesterol and phospholipids.

The most relevant and peculiar properties of naturally occurring BA are their detergency and ability to form mixed micelles with phospholipids and cholesterol and other lipids in bile and this can be evaluated by experimentally measuring the Critical Micellar Concentration (CMC) of pure systems and even more complex ones.

The structural modification is able to modify the lipophilicity and, as a consequence, their partition in a lipid domain and therefore the extent of their intestinal passive absorption. The ionization constant is another important property to study

### **1.3.1. Critical Micellar Concentration**

BA (salts) self-associate to form micelles over a broad range of concentration, as compared to that of typical ionic detergents, since the pattern of association is more stepwise (dimers, tetramers) (Hofmann et al. 1984; Mukerjee et al. 1984). In the past, Roda et al (Roda et al., 1983) used a dynamic method for measuring surface tension based on a maximum bubble pressure principle to determine the CMC of a large number of BA. This work demonstrated that the structure of both the nucleus and the side chain influences the CMC. For the nucleus, the key factor influencing self-association appeared to be the contiguous hydrophobic area ( $\beta$  face is shown in figure 1.8). Any decrease in this hydrophobic area raised the CMC, such that BA in which both sides of the molecule were hydrophilic did not form micelles even at high concentrations. Decreasing the side chain length increased the CMC. Amidation with



glycine or taurine had little effect on the reduction of CMC values in respect to the C-24 free BA: the polarity of the amide bond compensated for the increased length of the side chain caused by glycine or taurine. Natural BA possess relatively low CMC values (< 10 mM) because of the striking asymmetry of their nuclear structure having all the hydroxyls on the same side and therefore facilitating the back-to-back micelles formation and because of their negative charged five Carbon atoms side chain.

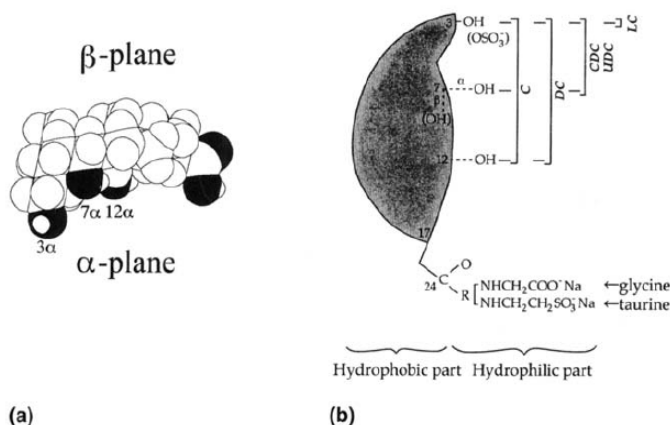


Figure 1.8: Molecular structure (a) and the scheme of amphipathic structure (b) salts. R: side chain of glycine and taurine; C: cholate; DC: deoxycholate; CDC: deoxcholate; UDC: ursodeoxycholate; LC: lithocholateholate. (From Hofmann et al. 1988).

### 1.3.2. Water solubility

The solubility of a BA is mainly related to the nature of the solid state and to the possibility to ionize in water.

In the case of ionizable molecules like unconjugated natural BA, the dissociation constant is the key parameter since the protonated form is usually almost insoluble while the ionized species is much more soluble (Fini et al. 1985). The solubility in the case of a weak acid increases with the pH according to the equation:

$$S_t = S_0 [1 + 10^{(pH - pK_a)}]$$

$$\text{Where } S_t = [HA] + [A^-]$$

$$S_0 = [HA]$$

The solubility of the protonated species were obtained by performing measurements at  $pH = 1$  (at least two units below the  $pK_a$  of the common carboxylated BA ( $pK_a = 5$ ) and even when amidated with glycine ( $pK_a = 3.9$ ).

When used as a drug, the solubility affects both the release-dissolution of the drug from the formulation and its intestinal absorption after oral administration (Figure 1.9). When the drug is administered intravenously, the role of the solubility is even more critical because it can lead to precipitation of solids within the blood vessels with serious consequences.

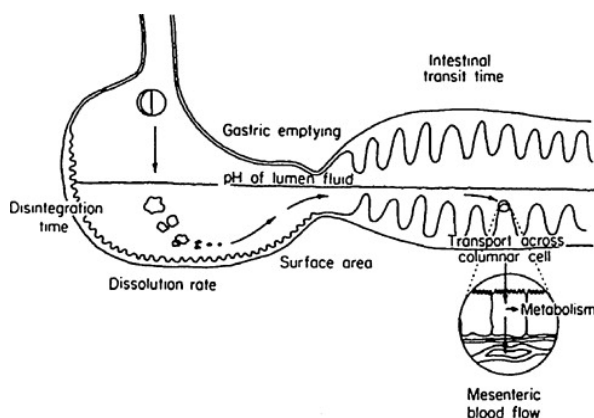


Figure 1.9: Factors affecting the rate of absorption of drug from the gastrointestinal tract (From Goole et al., 2010)

### 1.3.3. Lipophilicity of the molecule: the value of $\text{LogP}_{O/W}$

The  $\text{LogP}_{O/W}$  is an index of the lipophilicity of the molecule. It is calculated by means of an equilibrium distribution at a given pH of the molecule between two phases, consisting of water and 1-octanol. Historically, the use of 1-octanol was chosen because it reflects the behavior of the lipid components of cell membranes quite well in its properties, thus making it possible to simulate "in vitro" what would happen to a solute in its distribution between the external aqueous extract of living cell and the lipid layer on its membrane.

The partition properties in two immiscible phases are usually described by the partition coefficient (P) which refers to a single chemical species and is distinct from the distribution coefficient (D) which is the ratio between the total concentration (protonated and ionized form) in the two phases (Roda et al. 1990a).

Solutes that display some preference for the nonpolar phase ( $\text{logP} > 0$ ) are termed lipophilic or hydrophobic, while solutes are classified as hydrophilic (lipophobic) when  $\text{logP} < 0$ . The terms lipophilicity and hydrophobicity are often considered synonymous.

Lipophilicity can be expressed as a function of bulk (excluded volume) and polarity of the solute. Hydrophobicity refers to the first of these two parameters and is due to Van der Waals and hydrophobic forces. Hence, lipophilicity = hydrophobicity - polarity (Van De Waterbeemd et al. 1987). The calculation of the intrinsic partition coefficient from the experimentally determined distribution coefficient requires accurate knowledge of the dissociation constants of the BA studied (Fini et al. 1982; Fini et al. 1987). The general equation used for the calculation of logP from logD using this simplification is:

$$\text{LogP} = \text{LogD} + \text{Log}(1 + 10^{\text{pH} - \text{pK}_a})$$

Since BA molecules with a significant lipophilic component (Roda et al. 1990a) is a predictable distribution in the non-polar phase (octanol) both of the protonated component that of the ionized.

According to these findings, both ionized and protonated species must be considered to partition in the 1-octanol phase and, consequently, the distribution coefficient D which takes this into account, must be defined:

$$D = \frac{[\text{HA}]_{\text{oct}} + [\text{A}^-]_{\text{oct}}}{[\text{HA}]_{\text{w}} + [\text{A}^-]_{\text{w}}}$$

where [HA] and [A<sup>-</sup>] are the concentrations of protonated and ionized species in 1-octanol (oct) and water (w), respectively. Combining this equation with that relating to the dissociation constant of a weak acid is obtained:

$$D = \frac{P'_{\text{HA}} [\text{H}^+] + P'_{\text{A}} K_a}{[\text{H}^+] + K_a}$$

where P'<sub>HA</sub> and P'<sub>A</sub> are the intrinsic partition coefficients of HA and A<sup>-</sup>, respectively, and K is the dissociation constant of the BA.

#### 1.3.4. Affinity binding to serum albumin

The bioavailability of a drug is influenced by its binding and affinity for plasma proteins in two opposite way. The binding to protein reduces the fraction of free drug, potentially pharmacologically active.

On the other hand evidence has been presented that the uptake of BA similarly to fatty acids is mediated by a (a)specific receptor on the liver cell surface (Weisieger et al. 1981; Roda et al. 1982). The existence of a receptor for albumin on the hepatocytes may be responsible for the efficient hepatic extraction of those molecules which are most tightly bound to the albumin (Cowen et al. 1975).

The interaction of human serum albumin with BA (BA) has been previously studied by equilibrium dialysis technique using  $^3\text{H}$ - and  $^{14}\text{C}$ -labeled BA (Roda et al. 1982). In this article the authors showed that the affinity constant of a BA for albumin decreases with an increase in the number of hydroxy groups and also with the replacement of 7-hydroxy by 7-keto groups. The affinity constant is similar for glycine and taurine conjugated BA, but is slightly higher for unconjugated than conjugated forms (Fini et al. 1987; Aldini et al. 1982). Hepatocyte uptake of BA returning from the intestine is not 100% efficient. The efficiency of hepatic uptake depends on the BA structure: trihydroxy > dihydroxy, and conjugated BA > unconjugated BA (Hofmann et al. 1994; Aldini et al. 1984). According to these data we expected that the new BA analogues will have difference in the binding with albumin and therefore in their pharmacokinetics.

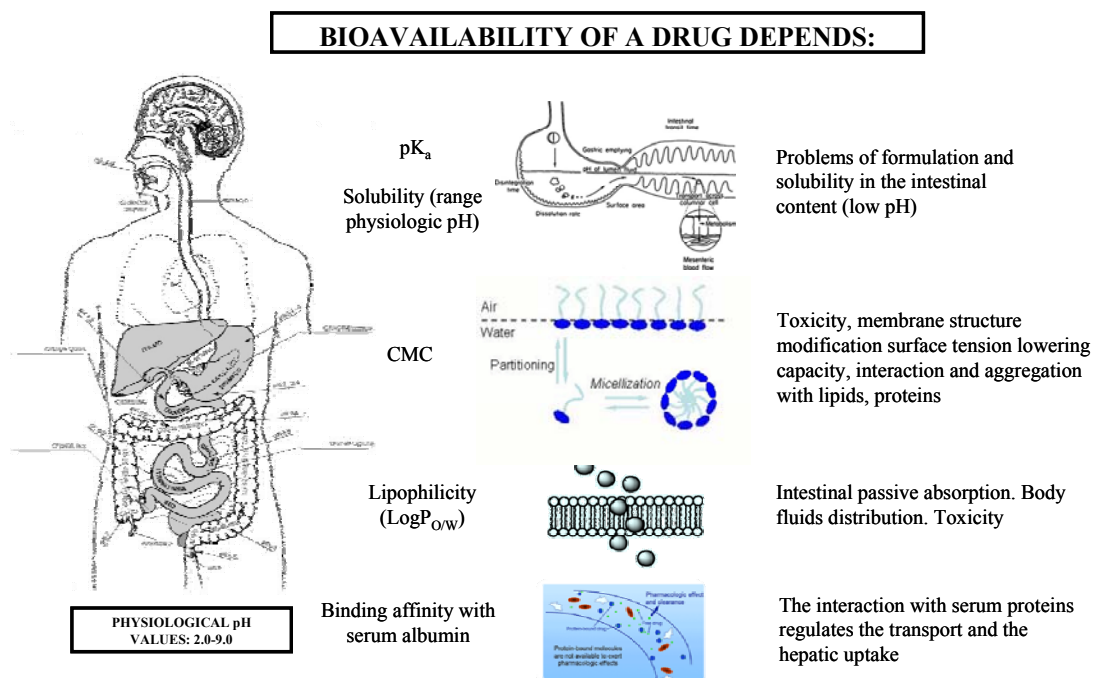


Figure 1.10: Significance of the physico-chemical properties.

## 1.4. AIM AND RATIONALE

This thesis is part of a more general research activities carried out in the Professor Roda Laboratory in collaboration with Professor Pellicciari group at the University of Perugia and InterceptPharmaceuticals Company related to the study of new synthetic analogues of BA as potential new drugs.

Although the literature covers numerous articles on the physical-chemistry properties, biochemistry, metabolism, physiology and pathophysiology of endogenous BA, many aspects are still unknown. One of the limitations for accurate biochemical and metabolic study is due to the complexity of the BA metabolism different from human and animal species resulting in a highly variable composition of BA in different organs and compartments of the enterohepatic circulation producing many metabolites at very low concentrations. The analytical characterization is therefore extremely difficult and time consuming. In order to investigate aspects of the physiology and pathophysiology of endogenous BA and the pharmacology of new synthetic analogues, the present work has been developed in two phases:

- Development of analytical methods for studies of the physico-chemical properties of synthetic analogues in comparison with natural BA. Combined HPLC-Electrospray-Mass Spectrometry with efficient chromatographic separation of all studied BA and their metabolites, identified the parent ion generated by ESI source have applied to the analysis of BA in matrices.
- Study of the structure-activity in vivo of new synthetic analogues of CA and CDCA and their tauro and glyco-conjugates using suitable animal model consisting of a bile fistula rat.

The analytical methods have been used for the characterization, by means of chemical-physical measurement, of their behavior in aqueous solution with particular regard to detergency evaluated by experimentally measuring the Critical Micellar Concentration (CMC), lipophilicity evaluated experimentally by the LogP, water solubility and albumin binding of the new analogues in comparison with natural BA and previously studied analogues.

The rationale for the study of synthetic analogues of CA and CDCA was to design compounds that are not only active on the target receptors but in part more

metabolically stable, such as resistant to intestinal bacterial 7-dehydroxylation responsible for the formation of potentially toxic metabolites.

Another objective is to keep the hepatic uptake and intestinal absorption of these compounds efficient.

The pharmacological screening of their activity toward the specific receptors was done by the group of Professor Pellicciari (Rizzo et al. 2010) as a first screening, before subjecting the molecules to additional characterization. Table 1.3 reports the data of activity ( $EC_{50}$ ) of these molecules to receptors FXR and TGR5; new candidates for a second level screening will be selected on the basis of these data.

BA activity	TGR5 and FXR potency	
	$EC_{50}$ ( $\mu$ M)	
	TGR5 *Agonist potency ( $\mu$ M)	FXR **Agonist potency ( $\mu$ M)
Natural BA		
CDCA	30	13
CA	40	NA
LCA	0.58	20
Synthetic analogues of 6-Ethyl-CDCA		
INT-747	15	0.15
INT-855	0.56	11.8
Synthetic sulphonate and sulphate analogue of 6-Ethyl-CDCA		
INT-767	0.63	0.03
Synthetic carboxylated analogues of 6-Ethy-CA		
INT-777	0.9	> 100
INT-1075	22.5	44
Synthetic sulphonates and sulphate analogues of 6Ethyl-CA		
INT-1244	0.7	7.0
INT-2021	1.1	3.0
INT-2023	1.6	0.6
Synthetic carboxylates analogues of containing a 16 $\beta$ - hydroxyl		
INT-1212	0.65	11.5
INT-2024	1.2	55
Taurine and glycine conjugated analogues		
T-INT-777	7	>100
T-INT-1212	5.4	8
G-INT-777	5.5	>100

\*=*AlphaScreen* FXR; \*\*=*FRET (cAMP) NCI-H716 cells* TGR5

The structural changes must however ensure that the molecule maintains optimum physico-chemical properties in terms of acidity, solubility, detergency and lipophilicity. As previously defined on the basis of extensive structure-activity relationship studies carried out in the laboratory.

More recently, up to thirteen new synthetic analogues have therefore been synthesized, and studied in the last 6 years. They can be divided into two main groups: unconjugated and steroid modified BA and BA conjugated with taurine or glycine or pseudo-conjugates (sulphonate and sulphate analogue).

The first group includes derivatives modified by introducing in the steroidal ring an Ethyl group in position C-6 and / or a Methyl in position C-23.

These derivatives were selected on the BA is of their potency toward the target receptor and on the mean time to increase the metabolic stability toward 7-dehydroxylation and side chain modifications including amidation or deamidation of the corresponding conjugated analogue.

The second group consists of glyco-conjugates or tauro-conjugates of synthetic analogues or sulphonate and sulphate conjugates of synthetic analogues, in order to avoid both hepatic conjugation to obtain an efficient secretion of bile and high metabolic stability of these conjugates.

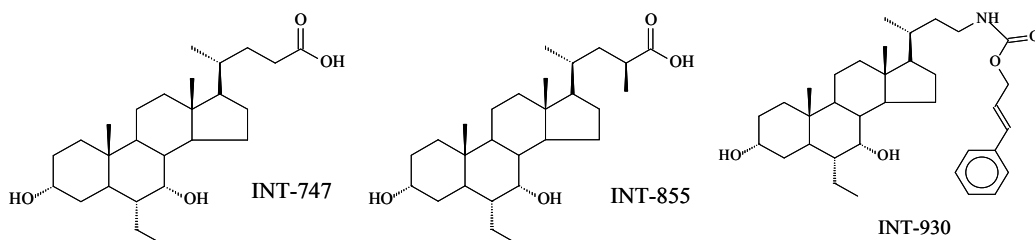
These reference naturally occurring BA are cholic and chenodeoxycholic acid.

In this thesis, the main physico-chemical properties of the more recently developed analogues were measured. The intestinal absorption, hepatic uptake and metabolism and biliary secretion of new molecules compared with the natural analogues were studied in the bile fistula rat model after intravenous infusion (iv) and duodenal infusion (id) administration.

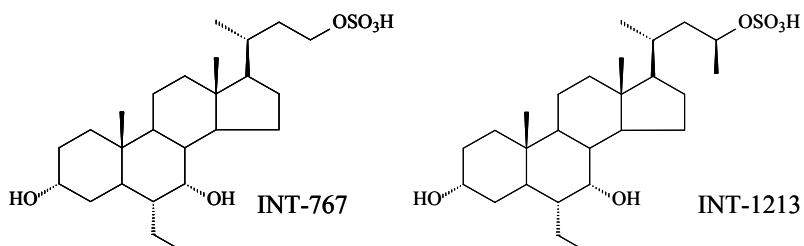
The new BA analogues studied are: INT-2021, INT-2023, INT-2024, T-INT-1212, T-INT-777, INT-1057 and G-INT-777. The results were compared with those obtained in the previous years using the same experimental protocol in the laboratory of Professor Roda which included: INT-747 (Roda et al. 2008, 2011 report), INT-930 (Roda et al. 2009 report), INT-767 (Roda et al. 2008, 2008a report), INT-777 (Roda et al. 2009, 2009a report), INT-1244 (Roda et al. 2009 report), INT-1212 (Roda et al. 2009 report) and INT -855 (Roda et al. 2010 report).

All the molecules studied in this thesis and classified according to their chemical structure are summarized below.

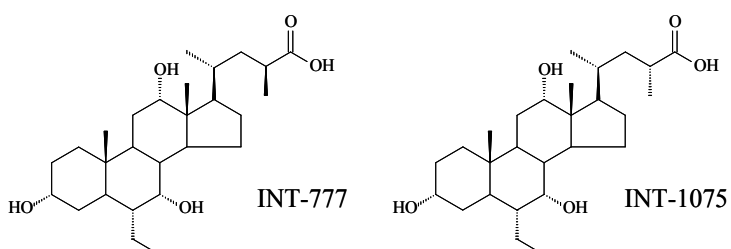
**Synthetic analogues of 6-Ethyl-CDCA:**



**Synthetic sulphonate and sulphate analogues of 6-Ethyl-CDCA:**

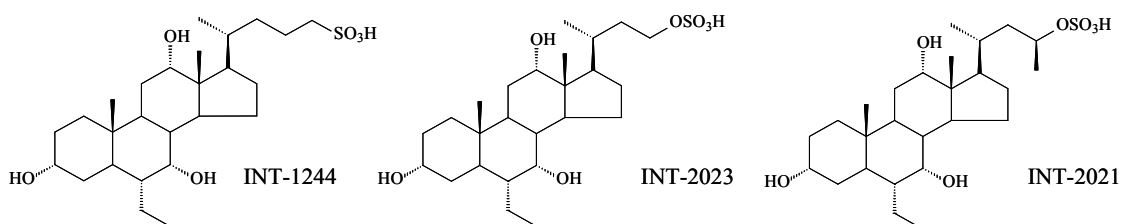


**Synthetic carboxylated analogues of 6-Ethyl-CA:**

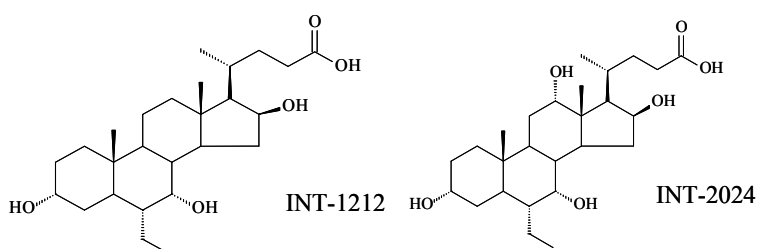




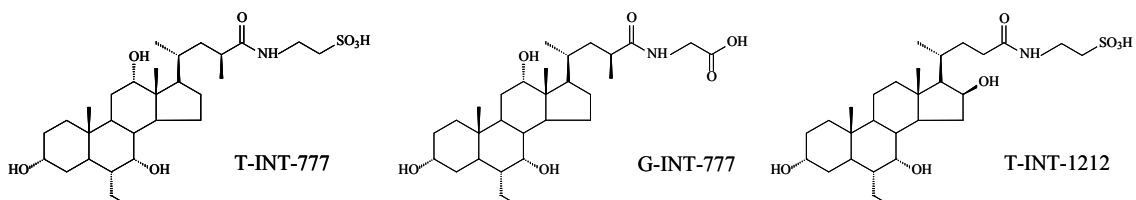
**Synthetic sulphonates and sulphate analogues of 6Ethyl-CA:**



**Synthetic carboxylates analogues of CDCA and CA containing a 16 $\beta$ -hydroxyl:**



**Taurine and glycine conjugated analogues:**



## 2. METHOD HPLC-ESI-MS/MS

The quali-quantitative determination of BA is extremely complex because, in addition to numerous forms which are formed of the BA (free, glyco, tauro and sulphates conjugates), in some biological fluids such as blood, bile and urine, their concentration is extremely variable (Roda et al. 1995).

The old methods reported in the literature before the introduction of High Performance Liquid Chromatography – Electrospray tandem mass spectrometry (HPLC-ES-MS/MS) for the analysis of the different forms of BA, include a clean-up step of the analytes from the biological matrix and complex group separation (free, tauro and glyco conjugates, sulphates), by anion exchange resins (Scalia et al. 1990; Scalia et al. 1990a) and analysed by HPLC only in those fluids with BA concentration at mmolar level. Gas liquid chromatography has been extensively used for the analysis of BA in serum at molar level however derivatization steps are required (hydrolysis of the amide bond and solvolysis of the ether sulphates and derivatization to methyl esters trisilyl ethers, to make them thermostable and volatile) (Karlaganis et al. 1980; Almè et al. 1977). In the case of liquid chromatography their detection by spectrophotometer is insensitive and nonspecific as not presenting strong chromophore groups.. Methods may be used derivatization pre- or post-column formation of fluorescent derivatives (Cavrini et al. 1993; Ishii et al. 1983) or other detectors (eg electrochemical, Kamada et al. 1982). Roda *et al.* (Roda et al. 1992) have developed a system using a universal detector to light scattering allows the revelation with equal sensitivity of BA both free and conjugated without the need for derivatization.

The use of HPLC combined with mass spectrometry with Electrospray interface open a new era in BA analysis offering the possibility to directly analyse all the BA form in any biological fluid or organ and all the previous methodology have been full replaced (Griffiths et al. 2013).

In this work we have developed a new method for analysis of bile samples collected at different times during the iv and id experiments were analyzed to determine the concentration of the administered analogues and their main metabolites in bile.

Using this method, the concentration of BA in the different samples admitted to the physico-chemical property screening project were analyzed (see Chapter 3).

## **2.1. Material and methods**

### **2.1.1. Chemicals**

Solvent: All solvents were of high purity analytical grade and used without further purification. All solvents were: Water LiChrosolv® for HPLC, Merck; Acetonitrile, LiChrosolv® for HPLC, Merck; Methyl alcohol RPE, Glacial acetic acid RPE, Carlo Erba Reagents.

Analytical Equipment: The following equipment was used for the HPLC-ES-MSMS analysis: Vortex mixer, Heidolph; Pipettes Eppendorf, Gilson; Triple quadrupole mass spectrometer QUATTRO-LC (MICROMASS); WATERS ALLIANCE 2695 separations module (solvent and sample management platform); HPLC Luna Phenyl-Hexyl Column 4µm, 150 x 2.1 mm protected by a SecurityGuard Phenyl 4.0 x 2.0 mm i.d. guard column, both supplied by Phenomenex.

Natural BA: Chenodeoxycholic acid (CDCA), glycochenodeoxycholic acid (G-CDCA) and taurochenodeoxycholic acid (T-CDCA), cholic acid (CA), taurocholic acid (T-CA) and glycocholic acid (G-CA) were purchased from Sigma (St. Louis, MO). All chemical structures are summarized in Table 2.1.

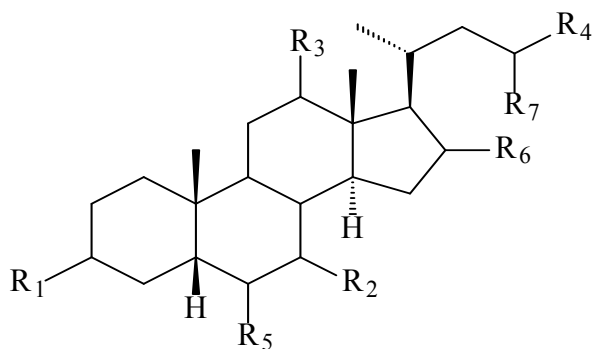


Table 2.1: Natural BA.

Natural BA	C3-R <sub>1</sub>	C7-R <sub>2</sub>	C12-R <sub>3</sub>	C23-R <sub>4</sub>	C6-R <sub>5</sub>	C16-R <sub>6</sub>	C23-R <sub>7</sub>
CA	OH ( $\alpha$ )	OH ( $\alpha$ )	OH ( $\alpha$ )	-CO-OH	H	H	H
T-CA	OH ( $\alpha$ )	OH ( $\alpha$ )	OH ( $\alpha$ )	-CO-NH (CH <sub>2</sub> ) <sub>2</sub> SO <sub>3</sub> <sup>-</sup>	H	H	H
G-CA	OH ( $\alpha$ )	OH ( $\alpha$ )	OH ( $\alpha$ )	-CO- NH(CH <sub>2</sub> )COO <sup>-</sup>	H	H	H
CDCA	OH ( $\alpha$ )	OH ( $\alpha$ )	-	-CO-OH	H	H	H
T-CDCA	OH ( $\alpha$ )	OH ( $\alpha$ )	-	-CO- NH(CH <sub>2</sub> ) <sub>2</sub> SO <sub>3</sub> <sup>-</sup>	H	H	H
G-CDCA	OH ( $\alpha$ )	OH ( $\alpha$ )	-	-CO- NH(CH <sub>2</sub> )COO <sup>-</sup>	H	H	H

Synthetic BA: The present work was carried out on the more recent BA analogues under study in the Bioanalytical laboratory that include: INT-2021, INT-2023, INT-2024, T-INT-1212, T-INT-777, G-INT-777. Data regarding INT-777, INT-1212 and other INT analogues derive from previous studies.

Internal standards used are 6-ECDC (INT-747), its tauro- and glyco-conjugates.

Pure crystalline powder of each compound were synthesized, and purified (purity > 99 % as documented by HPLC-ES-MS-MS analysis) in the laboratory of Prof. Pellicciari (Institute of Pharmaceutical Chemistry, University of Perugia, Italy).

All chemical structures are summarized in Table 2.2.

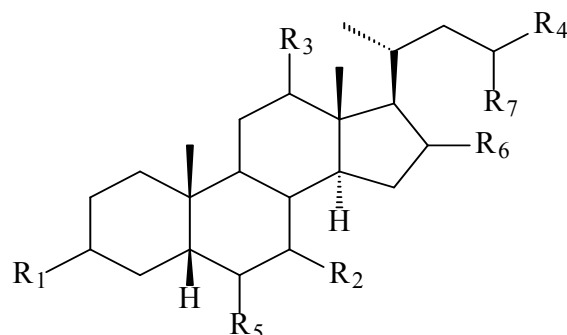


Table 2.2: Synthetic BA.

Synthetic BA	C3-R <sub>1</sub>	C7-R <sub>2</sub>	C12-R <sub>3</sub>	C23-R <sub>4</sub>	C6-R <sub>5</sub> ( $\alpha$ )	C16-R <sub>6</sub>	C23-R <sub>7</sub>
INT-747	OH ( $\alpha$ )	OH ( $\alpha$ )	-	-CO-OH	-CH <sub>2</sub> CH <sub>3</sub>	H	H
INT-777	OH ( $\alpha$ )	OH ( $\alpha$ )	OH ( $\alpha$ )	-CO-OH	-CH <sub>2</sub> CH <sub>3</sub>	H	-CH <sub>3</sub> (S)
T-INT777	OH ( $\alpha$ )	OH ( $\alpha$ )	OH ( $\alpha$ )	-CO- NH(CH <sub>2</sub> ) <sub>2</sub> SO <sub>3</sub> <sup>-</sup>	-CH <sub>2</sub> CH <sub>3</sub>	H	-CH <sub>3</sub> (S)
G-INT777	OH ( $\alpha$ )	OH ( $\alpha$ )	OH ( $\alpha$ )	-CO- NH(CH <sub>2</sub> )COO <sup>-</sup>	-CH <sub>2</sub> CH <sub>3</sub>	H	-CH <sub>3</sub> (S)
INT-2021	OH ( $\alpha$ )	OH ( $\alpha$ )	OH ( $\alpha$ )	-CH-OSO <sub>3</sub> <sup>-</sup>	-CH <sub>2</sub> CH <sub>3</sub>	H	-CH <sub>3</sub> (S)
INT-2023	OH ( $\alpha$ )	OH ( $\alpha$ )	OH ( $\alpha$ )	-CH <sub>2</sub> -OSO <sub>3</sub> <sup>-</sup>	-CH <sub>2</sub> CH <sub>3</sub>	H	H
INT-2024	OH ( $\alpha$ )	OH ( $\alpha$ )	OH ( $\alpha$ )	-CO-OH	-CH <sub>2</sub> CH <sub>3</sub>	OH( $\beta$ )	H
INT-1212	OH ( $\alpha$ )	OH ( $\alpha$ )	-	-CO-OH	-CH <sub>2</sub> CH <sub>3</sub>	OH( $\beta$ )	H
T-INT-1212	OH ( $\alpha$ )	OH ( $\alpha$ )	-	-CO- NH(CH <sub>2</sub> ) <sub>2</sub> SO <sub>3</sub> <sup>-</sup>	-CH <sub>2</sub> CH <sub>3</sub>	OH( $\beta$ )	H

### 2.1.2. Calibration curve

Stock solutions were prepared in methanol at 1 mmol/l and working solutions were prepared by diluting appropriate volumes of the stock solution. The stock solution was stored in screw cap disposable glass tubes at approximately -20°C. These stock solutions were further diluted with methanol to obtain working solutions containing all the BA studied for the individual experiments for administration in the rat and for samples from the physico-chemical properties. For purposes of quantification, calibration samples were prepared by adding the appropriate amount of the corresponding BA working solution to bile samples collected at time zero (before

infusion of the analogue) and diluted with mobile phase 1:10 (v/v) or directly with mobile phase for the samples from the physico-chemical properties. INT-747 and its glyco- and tauro- conjugates were used as the internal standards respectively to quantify the free analogues and glyco- and tauro- conjugates.

A 6-point calibration curve was prepared daily. Calibration samples were obtained in the 0.1 to 20  $\mu\text{mol/l}$  concentration range prepared in the bile matrix diluted (1:10 v/v with mobile phase) and only in mobile phase. Quality control (QC) samples were prepared at three concentrations, starting from the working solutions used for the calibration curve: low level: 0.3  $\mu\text{mol/l}$ , medium level: 8.0  $\mu\text{mol/l}$  and high level: 17.5  $\mu\text{mol/l}$ . At each day of analysis, the three concentrations of QC samples were assayed in duplicate.

### **2.1.3. Sample preparation**

#### **Bile samples**

Rat bile samples were brought to room temperature, briefly stirred, and diluted 1:1000, 1:100 or 1:10 (v/v) (bile samples from femoral infusion and from duodenal infusion) with ammonium acetate buffer 15 mM pH 8 and acetonitrile : methanol (3:1 v/v) in ratio 65:35= aqueous solvent: organic solvent (v/v). The final solution was transferred to an autosampler vial and 5  $\mu\text{L}$  was injected onto the chromatographic column. When samples were found to be outside the linearity range, they were diluted and reanalyzed.

#### **Samples from the physico-chemical properties**

The samples from Ws, LogP(A<sup>-</sup>) and albumin binding were brought to room temperature and diluted 1:100 or 1:10 (v/v) with ammonium acetate buffer 15 mM pH 8 and acetonitrile : methanol (3:1 v/v) in ratio 65:35= aqueous solvent: organic solvent (v/v). The final solution was transferred to an autosampler vial and 5  $\mu\text{L}$  was injected onto the chromatographic column. When samples were found to be outside the linearity range, they were diluted and reanalyzed.

#### 2.1.4. Quantification

Calibration curves were generated by plotting the peak area ratio of the respective compound to the corresponding internal standard versus the nominal concentration. The line of best fit was determined by linear-weighted (1/x) least-squares regression. The linearity acceptance criterion for the correlation coefficient was 0.99, or better. Each back calculated standard concentration should be within  $\pm 15\%$  deviation from the nominal value, except for the LLOQ, for which the maximum acceptable deviation was  $\pm 20\%$ .

#### 2.1.5. Instrumentation: HPLC-ES-MS/MS analysis

Rat bile samples (see Chapter 4) and samples of the physico-chemical property studies (see Chapter 3) were analyzed by liquid chromatography using a 2695 Alliance system (Waters, Milford, MA) separation module coupled with autosampler. The autosampler was maintained at 7°C. The analytical column was a Luna Phenyl-Hexyl (150x2.0mm i.d., 4  $\mu\text{m}$  particle size), protected by a SecurityGuard Phenyl 4 x 2.0 mm i.d. guard column, both supplied by Phenomenex. BA were separated in elution gradient using 15 mM ammonium acetate buffer (pH = 8.00) as mobile phase A and acetonitrile : methanol = 75:25 v/v as mobile phase B. The analysis was performed in the gradient mode, according to the following gradient table.

Table 2.3: Elution gradient

Time (min)	A%	B%	Flow (ml/min)	Curve
0.00	65	35	0.150	1
10.00	65	35	0.150	1
10.30	55	45	0.150	6
21.00	55	45	0.150	1
21.30	0	100	0.150	6
23.30	0	100	0.150	1
24.00	65	35	0.150	6
35.00	65	35	0.150	1

Solvents A and Solvent B were previously filtered using a 0.45  $\mu\text{m}$  Millipore filter. Elution was performed at a flow rate of 0.15 ml/min. Sample injection volume was 5  $\mu\text{L}$  and the column was maintained at 45°C.

The HPLC was connected to a Quattro-LC (triple quadrupole of MicroMass) MS system operating with an electrospray (ES) ionization source in the negative mode with the following parameters.

Table 2.4: Tuning parameters optimized

<b>Instrumental parameters</b>	<b>Value</b>
Capillary:	3.0 KVolts
	60 volts Free-BA
Cone:	40 volts Glyco-BA
	70 volts Tauro-BA
Extractor:	1 volts
RF lens:	0.50 volts
Source block temp.:	120°C
Desolvation temp.:	180°C
<b>MS</b>	
Entrance:	1.0 volts
Exit:	1.0 volts
Ion energy:	1.5 volts
LM resolution:	12.0
HM resolution:	12.0
<b>MS2</b>	
Ion energy:	3.0 volts
LM resolution:	12.0
HM resolution:	12.0
<b>Pressure</b>	
Analyser vacuum:	3.4e <sup>-5</sup> mBar
Gas cell:	2.6e <sup>-3</sup> mBar
<b>Flows</b>	
Nebulizer (Nitrogen):	87 lit/hr
Desolvation gas (Nitrogen):	800 lit/hr
<b>Multiplier</b>	650 volts



Instrument optimization was performed by direct infusion and manual tuning of each BA. Chromatograms were acquired using the mass spectrometer in multiple reaction monitoring (MRM) mode. Collision energies (by Argon) were performed for each BA. MassLynx software version 4.0 was used for data acquisition and processing. In addition, using mass spectrometry both in single MS and tandem MS/MS configurations, experiments were performed to identify metabolites.

### 2.1.6. Identification of the metabolites

Potential or expected metabolites including those conjugated with sulphate, glucuronic acid or dehydroxylated, decarboxylated, oxo and epimer derivatives (epimers have the same m/z ratio but often different retention time) were investigated, even if the standards necessary for their quantization were not available. These compounds were identified according to the m/z values.

The table below summarizes some rules for studying the metabolism of BA.

General rules for the identification of BA metabolites in mass spectrometry			Acquisition mode
Interpretation of the profiles for in vivo experiments:	Metabolite	$[M-H]^-_0 < [M-H]^-_1$	SIR
	Conjugated species	$[M-H]^-_0 > [M-H]^-_1$	MRM/SIR
	Analogues	$[M-H]^-_0 \sim [M-H]^-_1$	MRM
	Isomers	$[M-H]^-_0 = [M-H]^-_1$	MRM/SIR
Examples:	Taurine-conjugated	$[M-H]^-_0 + 107$	MRM
	Glycine-conjugated	$[M-H]^-_0 + 57$	MRM
	Glucuronide-conjugated	$[M-H]^-_0 + 176$	MRM/SIM
	Sulphate-conjugated	$[M-H]^-_0 + 80$	SIM
	Dehydroxylated-derivatives	$[M-H]^-_0 - 16$	SIM
	Decarboxylated-derivatives	$[M-H]^-_0 - 44$	SIM
	Oxo-derivatives	$[M-H]^-_0 - 2$	SIM

*$[M-H]^-_0$ =ion of the compound studied;  $[M-H]^-_1$ =ion of the Metabolite/Analogue/Conjugated/Isomer*

Taurine and glycine conjugates were identified in tandem mass spectrometry by monitoring the specific ion transitions in MRM mode (in this mode both quadrupoles

are fixed to detect one selected precursor ion and one, or more, selected product ions produced in the collision cell. The instrument does not make a full scan of all ions but only those of interest to us and this increases the sensitivity (Figure 2.1).

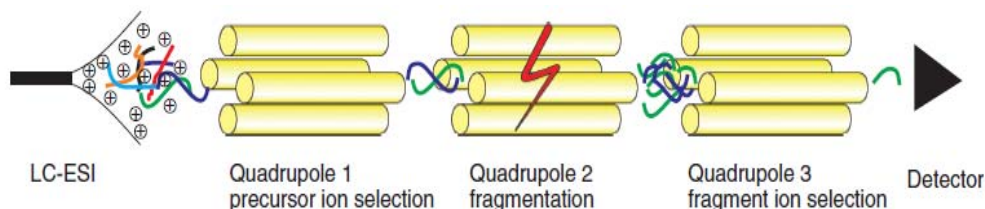
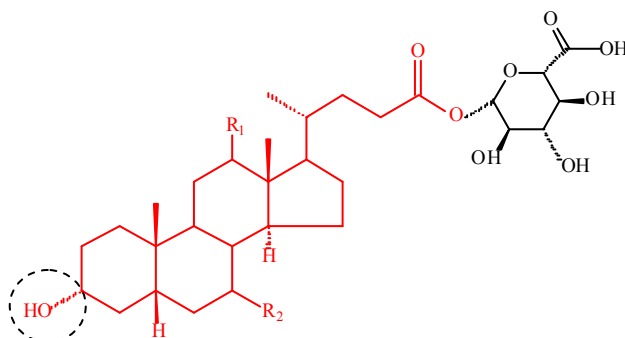


Figure 2.1: MRM analysis on QQQ MS. Several analytes are coeluting from the chromatographic system. The specific  $m/z$  selection in the first quadrupole filters out most coeluting ions. However, owing to identical mass, one interfering ion (blue) remains. In quadrupole 2, the analytes are fragmented. The  $m/z$  selection in the third quadrupole filters out all the fragments of the blue analyte and leaves only a particular fragment of the green analyte for specific detection (From Lange et al. 2008).

All other conjugates were monitored in tandem mass spectrometry in a selected-ion reaction (SIR) mode with a negative electrospray ionization (ESI) interface by the following ions (rules summarized in the Table above). The metabolism results of each BA are described in section 4.1.2.

In some experiments the glucuronide conjugates were identified also in tandem mass spectrometry (in MRM mode) by monitoring the specific ion transition  $m/z [M-H]^- \rightarrow 175$  (transition representative of glucuronide conjugate, there are other specific fragments from the spectra of glucuronide group they are 113, 85, 75  $m/z$  but in our case the mass peak  $m/z$  175 was more intense than other) in bile sample only diluted 1:10 (v/v) in mobile phase. In addition, setting a lower cone voltage value (35 V), the double charged ion would be recorded.



As a test of the presence of the glucuronide conjugate were also made tests using the enzyme  $\beta$ -glucuronidase (from Sigma Aldrich used for the enzymatic hydrolysis of

glucuronides prior to analysis) and treatment the sample with and without the enzyme in order to see if the signals of Free form or Glucuronidase form will change. That is, in the sample with the enzyme will increase the signal of the free form of BA (monitored in MRM mode) and will drop the signal glucuronide (monitored in MRM and SIR depends on the case and the complexity of the chromatographic profiles obtained). So in this case we can confirm the presence of glucuronide form.

### **2.1.7. Method validation**

In terms of linearity, accuracy and precision, the bioanalytical method used in this study fulfils the compliance criteria described by the FDA Guidance for the industry: bioanalytical method validation.

The limit of quantification (LOQ) of the different analytes was calculated using a signal-to-noise ratio of 5 from data obtained for spiked bile samples diluted 1:10 (v/v) with mobile phase. In addition, the coefficients of variation at this concentration were calculated for each BA. The limit of detection (LOD) of the different analytes was calculated using a signal-to-noise ratio of 3 from data obtained for spiked bile samples diluted 1:10 (v/v) with mobile phase.

Each back calculated standard concentration should be within  $\pm 15\%$  deviation from the nominal value, except for the LOQ, for which the maximum acceptable deviation was  $\pm 20\%$ .

Intra-day and inter-day precision and accuracy were determined by analyzing individual BA in three different QCs corresponding low (0.3  $\mu\text{mol/l}$ ), medium (8.0  $\mu\text{mol/l}$ ) and high (17.5  $\mu\text{mol/l}$ ) representative concentrations.

The IS concentration (1  $\mu\text{mol/l}$  for INT-747, T-INT-747 and G-INT-747) was maintained constant in all the QCs. Each QC was analyzed five times in three different experimental sample batches. The acceptance criteria for precision within and between batches, expressed as a coefficient of variation (CV), were  $\pm 20\%$  for the LLOQ and  $\pm 15\%$  or better for the other concentrations. Accuracy is expressed as the relative measurement error (RME) and was calculated using the following formula:  $\text{RME (\%)} = 100 \times (\text{calculated concentration} - \text{nominal concentration})/\text{nominal concentration}$ . The

acceptance criteria were  $\pm 20\%$  for within and between batches for the LLOQ and  $\pm 15\%$  or better for the other concentrations.

The biological matrices contain numerous endogenous substances that may interfere with analysis and generate a matrix effect if coelute with the analyte resulting decrease (ion suppression) or increase instrumental response. The matrix effect was calculated as the ratio of the analyte in mobile phase with respect to the analyte in the bile sample (collected at time zero and diluted 1:10 (v/v) with mobile phase) fortified at the end of the process. The total recovery was not determined because the sample pretreatment is only a dilution of bile sample and not an extraction or clean-up procedure as for samples from the physico-chemical properties.

## **2.2. Results and Discussion**

### **2.2.1. Optimization of chromatographic conditions**

The optimization of the chromatographic analysis for all analytes is based on the peak resolution, the retention time, analysis time and the need to obtain the highest signal-to-noise (S/N); a suitable pH value and a suitable solvent for the mobile phase were therefore evaluated.

The best result in terms of ESI response, resolution of peak and time of chromatographic run is obtained with a Luna Phenyl-Hexyl (150x2.0mm i.d., 4  $\mu\text{m}$  particle size) hydrophobic column ideal for the retention of acids, protected by a SecurityGuard Phenyl 4 x 2.0 mm i.d. guard column, both supplied from Phenomenex.

BA were separated in elution gradient using 15 mM ammonium acetate buffer (pH = 8.00) as mobile phase A and acetonitrile : methanol = 75:25 v/v as mobile phase B. In analytical conditions optimal retention times average (n = 20) are reported in the following table 2.5.

Table 2.5: Retention times of the different BA

BA	Free- BA	Glycine - BA	Taurine - BA
	$t_R$	$t_R$	$t_R$
CA	6	6.4	7.1
CDCA	12.8	11.8	13.8
INT-747(IS)	23.3	21.9	20.9
INT-777	10.3	7.5	8.7
INT-1212	8.3	NA	10.5
INT-2021	16.6	NF	NF
INT-2023	21.9	NF	NF
INT-2024	5.4	NF	6.4*

NA= not available;  $t_R$ = minutes; NF= not formed; \*= not standard available

It was possible to use the same matrix, with bile collected before the infusion in the rat diluted 1:10 (v/v) with mobile phase, to plot the calibration curve because the BA that we analyse are synthetic BA, with structural modifications, that are not found in this sample. To quantify TCDCA and CDCA, we had no problems since TCDCA and even the free form CDCA are almost absent in the rat bile and therefore the signals are negligible compared to those found after the administration of these compounds.

The conditions of "purge" of the column and reconditioning guarantee the stability of the pressure of the chromatographic column and as well as repeat times reproducible (standard deviation of time retention is  $\pm 0.1$  min. for each BA studied) for at least 50 consecutive injections.

The injection volume of 5 $\mu$ l was chosen as the optimum volume in terms of peak amplitude, signal-to-noise ratio and stability of the system during an analysis cycle (lasting 42 hours).

Figures 2.2 and 2.3 show a typical chromatogram obtained in MRM mode acquisition from analysis of bile sample containing 10  $\mu$ M of the respectively reported analytes, IS in bile matrices diluted 1:10 with mobile phase and blank bile samples in matrix.

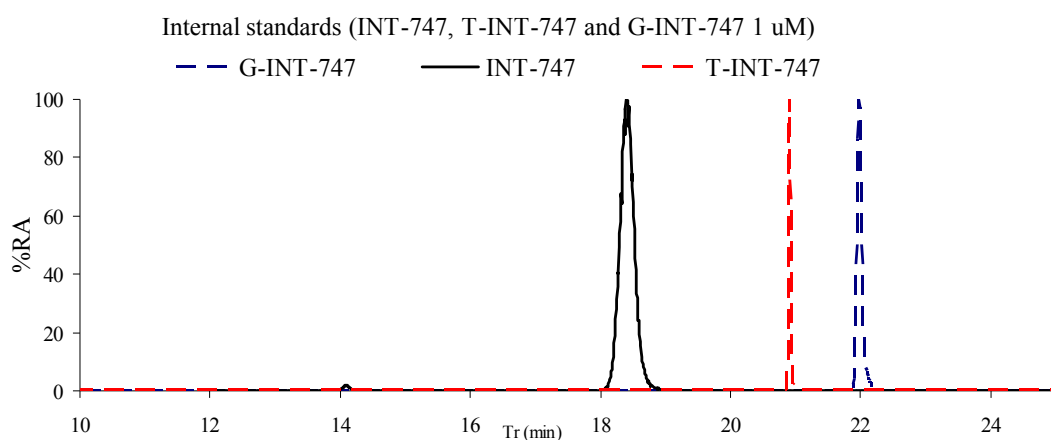


Figure 2.2: Example of RIC chromatogram (acquired in MRM mode) obtained from the analysis of bile (taken prior to infusion of the synthetic BA) diluted with mobile phase and after spiking with ISs (INT-747, T-INT-747 and G-INT-747 at the concentration of 1  $\mu\text{M}$ ) used to build the calibration curve.

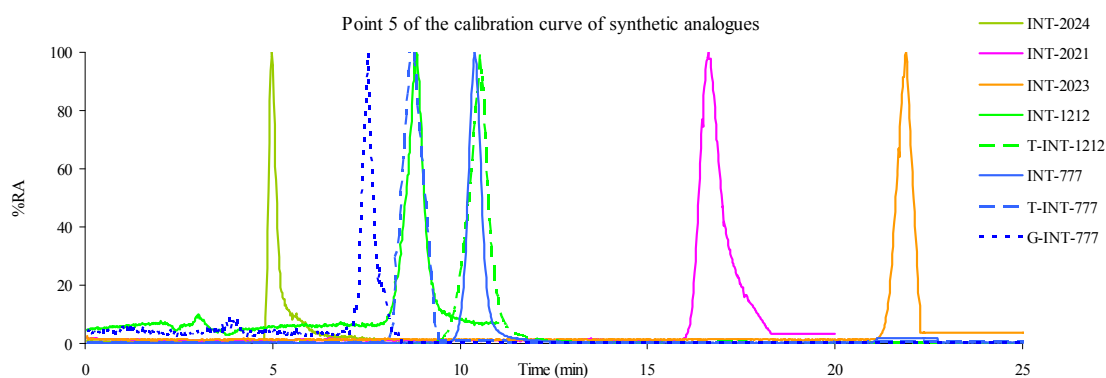


Figure 2.3: Example of RIC chromatogram (acquired in MRM mode) obtained from the analysis of bile (taken prior to infusion of the synthetic BA) diluted with mobile phase and after spiking with synthetic analogues (at the concentration of 10  $\mu\text{M}$ ) used to build the calibration curve.

Table 2.6 reports the values of intensity of the chromatographic peaks expressed as eV obtained from the chromatographic run, in matrix. This is equivalent to point five of the calibration curve.

Synthetic analogues	Chromatogram peak intensity at [C]= 10 $\mu$ M
INT-2024	6.49E+04
INT-2021	8.60E+04
INT-2023	5.72E+04
INT-1212	1.82E+05
T-INT-1212	2.35E+06
INT-777	1.54E+06
T-INT-777	1.07E+05
G-INT-777	2.03E+04
INT-747	9.53E+06
T-INT-747	6.28E+04
G-INT-747	4.89E+05

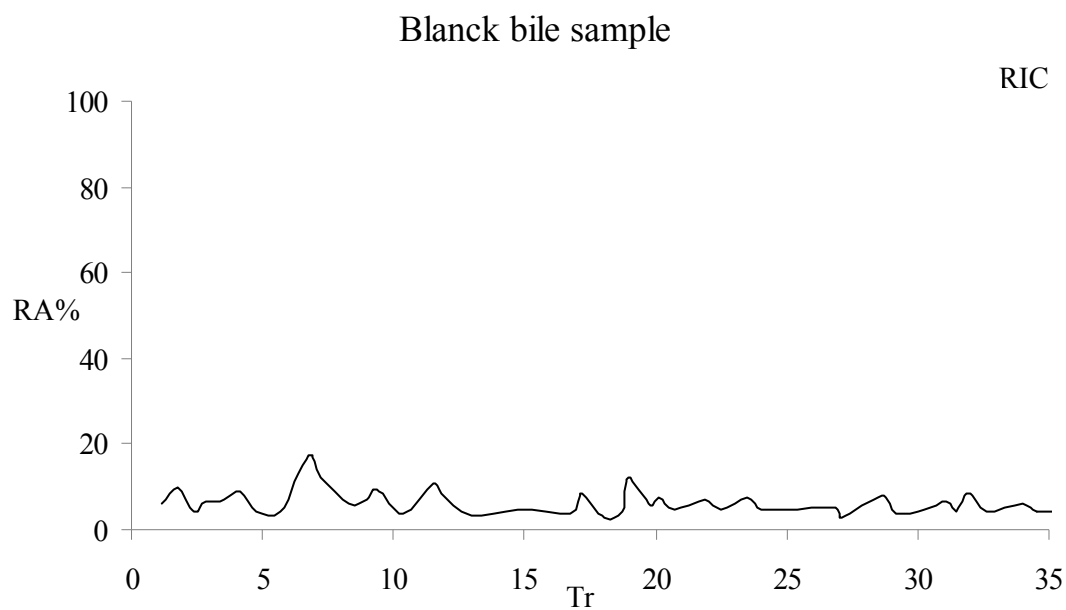


Figure 2.4: Example of blank chromatogram (acquired in MRM mode) obtained from the analysis of bile (taken prior to infusion of the synthetic BA) diluted with mobile phase used to build the calibration curve. RIC= reconstitute ion current (of all analogues searched).

## 2.2.2. Optimization of mass spectrometry conditions

The mass spectrometry optimization is obtained by evaluating both ionization modes and the effect of different compositions of the mobile phase to find the optimal conditions for the ESI source.

The use of solvents containing weak acids usually leads to a higher signal-to-noise ratio, but in this case of BA a better signal is obtained using a basic pH. Instrument optimization was performed by direct infusion (conditions of infusions: flow rate = 40  $\mu$ l/min; Solutions = 0.02 mM in 50:50 (v/v) = buffer : organic solvent (acetonitrile : methanol = 75:25 (v/v)) and manual tuning of each BA, a summary table 2.7 of the compound infusions is shown below.

Table 2.7: BA and their ions used in the HPLC–ESI-MS/MS analysis.

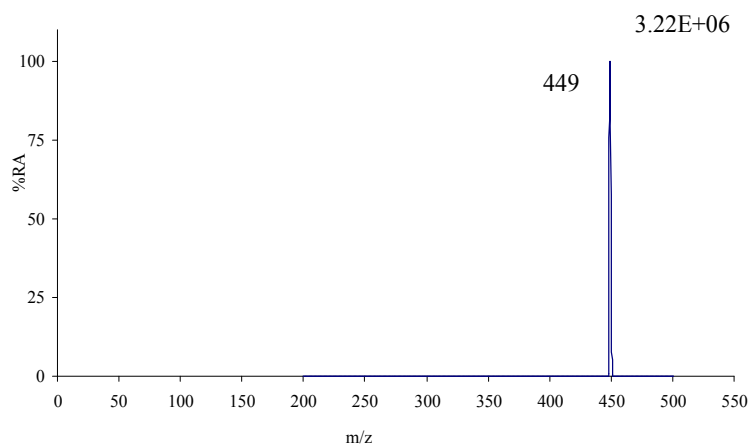
BA	Free- BA		Glycine - BA		Taurine - BA	
	P.I. [M-H] <sup>-</sup> →product ion (m/z)	CE	P.I. [M-H] <sup>-</sup> →product ion (m/z)	CE	P.I. [M-H] <sup>-</sup> →product ion (m/z)	CE
CA	407→407	15	464→74	40	514→80	60
CDCA	391→391	15	448→74	40	498→124	50
INT-747(IS)	419→419	20	476→74	40	526→107	60
INT-777	449→449	15	506→74	60	556→80	60
INT-1212	435→435	15	492→492	15	542→542	15
INT-2021	501→501	5	NA	-	NA	-
INT-2023	487→487	5	NA	-	NA	-
INT-2024	451→451	5	NA	-	558→124*	40

*P.I.* = Precursor ion; *CE*= collision energy; *NA* = not available; *IS*= internal standards; \*=not standard available

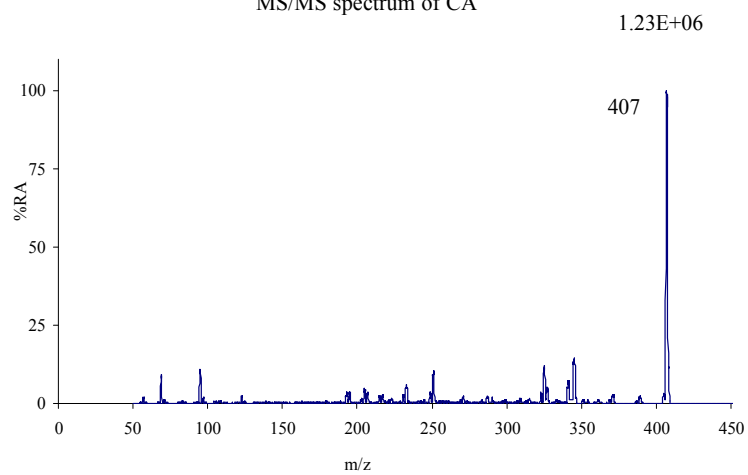
The figures below report some examples of MS/MS mass spectra of INT-777, CA, T-INT-777, T-CA, G-CA and G-INT-777 compounds acquired after instrument optimization.



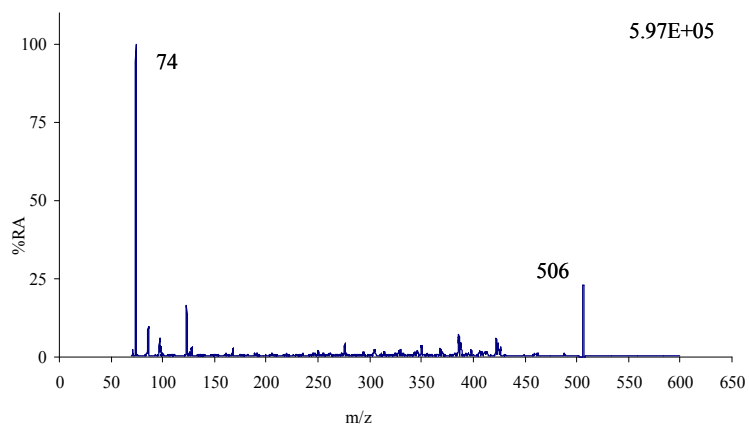
MS/MS spectrum of INT-777



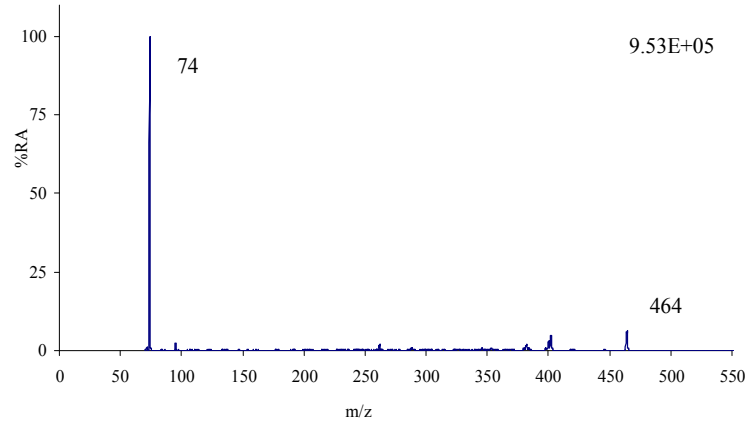
MS/MS spectrum of CA



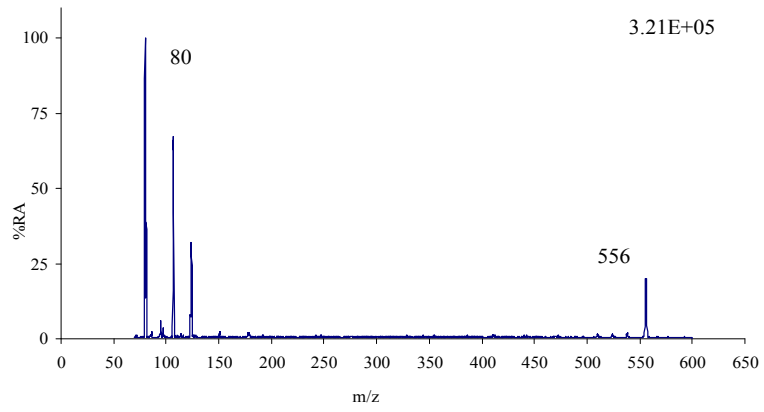
MS/MS spectrum of G-INT-777



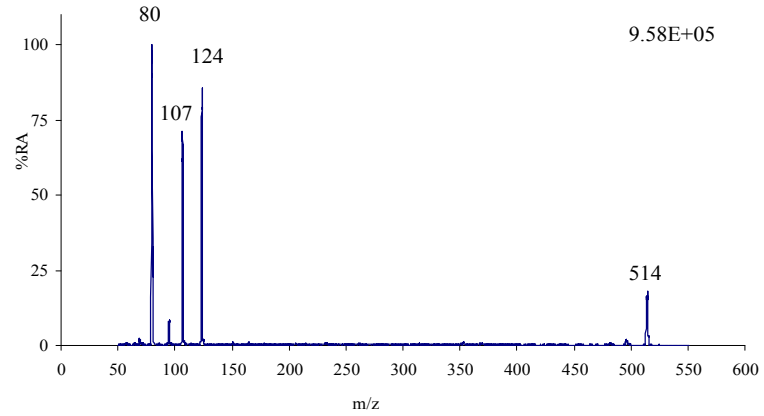
MS/MS spectrum of G-CA



MS/MS spectrum of T-INT-777



MS/MS spectrum of T-CA



The value of the intensity reported in the different MSMS spectra ( in eV) suggests that the structural modifications performed on the new BA analogues, compared to the natural BA, do not affect the ionization with a similar response in ESI source both free, glycine and taurine BA.

### 2.2.3. Method validation

The HPLC-ES-MS/MS method was validated in terms of accuracy, precision and linearity. Overall accuracy and precision were appropriate for all the determinations.

The average recovery due to the effect matrix for all analytes is 97% while for the internal standards are 100% (CV% < 2), thus confirming the absence of the matrix effect in optimized conditions.

Table 2.8 shows the parameters for the calibration curve derived from the statistical analysis of six calibration curves (obtained in duplicate) obtained in bile matrix.

Table 2.8: Parameters for the calibration curve obtained for each BA.

BA	Slope ( $\pm$ sd)	Intercepts ( $\pm$ sd)	R <sup>2</sup>	IS
G-INT-777	6.64E-04 $\pm$ 1.2E-04	5.88E-03 $\pm$ 2.3E-03	0.992	G-INT-747
T-INT-777	1.65E-04 $\pm$ 0.3E-04	-3.85E-04 $\pm$ 2.2E-04	0.993	T-INT-747
INT-777	2.83E-03 $\pm$ 0.8E-03	1.87E-02 $\pm$ 0.4E-02	0.995	INT-747
T-INT-1212	2.36E-04 $\pm$ 1.1E-04	-6.48E-03 $\pm$ 2.0E-03	0.997	T-INT-747
INT-1212	1.56E-07 $\pm$ 0.4E-07	-1.60E-04 $\pm$ 0.4E-04	0.999	INT-747
INT-2021	3.05E-04 $\pm$ 0.8E-04	-8.32E-02 $\pm$ 3.0E-02	0.997	INT-747
INT-2023	1.89E-04 $\pm$ 0.7E-04	-2.06E-02 $\pm$ 1.0E-02	1.000	INT-747
INT-2024	5.62E-05 $\pm$ 2.0E-05	2.58E-02 $\pm$ 0.9E-02	0.993	INT-747
T-CDCA	5.57E-04 $\pm$ 1.8E-04	-4.35E-03 $\pm$ 1.3E-03	0.997	T-INT-747
CDCA	5.78E-04 $\pm$ 3.2E-04	1.15E-03 $\pm$ 0.5E-03	0.995	INT-747
T-CA	8.09E-04 $\pm$ 3.2E-04	9.21E-03 $\pm$ 0.5E-03	0.996	T-INT-747
CA	7.62E-04 $\pm$ 3.2E-04	-1.45E-02 $\pm$ 0.3E-02	0.996	INT-747

The calibration curves show good linearity in the range of concentration between 0.1 and 20  $\mu$ M. This concentration range proved to be suitable for analyzing both the bile samples appropriately diluted with mobile phase (1:1000, 1:100 and 1:10 v/v) that the

samples of the physico-chemical properties because the method don't shows the matrix effect and so the validation parameters obtained in the mobile phase or in bile diluted, as matrix, did not change the values of precision, accuracy and linearity.

Therefore we performed calibration curves in mobile phase for the samples of the physico-chemical properties and in bile diluted for bile samples from rat.

Intra-day and inter-day accuracy, measured as RME, ranged from -7.7% to 8.0%. Precision, measured as CV (%), was below 10.0% and 9.4% for intra- and inter-day, respectively (Table 2.9). In terms of linearity, the regression coefficients for all the calibration curves of the BA were higher than 0.992.

Table 2.9: The precision, accuracy for each BA.

BA	Intra-day Validation						Inter-day Validation					
	Precision (cv%)			Accuracy (RME %)			Precision (cv%)			Accuracy (RME %)		
	L	M	H	L	M	H	L	M	H	L	M	H
CDCA	2.4	5.2	6.2	2.1	-0.5	1.3	3.2	3.4	2.3	1.1	-0.7	1.2
T-CDCA	3.8	3.1	3.3	0.1	6.3	2.2	3.2	2.6	3.3	0.1	6.2	1.1
G-CDCA	5.0	7.0	2.0	2.8	2.6	5.0	7.0	2.0	6.0	1.8	1.6	5.0
CA	2.1	9.4	1.7	0.7	0.3	4.2	5.2	3.3	9.4	0.4	0.2	4.1
T-CA	5.6	3.8	1.4	5.2	-0.7	1.4	3.8	2.6	3.8	5.1	-0.4	1.4
G-CA	1.2	1.7	4.7	0.4	3.5	-2.6	2.7	3.3	3.6	0.4	2.5	-1.6
INT-777	7.8	2.4	2.5	1.8	2.7	0.2	2.2	6.8	3.4	1.8	1.4	0.1
T-INT-777	10	2.6	2.8	1.2	4.1	0.8	2.6	30	3.6	1.1	4.1	0.8
G-INT-777	7.0	1.3	4.8	4.4	2.2	2.5	2.3	6.0	3.3	4.4	1.1	1.5
INT-1212	4.5	5.0	9.0	2.8	3.7	1.1	3.0	4.2	2.0	1.8	2.4	1.1
T-INT-1212	2.0	7.3	6.8	-0.2	2.2	3.2	7.3	3.0	6.3	-0.1	1.1	2.1
INT-2021	5.7	2.1	4.7	2.2	5.6	-0.6	2.2	2.6	3.3	1.1	5.6	-0.6
INT-2023	5.8	2.5	3.3	3.1	-7.7	5.0	2.3	2.8	3.2	2.1	-4.4	5.0
INT-2024	1.6	6.1	2.3	1.1	8.0	4.9	6.2	3.6	6.3	1.1	8.0	4.9

Precision is expressed as a coefficient of variation (%). Accuracy is expressed as the relative error (RME) and is calculated using the following formula:  $RME (\%) = 100 \times (\text{calculated concentration} - \text{nominal concentration}) / \text{nominal concentration}$ . L: low concentration (0.3  $\mu\text{mol/l}$ ); M: medium concentration (8.0  $\mu\text{mol/l}$ ); H: high concentration (17.5  $\mu\text{mol/l}$ ).

The LOQ values (signal-to-noise ratio, 5) for bile samples were between 0.005 and 0.01  $\mu\text{M}$ . The LOD values (signal-to-noise ratio, 3) for bile samples were between 0.001 and 0.02  $\mu\text{M}$ . The following are the values of LOD and LOQ for each BA analyzed (Table 2.1.0.).

Table 2.1.0: Limit of quantification and Limit of detection ( $\mu\text{M}$ ) of the different BA.

BA	LOQ ( $\mu\text{M}$ )	LOD ( $\mu\text{M}$ )	BA	LOQ ( $\mu\text{M}$ )	LOD ( $\mu\text{M}$ )
CDCA	0.01	0.002	INT-777	0.005	0.001
T-CDCA	0.01	0.003	T-INT-777	0.007	0.003
G-CDCA	0.01	0.0004	G-INT-777	0.01	0.003
CA	0.01	0.003	INT-1212	0.01	0.002
T-CA	0.01	0.003	T-INT-1212	0.01	0.01
G-CA	0.01	0.003	INT-2021	0.01	0.003
INT-747	0.04	0.01	INT-2023	0.01	0.003
T-INT-747	0.09	0.02	INT-2024	0.01	0.004
G-INT-747	0.09	0.02			

## 2.2.4. Pharmacokinetics (biliary secretion) and hepatic metabolism of the administered analogues: iv and id infusion.

The data refer to the samples from the physico-chemical properties are summarized in chapter 3 sections 3.2.2. for Ws, 3.2.3. for LogP(A<sup>-</sup>) and 3.2.4. for albumin binding.

The data refer to the secretion rate of the more recent BA analogues recovered in bile as such after duodenal and femoral infusion at a dose of 1 µmol/min/kg (Tables 2.1.1, 2.1.2, 2.1.3 and 2.1.4).

Table 2.1.1: INT-2021, INT-2023, and INT-2024 concentrations in µmol/l and secretion values in µmol/min/kg obtained from rat bile samples collected during the duodenal infusion (1 hour ranging from 75 to 135 minutes).

Time (min)	INT-2021 (n=3)		INT-2023 (n=3)		INT-2024 (n=3)	
	Conc.±SD	Secretion±SD	Conc.±SD	Secretion±SD	Conc.±SD	Secretion±SD
ID	(µmol/l)	(µmol/min/kg)	(µmol/l)	(µmol/min/kg)	(µmol/l)	(µmol/min/kg)
75	n.d.	-	n.d.	-	n.d.	-
90	3.0±2.0	0.00011±0.00007	1.8±0.8	0.00008±0.00001	4.78±0.01	0.0002±0.0002
105	6.0±1.0	0.00011±0.00001	24±3	0.0012±0.0001	92.24±0.01	0.004±0.004
120	21±7	0.0003±0.0002	120 ±20	0.0063±0.0008	400±100	0.020±0.006
135	16.0±7.0	0.0007±0.0002	378±3	0.0186±0.0002	800±200	0.036±0.007
150	23.0±9.0	0.0006±0.0003	920±30	0.044±0.002	800±400	0.036±0.003
165	70±20	0.0008±0.0006	1200±100	0.057±0.005	1200±600	0.08±0.01
180	110±20	0.004±0.001	1000±400	0.05±0.02	860±90	0.036±0.003
195	77±6	0.0030±0.0002	7000±300	0.04±0.02	770±80	0.03±0.03
210	60±20	0.0002±0.0006	700±100	0.037±0.007	420±70	0.017±0.005
225	72±7	0.0022±0.0002	500±0.3	0.03±0.02	270±50	0.011±0.003
240	70±30	0.0022±0.0009	500±0.3	0.03±0.01	130±30	0.005±0.004
255	60±40	0.002±0.001	500±0.4	0.02±0.02	140±70	0.006±0.005

*n.d.* = not detected; - = not calculated

Table 2.1.2: T-INT-777, G-INT-777, and T-INT-1212 concentration and secretion values obtained from rat bile samples collected during the duodenal infusion (1 hour ranging from 75 to 135 minutes).

Time (min)	T-INT-777 (n=3)		G-INT-777 (n=3)		T-INT-1212 (n=3)	
	Conc.±SD	Secretion±SD	Conc.±SD	Secretion±SD	Conc.±SD	Secretion±SD
<b>ID</b>	(µmol/l)	(µmol/min/kg)	(µmol/l)	(µmol/min/kg)	(µmol/l)	(µmol/min/kg)
75	n.d.	-	n.d.	-	n.d.	-
90	5.0±1.0	0.030±0.005	0.2±0.1	0.001±0.001	n.d.	-
105	6.0±1.0	0.030±0.008	0.9±0.2	0.005±0.003	0.3±0.1	0.001±0.001
120	7.0±1.0	0.04±0.01	2.0±1.0	0.008±0.004	2.5±0.5	0.008±0.001
135	11.0±3.0	0.06±0.01	100±20	0.66±0.02	4.0±1.0	0.014±0.003
150	19.0±4.0	0.13±0.02	3.0±0.2	0.50±0.04	5.0±1.0	0.020±0.002
±165	10.0±2.0	0.11±0.06	2.5±0.5	0.10±0.02	3.3±0.8	0.020±0.002
180	14.0±5.0	0.10±0.03	3.3±0.6	0.03±0.01	4.8±0.9	0.016±0.003
195	11.0±2.0	0.100±0.005	2.5±0.8	0.012±0.002	2.5±0.5	0.013±0.006
210	20.0±3.0	0.100±0.003	2.1±0.5	0.008±0.003	2.5±0.7	0.012±0.004
225	20.0±6.0	0.09±0.01	2.3±0.3	0.008±0.006	3.6±0.8	0.012±0.002
240	20.0±3.0	0.080±0.005	3.5±0.2	0.015±0.003	3.5±0.7	0.012±0.002

*n.d.* = not detected; - = not calculated

Table 2.1.3: INT-2021, INT-2023, and INT-2024 concentration and secretion values obtained from rat bile samples collected during the femoral infusion (1 hour ranging from 75 to 135 minutes).

Time (min)	INT-2021 (n=3)		INT-2023 (n=3)		INT-2024 (n=3)	
	Conc.±SD (µmol/l)	Secretion±SD (µmol/min/kg)	Conc.±SD (µmol/l)	Secretion±SD (µmol/min/kg)	Conc.±SD (µmol/l)	Secretion±SD (µmol/min/kg)
<b>IV</b>						
75	n.d.	-	n.d.	-	n.d.	-
90	n.d.	-	50±30	2.02±0.03	n.d.	-
105	6900±2900	400±200	6511.3±0.7	300±200	13700±200	720±9
120	10800±3600	0.79±0.05	11900±5200	0.5±0.1	17200±1700	0.88±0.09
135	9100±3500	0.5±0.2	14400±2900	0.69±0.04	18800±800	1.00±0.08
150	6300±6200	0.3±0.2	14300±1200	0.69±0.04	19300±40	0.923±0.002
165	7300±4200	0.3±0.2	10100±1000	0.52±0.04	4100±2400	0.2±0.1
180	7400±900	0.3±0.2	3900±800	0.3±0.2	1500±1100	0.07±0.05
195	4700±600	0.2±0.1	1100±300	0.07±0.03	900±600	0.04±0.03
210	1100±1000	0.04±0.03	480±50	0.028±0.006	500±400	0.02±0.02
225	1600±900	0.05±0.04	200±100	0.0130±0.0009	300±200	0.02±0.01
240	680±70	0.02±0.01	170±10	0.0098±0.0004	200±100	0.010±0.007
255	500±400	0.010±0.009	148±7	0.0084±0.0003	140±90	0.006±0.004

*n.d.* = not detected; - = not calculated



Table 2.1.4: T-INT-777, G-INT-777, and T-INT-1212 concentration and secretion values obtained from rat bile samples collected during the femoral infusion (1 hour ranging from 75 to 135 minutes).

Time (min)	T-INT-777 (n=3)		G-INT-777 (n=3)		T-INT-1212 (n=3)	
	Conc.±SD	Secretion±SD	Conc.±SD	Secretion±SD	Conc.±SD	Secretion±SD
<b>IV</b>	( $\mu\text{mol/l}$ )	( $\mu\text{mol/min/kg}$ )	( $\mu\text{mol/l}$ )	( $\mu\text{mol/min/kg}$ )	( $\mu\text{mol/l}$ )	( $\mu\text{mol/min/kg}$ )
75	n.d.	-	n.d.	-	n.d.	-
90	60±10	0.48± 0.07	99.0±2.0	0.72±0.05	100±20	0.66± 0.01
105	160±20	0.93±0.10	113.0±2.0	0.83±0.07	140±30	0.96± 0.06
120	170±30	0.98±0.07	140±10	0.98±0.05	150±50	0.91± 0.07
135	20.0±1.0	0.11±0.05	2.0±1.0	0.20±0.05	110±10	0.50± 0.08
150	6.0±1.0	0.020±0.005	22.0±2.0	0.09±0.06	20±10	0.12± 0.02
165	4.0±1.0	0.020±0.005	7.0±0.2	0.040±0.001	10±1.0	0.04± 0.01
180	2.0±0.6	0.010±0.001	2.0±0.1	0.014±0.004	4.0±1.0	0.011± 0.001
195	1.0±0.2	0.004±0.001	2.0±0.1	0.006±0.001	3.0±1.0	0.015± 0.004
210	1.0±0.1	0.003±0.001	1.0±0.2	0.005±0.001	2.0±1.0	0.006± 0.001
225	1.0±0.2	0.002±0.001	1.0±0.2	0.003±0.001	2.0±1.0	0.007± 0.002
240	1.0±0.1	0.003±0.001	1.0±0.2	0.002±0.001	1.0±1.0	0.004± 0.001

*n.d.* = not detected; - = not calculated

A preliminary screen was carried out to search for possible metabolites among the new analogues studied (INT-2023, INT-2021, INT-2024, T-INT-777, G-INT-777 and T-INT-1212), the only BA that it is metabolized was INT-2024 that forms its tauro-conjugate and it's chromatographic profile acquire in MRM mode in show below in Figure 2.5.

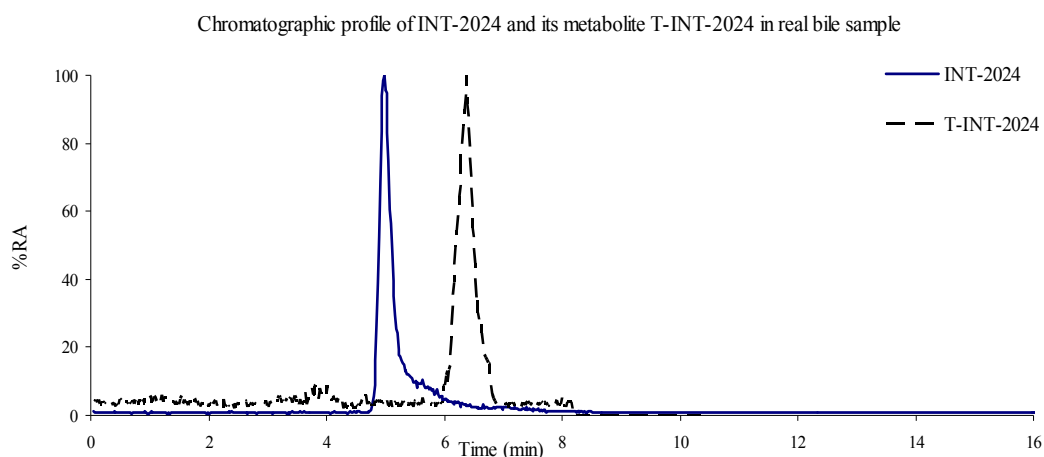


Figure 2.5: Example of RIC chromatogram (acquired in MRM mode) obtained from the analysis of bile (taken prior to infusion of the synthetic BA INT-2024) diluted with mobile phase 1:10 (v/v).

Tauro- conjugate metabolite of INT-2024 were also estimated even though standard was not available to us. Opportune corrective factors, to take into account the different responses in ES-MS/MS between free and taurine conjugated species, were estimated and applied to the area values obtained from HPLC-MRM dataset chromatograms. In the table in the section 2.2.2. there are the parameters of mass spectrometry used for follow the taurine metabolite. Finally, calibration curves obtained for the free BA were used to estimate taurine conjugated metabolites.

Table 2.1.5: Metabolite T-INT-2024 formed to infusion of INT-2024.

Time	T-INT-2024 (n=3)		Time	T-INT-2024 (n=3)	
(min)	Conc.±SD	Secretion±SD	(min)	Conc.±SD	Secretion±SD
ID	(mmol/l)	( $\mu\text{mol}/\text{min}/\text{kg}$ )	IV	(mmol/l)	( $\mu\text{mol}/\text{min}/\text{kg}$ )
75	n.d.	-	75	n.d.	-
90	n.d.	-	90	n.d.	-
105	0.18±0.09	0.009±0.001	105	2.1±1.7	0.11±0.01
120	0.4±0.1	0.02±0.01	120	1.6±0.8	0.08±0.02
135	0.5±0.2	0.02±0.02	135	2.04±0.04	0.10±0.03
150	0.7±0.6	0.04±0.02	150	0.7±0.2	0.03±0.01
165	0.6±0.1	0.03±0.01	165	0.2±0.1	0.009±0.002
180	0.5±0.4	0.022±0.003	180	0.09±0.06	0.0040±0.0005
195	0.4±0.3	0.01±0.01	195	0.05±0.04	0.00203±0.00008
210	0.2±0.1	0.007±0.007	210	0.02±0.02	0.0010±0.0003
225	0.07±0.07	0.003±0.002	225	0.02±0.01	0.00086±0.00007
240	0.2±0.1	0.008±0.01	240	0.006±0.002	0.0003±0.0002

*n.d.* = not detected; - = not calculated

The concentration and secretion values obtained from rat bile samples collected during the femoral infusion (1 hour ranging from 75 to 135 minutes).

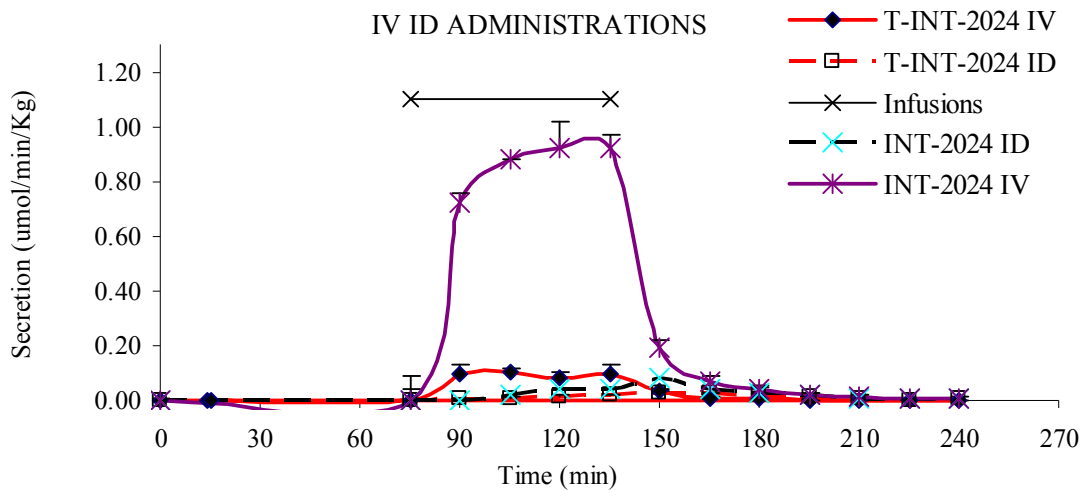


Figure 2.6: Comparison of INT-2024 and its Tauro-INT-2024 (also estimated) derivative mean secretion rates vs time in ID and IV experiments at 1  $\mu\text{mol}/\text{kg}/\text{min}$  for 1 h (n=3). Standard deviations are also reported.

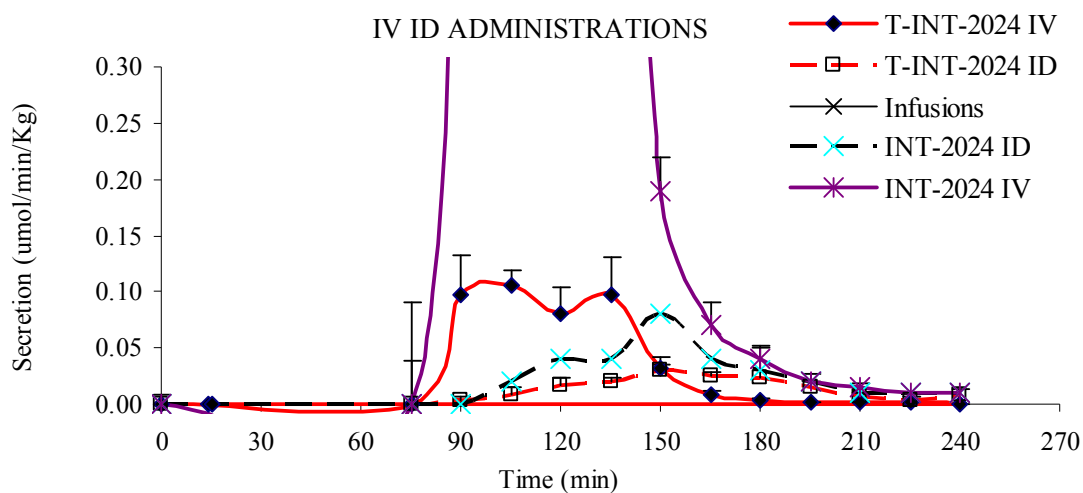


Figure 2.7: Zoom display of Figure 2.6.

This molecule is mainly secreted as such and only slightly metabolized by the liver. The main metabolite is the taurine conjugated specie and it wasn't detected glucuronide specie.

Data regarding other analogues, that have been studied before, and their metabolism and conclusions are discussed in sections 4.2. and 4.3.

### **2.3. Conclusions**

An improved HPLC-ESI-MS/MS method was developed for the determination of the synthetic BA and their major metabolites in bile that meets the general acceptance criteria established for bioanalytical studies applied in the pharmaceutical field.

In the analyzed range the method is accurate, precise, selective and sensitive to enable the analysis of molecules of interest in bile samples.

The method does not require pre analytical extraction and the analyses can be performed after a simple dilution step, minimizing the analytical variability and the analysis time.

The use of three internal standards (INT-747, T-INT-747 and G-INT-747) with similar structure to the analytes studied in this work and the use of the calibration curves in diluted bile made it possible to compensate the effect of suppression of the signal and to reduce the problems of inaccuracy.

The value of LOQ estimated for all analytes is suitable for quantifying the levels of concentration of analogues generally found in bile samples collected during the bile fistula rat studies.

### 3. PHYSICO-CHEMICAL PROPERTIES

The new BA analogues were submitted to complete physico-chemical properties characterization following protocols previously developed and optimized in our laboratory (Hofmann et al. 1984; Roda et al. 1990a; Roda et al. 1982; Roda et al. 1883; Roda et al. 1888). These studies were previously applied for the screening of naturally occurring BA (Roda et al. 1888; Aldini et al. 1996; Aldini et al. 1996a; Aldini et al. 1982) and a large series of new BA analogues were developed in R. Pellicciari's laboratory (Pellicciari et al. 1984; Roda et al. 1987; Roda et al. 1988; Roda et al. 1990; Roda et al. 1994; Roda et al. 1995). The physico-chemical properties were selected to:

- 1) define the behavior in aqueous solutions and in biological fluids
- 2) establish their potential toxicity to biological membranes
- 3) study their pharmacokinetics, pharmacodynamics, and biodistribution in the different biological fluids and organs.

Analyses of comparative data with natural analogues were also performed and are discussed.

#### 3.1. Material and Methods

##### 3.1.1. Chemicals

Natural BA: Chenodeoxycholic acid (CDCA), glycochenodeoxycholic acid (G-CDCA), taurochenodeoxycholic acid (T-CDCA), deoxycholic acid (DCA), cholic acid (CA), taurocholic acid (T-CA), glycocholic acid (G-CA) were purchased from Sigma (St. Louis, MO). Ursodeoxycholic acid (UDCA) was kindly supplied by Giuliani Spa, Milan, Italy. All chemical structures are summarized in the Table below.

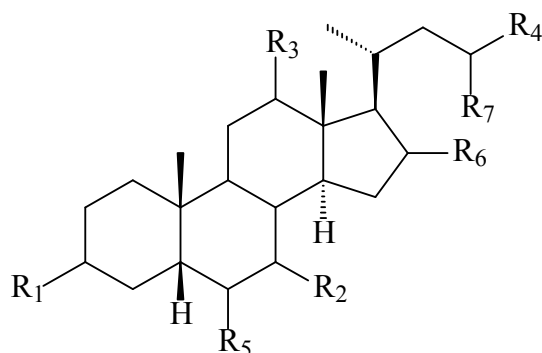


Table 3.1: Natural BA.

Natural BA	C3-R <sub>1</sub>	C7-R <sub>2</sub>	C12-R <sub>3</sub>	C23-R <sub>4</sub>	C6-R <sub>5</sub>	C16-R <sub>6</sub>	C23-R <sub>7</sub>
CA	OH ( $\alpha$ )	OH ( $\alpha$ )	OH ( $\alpha$ )	-CO-OH	H	H	H
T-CA	OH ( $\alpha$ )	OH ( $\alpha$ )	OH ( $\alpha$ )	-CO-NH (CH <sub>2</sub> ) <sub>2</sub> SO <sub>3</sub> <sup>-</sup>	H	H	H
G-CA	OH ( $\alpha$ )	OH ( $\alpha$ )	OH ( $\alpha$ )	-CO- NH(CH <sub>2</sub> )COO <sup>-</sup>	H	H	H
CDCA	OH ( $\alpha$ )	OH ( $\alpha$ )	-	-CO-OH	H	H	H
T-CDCA	OH ( $\alpha$ )	OH ( $\alpha$ )	-	-CO- NH(CH <sub>2</sub> ) <sub>2</sub> SO <sub>3</sub> <sup>-</sup>	H	H	H
G-CDCA	OH ( $\alpha$ )	OH ( $\alpha$ )	-	-CO- NH(CH <sub>2</sub> )COO <sup>-</sup>	H	H	H
DCA	OH ( $\alpha$ )	-	OH ( $\alpha$ )	-CO-OH	H	H	H
UDCA	OH ( $\alpha$ )	OH ( $\beta$ )	-	-CO-OH	H	H	H

Synthetic BA: The present work was carried out on the more recent BA analogues under study in the Bioanalytical laboratory that include: INT-2021, INT-2023, INT-2024, T-INT-1212, T-INT-777 and G-INT-777.

Data regarding INT-747, INT-1075, INT-767, INT-777, INT-1244, INT-1212 and INT-855 previously developed and fully characterized are also included for a more comprehensive interpretation of the structure-activity relationship. All the molecules were synthesized, and purified in the laboratory of Prof. Pellicciari (Institute of Pharmaceutical Chemistry, University of Perugia, Italy). All the experiments were carried out using the sodium salts of the synthesized BA if containing a side chain carboxy group. The sodium salts were prepared by adding an equimolar amount of NaHCO<sub>3</sub> to the aqueous suspension of the free acid, which was heated to 80°C, mixed

in an ultrasound bath, and then solubilized in a suitable aqueous solvent for the infusion. All chemical structures are summarized in the Table below.

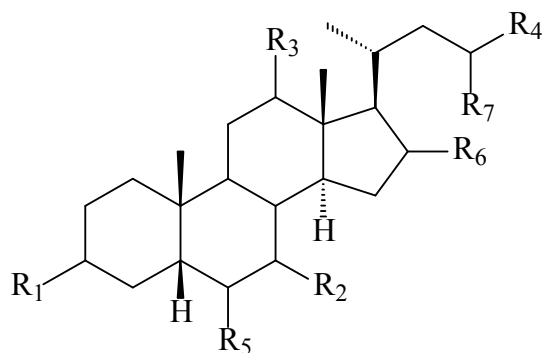


Table 3.2: Synthetic BA.

Synthetic BA	C3-R <sub>1</sub>	C7-R <sub>2</sub>	C12-R <sub>3</sub>	C23-R <sub>4</sub>	C6-R <sub>5</sub> ( $\alpha$ )	C16-R <sub>6</sub>	C23-R <sub>7</sub>
INT-747	OH ( $\alpha$ )	OH ( $\alpha$ )	-	-CO-OH	-CH <sub>2</sub> CH <sub>3</sub>	H	H
INT-777	OH ( $\alpha$ )	OH ( $\alpha$ )	OH ( $\alpha$ )	-CO-OH	-CH <sub>2</sub> CH <sub>3</sub>	H	-CH <sub>3</sub> (S)
T-INT777	OH ( $\alpha$ )	OH ( $\alpha$ )	OH ( $\alpha$ )	-CO- NH(CH <sub>2</sub> ) <sub>2</sub> SO <sub>3</sub> <sup>-</sup>	-CH <sub>2</sub> CH <sub>3</sub>	H	-CH <sub>3</sub> (S)
G-INT777	OH ( $\alpha$ )	OH ( $\alpha$ )	OH ( $\alpha$ )	-CO- NH(CH <sub>2</sub> )COO <sup>-</sup>	-CH <sub>2</sub> CH <sub>3</sub>	H	-CH <sub>3</sub> (S)
INT-1075	OH ( $\alpha$ )	OH ( $\alpha$ )	OH ( $\alpha$ )	-CO-OH	-CH <sub>2</sub> CH <sub>3</sub>	H	-CH <sub>3</sub> (R)
INT-2021	OH ( $\alpha$ )	OH ( $\alpha$ )	OH ( $\alpha$ )	-CH-OSO <sub>3</sub> <sup>-</sup>	-CH <sub>2</sub> CH <sub>3</sub>	H	-CH <sub>3</sub> (S)
INT-2023	OH ( $\alpha$ )	OH ( $\alpha$ )	OH ( $\alpha$ )	-CH <sub>2</sub> -OSO <sub>3</sub> <sup>-</sup>	-CH <sub>2</sub> CH <sub>3</sub>	H	H
INT-1244	OH ( $\alpha$ )	OH ( $\alpha$ )	OH ( $\alpha$ )	-CH <sub>2</sub> -SO <sub>3</sub> <sup>-</sup>	-CH <sub>2</sub> CH <sub>3</sub>	H	H
INT-2024	OH ( $\alpha$ )	OH ( $\alpha$ )	OH ( $\alpha$ )	-CO-OH	-CH <sub>2</sub> CH <sub>3</sub>	OH( $\beta$ )	H
INT-930	OH ( $\alpha$ )	OH ( $\alpha$ )	-	-NH-CO-O- CH <sub>2</sub> (CH) <sub>2</sub> -Ph	-CH <sub>2</sub> CH <sub>3</sub>	H	H
INT-1212	OH ( $\alpha$ )	OH ( $\alpha$ )	-	-CO-OH	-CH <sub>2</sub> CH <sub>3</sub>	OH( $\beta$ )	H
T-INT-1212	OH ( $\alpha$ )	OH ( $\alpha$ )	-	-CO- NH(CH <sub>2</sub> ) <sub>2</sub> SO <sub>3</sub> <sup>-</sup>	-CH <sub>2</sub> CH <sub>3</sub>	OH( $\beta$ )	H
INT-855	OH ( $\alpha$ )	OH ( $\alpha$ )	-	-CO-OH	-CH <sub>2</sub> CH <sub>3</sub>	H	-CH <sub>3</sub> (S)
INT-1213	OH ( $\alpha$ )	OH ( $\alpha$ )	-	-CH-OSO <sub>3</sub> <sup>-</sup>	-CH <sub>2</sub> CH <sub>3</sub>	H	-CH <sub>3</sub> (S)
INT-767	OH ( $\alpha$ )	OH ( $\alpha$ )	-	-CH <sub>2</sub> -OSO <sub>3</sub> <sup>-</sup>	-CH <sub>2</sub> CH <sub>3</sub>	H	H



### 3.1.2. Critical Micellar Concentration

The critical micellar concentration (CMC) was evaluated by surface tension (ST) measurements using a maximum bubble-pressure method (Roda et al. 1983). The tensiometer was a Sensadyne 6000 (Chem-Dyne Research Corp., Milwaukee, WI) equipped with two glass probes of 0.5 and 4.0 mm in diameter connected to a source of compressed air. The bubble frequency was 1 bubble/sec in distilled water at 25°C (P=2.7 atm) and the calibration was made with double-distilled water and methanol. The ST of the BA solutions, as sodium salts in NaCl 0.15 M, was measured at various concentrations ranging from 0.10 to 50 mM. The ST values were plotted against the logarithm of the bile salt concentration; the regression lines corresponding to the two parts of the curve (monomeric and micellar phases) were calculated using the least squares method (Figure 3.1 below), and the intersection of the lines was taken as the CMC value. From the ST versus concentration curves, the ST value at the CMC (equilibrium between monomeric and micellar phases) was also calculated, giving information about the detergency power which is related to the size of the micelles with associated ST lowering capacity. The CMC was measured in NaCl 0.15 M to mimic physiological conditions (Mysels et al. 1973; Mukerjee et al. 1971). The CMC in water would be slightly higher but the values are not relevant for our purposes.

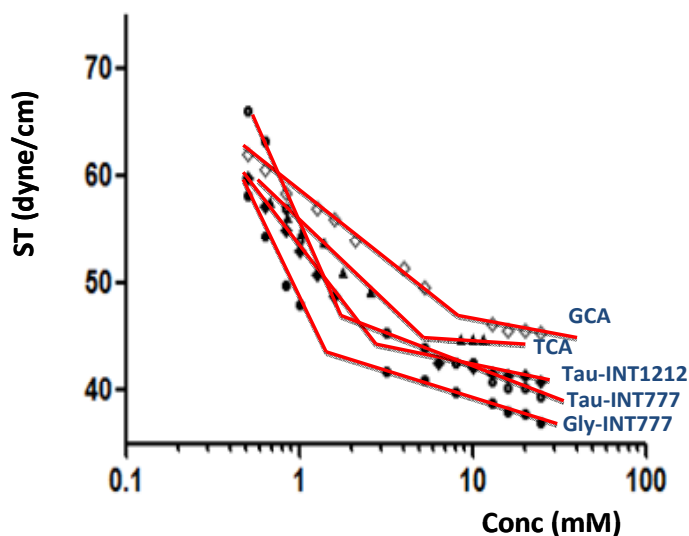


Figure 3.1: Surface tension (dyne/cm) plotted against the logarithm of the bile salt concentration (mM) in NaCl 0.15 M.

### 3.1.3. Water Solubility

The water solubility was determined only for side chain carboxylated BA INT-777, INT-1212, INT-855, INT-747 and INT-2024 since the protonated forms (at a low pH) of these compounds are quite insoluble. The sulfate and sulphonate analogues INT-1213, INT-767, INT-2021, INT-2023 and INT-1244 are highly water soluble at a pH range from 0 to 12, such as Tauro-INT-1212, Tauro-INT-777 and Glyco-INT-777. INT-930 is insoluble at all pH values.

A small amount (5 mg) of each solid BA was suspended in 5 mL of 0.1 M HCl; INT-930 was suspended in distilled water. After incubation and gentle mixing for 1 week at 25°C, the saturated solutions were filtered on a Millipore filter (0.22  $\mu\text{m}$ ) and the concentration of BA in the solution was measured by high performance liquid chromatography-electrospray ionization-mass spectrometry/mass spectrometry detection (HPLC-ESI-MS/MS), as reported in detail in Chapter 2, using a Phenyl-Hexyl column (150 mm x 2.1 mm internal diameter [id], 5 $\mu\text{m}$ ) and mobile phases of ammonium acetate buffer 15 mM pH 8 and acetonitrile:methanol (3:1 v/v) in ratio 65:35= aqueous solvent: organic solvent (v/v). The flow rate was 150  $\mu\text{l}/\text{min}$  and the column was maintained at 45°C. The mass spectrometry acquisition was performed in the multiple reaction monitoring mode using the electrospray source in negative ionization. Water solubility was expressed as  $\mu\text{mol}/\text{l}$ .

### 3.1.4. Octanol/Water Partition Coefficient

The 1-octanol/water partition coefficient ( $\text{LogP}(A^-)$ ) was evaluated using a conventional shake flask procedure (Roda et al. 1983) for the BA as anion. The experiments were carried out using a 0.1 mM bile salt solution buffered at pH 8 with 0.1 M phosphate buffer to ensure complete ionization of the BA. The  $\text{LogP}(A^-)$  values refer to the BA in the ionized form, not to the protonated species, and the initial concentration of each BA was below its own CMC value. The aqueous buffer was previously pre-saturated with 1-octanol (0.30 mg of 1-octanol are dissolved in 1 liter of water). Five ml of 1-octanol pre-saturated with buffer was then added and the samples were left to equilibrate for 4 days under continuous stirring at room temperature. After centrifugation, the two phases

were carefully separated by centrifuge. The BA concentration in the buffer phase, after dilution with the mobile phase, was measured by HPLC-ESI-MS/MS, as reported in detail in Chapter 2, using a Phenyl-Hexyl column (150 mm x 2.1 mm internal diameter [id]., 5µm) and mobile phases of ammonium acetate buffer 15 mM pH 8 and acetonitrile:methanol (3:1 v/v) in ratio 65:35= aqueous solvent: organic solvent (v/v). The flow rate was 150 µl/min and the column was maintained at 45°C. The mass spectrometry acquisition was performed in the multiple reaction monitoring (MRM) mode using the electrospray source in negative ionization. Octanol/Water partition coefficient was expressed as logarithmic ratio of the concentrations.

$$\text{LogP(A}^-) = \text{Log}_{10} ([\text{BA}]_{\text{1-octanol}}/[\text{BA}]_{\text{water}})$$

### **3.1.5. Albumin Binding**

The extent of albumin binding was evaluated by equilibrium dialysis at a fixed BA albumin ratio (Roda et al. 1982; Aldini et al. 1982; Scagnolari et al. 1984). Each BA was dissolved at a concentration of 100 µM in 5% bovine serum albumin (BSA fatty acid free from Sigma (St. Louis, MO))-saline solution (pH 7.2) and left to stand for 24 hours at 25°C. Two ml of this solution were dialyzed in cellulose sacs with molecular weight cut-off of 12,000 to 14,000 Dalton (Spectra/Por, Spectrum Medical Industries Inc., Los Angeles, CA) against 25 ml of saline solution. The system was equilibrated by gently shaking for 72 hours at 25°C. The BA concentrations of the dialyzed solution (corresponding to the free unbound fraction) and of the starting solution were determined with HPLC-ESI-MS/MS under the same conditions as the previous analysis. The percentage of albumin binding was calculated from the initial BA concentration and from the unbound concentration in the dialyzed fraction.

### **3.1.6. Critical micellar pH**

The critical micellar pH represents the pH at which a solid BA dissolves in a micellar phase. This is relevant to simulate the dissolution of the drug from the gastric content to the duodenal juice where the BA concentration is higher than the CMC.

This pH value is defined as critical micellar pH (CMpH) which, as well as experimentally, can be calculated from the pKa, the CMC and the solubility of the protonated form of that particular BA according to the equation:

$$\text{CMpH} = \text{pKa} + \log (\text{CMC}/\text{Ws})$$

## 3.2. Results and Discussion

### 3.2.1. Critical Micellar Concentration

All the studied BA analogues present amphipatic properties and behave like detergent-like natural occurring BA. All the data were obtained using the same analytical and physico-chemical methodologies to facilitate the comparative evaluation of the recent data obtained on INT-2024, INT-2021, INT-2023, INT-2024, T-INT-1212, T-INT-777 and G-INT-777 with those obtained in the previous studied analogues which include: INT-747, INT-1075, INT-767, INT-777, INT-1244, INT-1212 and INT-855 a more large series of other analogues and natural BA.

#### **Synthetic analogues of 6-Ethyl-CDCA:**

It has been previously reported that the relatively low CMC value of INT-747 (2.9 mM) quite similar to that of CDCA (3.0 mM) is related to the topographic distribution of the ethyl and hydroxyl groups: the ethyl group in position 6 is oriented in the  $\beta$  face, the back of the steroid, contributing to increase the lipophilicity of the surface of this moiety and therefore the tendency to form micelles via back to back interaction. Moreover the two  $3\alpha$  and  $7\alpha$  hydroxyl are oriented on the opposite face facilitating the growth of micelles fro dimer to tetramer and multiper via hydrogen bonding interaction.

#### **Synthetic sulphonate and sulphate analogue of 6-Ethyl-CDCA:**

INT-767 (1.3 mM) presents the lowest CMC of the studied analogues as a result of the ethyl group in position 6 and sulphate head in the side chain. The peculiar properties of the sulphate group gave INT-767 (synthetic derivative of CDCA) anionic surfactant like

properties (like sodium dodecyl sulphate) as a result of a negative charged head in the tail with a lipophilic steroid moiety. INT-1213 has not yet been admitted to this study

#### **Synthetic carboxylated analogues of 6-Ethyl-CA:**

INT-777 (2.0 mM) presented a lower CMC with respect to the natural CA analogues (9 mM) again as a result of the presence of the Ethyl group. However, it had a moderate detergency power as documented by the high surface tension values at the CMC higher in respect to CA or other analogues. The results suggest that this molecule is able to form micelles even at low concentrations but the micelles have a low aggregation number and size and are therefore characterized by a low detergency power (low detergency means low toxicity to membranes or cells).

#### **Synthetic sulphonates and sulphate analogues of 6Ethyl-CA:**

INT-1244 presented a CMC of 2.8 mM this value is within the range of a medium-high detergent molecule. The CMC was slightly higher than INT-767 (1.3 mM), suggesting that an additional hydroxyl group balances the presence of the 6-ethyl group. The behavior of the ST versus concentration suggests the formation of relatively large aggregates with consistent detergency. The CMC values suggest that this molecule is potentially less toxic than other CDCA analogues with a lower CMC, e.g. INT-767.

INT-2021 and INT-2023 (ethyl group in position 6 and sulphate 23 in the side chain) presenting a behavior of low detergency even if the 23 $\alpha$ -methyl in INT-2021 increases the CMC up to 5.6 mM compared to INT-2023 (2.6 mM) that has only the ethyl group in six position as a difference.

#### **Synthetic carboxylates analogues of CDCA and CA containing a 16 $\beta$ - hydroxyl:**

INT-1212 and INT-2024 presented relatively high CMC values (respectively 5.9 and 6.3 mM) with a low ST lowering capacity. This indicates that these compounds are moderate detergents and the micelles have a very low aggregation number. The presence of a hydroxyl group in the 16 $\beta$  position reduces the hydrophobic area responsible for back to back interactions and gives the molecule a low potential toxicity when accumulated in a given biological fluid or organ.

**Taurine and glycine conjugated analogues:**

The detergency of taurine / glycine conjugates of INT-777 and INT-1212 is higher, i.e. the CMC is lower than the corresponding free form as a result of increased side chain length. The CMC data are similar to natural occurring taurine/glycine conjugated BA such as TCA, GCA and TCDCA.

In general, BA with a CMC < 1 mM and a low ST tension value at the CMC in the order of 40 dyne/cm are detergents and potentially toxic if they accumulate in a target organ at a concentration higher than the CMC.

If the ST tension is > 45-50 dyne/cm, the BA forms aggregates at a low concentration but these micelles are small and therefore with less detergent power.

A CMC < 1mM and ST < 40 dyne/cm are criteria of exclusion or to admit the molecule to additional studies regarding their potential toxicity (membrane toxicity, cytotoxicity).

BA with a CMC > 20-30 mM behaves more likely an organic anion and not as an amphipatic molecule with different PK and biological effects.

All data of CMC are summarized in the Table 3.3 below (in mM  $\pm$  SD).

BA	CMC(b) 0,15 M Na <sup>+</sup> (mM)	BA	CMC(b) 0,15 M Na <sup>+</sup> (mM)
CDCA	3.2 $\pm$ 0.2	CA	9.0 $\pm$ 0.2
INT-747	2.9 $\pm$ 0.1	INT-777	2.0 $\pm$ 0.3
INT-767	1.3 $\pm$ 0.1	T-CA	4.0 $\pm$ 0.3
INT-1213	Not available	T-INT-777	1.4 $\pm$ 0.2
INT-855	-	G-CA	8.0 $\pm$ 0.1
INT-930	Not determined	G-INT-777	1.3 $\pm$ 0.3
INT-1212	5.9 $\pm$ 0.2	INT-1244	2.8 $\pm$ 0.1
T- INT-1212	2.7 $\pm$ 0.2	INT-2021	5.6 $\pm$ 0.2
T-CDCA	3.0 $\pm$ 0.1	INT-2023	4.1 $\pm$ 0.2
G-CDCA	2.0 $\pm$ 0.3	INT-2024	6.5 $\pm$ 0.4
DCA	3.0 $\pm$ 0.2	UDCA	10.0 $\pm$ 0.1
BA	ST <sub>CMC(c)</sub> Dyne/cm	BA	ST <sub>CMC(c)</sub> Dyne/cm
CDCA	45.5	CA	49.0
INT-747	48.8	INT-777	50.1
INT-767	47.9	T-CA	51
INT- 1213	Not available	T-INT-777	47.8
INT-855	-	G-CA	48.8
INT-930	Not determined	G-INT-777	43.8
INT-1212	52.4	INT-1244	43.4
T- INT-1212	43.6	INT-2021	38.3
T-CDCA	47	INT-2023	42.6
G-CDCA	45.2	INT-2024	43.2
DCA	50.2	UDCA	50.5

*b* CMC: Critical Micellar Concentration determined in 0,15 M NaCl water solution.

*c* ST<sub>CMC</sub>: Surface Tension at CMC in 0,15 M NaCl water solution.

### 3.2.2. Water Solubility

The water solubility was measured for the insoluble protonated species of the carboxylated BA at pH 1 to ensure complete protonation of the carboxyl group.

### **Synthetic analogues of 6-Ethyl-CDCA:**

All the new synthetic analogues studied present low solubility when protonated, as was observed in the previous studies for INT747, INT855, INT1212 and INT1244.

The water solubility of INT-747 and INT-855 was, respectively, 9 and 15  $\mu\text{M}$ , slightly lower than CDCA (32  $\mu\text{M}$ ), and comparable with that of UDCA (7  $\mu\text{M}$ ). The water solubility of INT-930 was very low as a result of the side chain modification and the lack of charged groups in the molecule. INT-930 remained practically insoluble at all the pH values since no ionizable groups are present in the molecule.

### **Synthetic carboxylated analogues of 6-Ethyl-CA:**

The water solubility of INT-777 was 99  $\mu\text{M}$  which is lower compared to the CA (273  $\mu\text{M}$ ). The presence of a C23-Methyl group and C6-Ethyl group in the compound INT-777 decreases the water solubility. Moreover, other factors are involved in determining the solubility, including the stability of the solid state as documented by differences in the melting points.

### **Synthetic sulphonate, sulphate, taurine and glycine conjugated analogues of 6-Ethyl-CDCA and 6Ethyl-CA :**

The sulphate and sulphonate compounds, INT-767, INT-1244, INT-2021, INT-2023, INT-1213 and taurine / glycine conjugates which are fully ionized even at low pH and in physiological conditions, were highly soluble in all biological fluids.

### **Synthetic carboxylate analogues of CDCA and CA containing a 16 $\beta$ - hydroxyl:**

INT-1212 is a synthetic analogue containing C6-Ethyl and two hydroxyl groups in position 3- $\alpha$  and 16- $\beta$  and INT-2024 a similar structure with one more hydroxyl group in position 12- $\alpha$ .

The water solubility of INT-1212 and INT-2024 were, respectively, 120, and 290  $\mu\text{M}$  which is higher than the corresponding trihydroxy BA and comparable with that of CA (273  $\mu\text{M}$ ). INT-2024 exhibited the highest solubility, perhaps due to the presence of the hydroxyl group in 12- $\alpha$ . The different position of the hydroxyl (16 $\beta$ -position) in the compound INT-1212 also slightly reduced the solubility when compared to the



conventional 3 $\alpha$ ,7 $\alpha$ ,12 $\alpha$ -trihydroxy BA (CA). Moreover these differences are better explained by the solid state properties.

**Glycine conjugated analogues:**

The natural BA conjugated with glycine (G-CA and G-CDCA) show different solubility values in comparison to the corresponding unconjugated BA; the Ws of CA is 273 mM while GCA 32 mM on the contrary CDCA 7 mM present lower value in respect to GCDCA (32 mM).

The relationship structure-solubility is mainly affected by the stability of the solids state and therefore more detailed studies on solid state should be performed.

The analogue conjugate with glycine (G-INT-777) shows a higher solubility compared to INT777, in fact the Ws for the INT-777 increased from 99 mM to 1700 mM for G-INT-777.

All data of Ws are reported in the Table 3.4 below (in  $\mu\text{M} \pm \text{SD}$ ).

BA	Ws (a) ( $\mu\text{M}$ )	BA	Ws (a) ( $\mu\text{M}$ )
CDCA	32 $\pm$ 4	CA	273 $\pm$ 10
INT-747	9 $\pm$ 1	INT-777	99 $\pm$ 7
INT-767	hs	T-CA	hs
INT -1213	hs	T-INT-777	hs
INT-855	15 $\pm$ 3	GCA	32 $\pm$ 3
INT-930	<0.02	G-INT-777	1700 $\pm$ 20
INT-1212	120 $\pm$ 9	INT 1244	hs
T- INT-1212	hs	INT-2021	hs
T-CDCA	hs	INT-2023	hs
G-CDCA	7 $\pm$ 1	INT-2024	290 $\pm$ 15
DCA	28 $\pm$ 2	UDCA	7 $\pm$ 1

*a Ws: water solubility refers to BA as protonated species*

*hs: high solubility*

### 3.2.3. Octanol/Water Partition Coefficient

The 1-octanol/water partition coefficient was measured for the ionized species to facilitate the comparison between the carboxyl and sulphate BA since the latter do not protonate even at very low pH values.

#### **Synthetic analogues of 6-Ethyl-CDCA:**

INT-747 and INT-855 (respectively 2.5 and 2.9) present a slightly higher lipophilicity with respect to other dihydroxy BA such as UDCA and CDCA. The increased lipophilicity is the result of the introduction of an ethyl group in position 6. The increase is even higher for INT-855 due to the presence of a C23-Methyl group. The tendency of these analogues to distribute in a lipid domain is therefore higher.

The logP of carbamate analogue INT-930 (4.0) was much higher than all the compounds, indicating that this compound accumulates preferentially in lipid domains. This is due to the side chain modification with the introduction of a relatively large moiety and without any charged group.

#### **Synthetic sulphonate and sulphate analogues of 6-Ethyl-CDCA:**

The INT-767 shows a logP of 2.0, a value slightly lower than INT-747 and natural CDCA and UDCA analogues, and this accounts for the contribution of the sulphate group and side chain. INT-767 has a tendency to accumulate in a lipid domain like INT 747, DCA, INT-930 and INT-855.

The sulphate analogue INT-1213 (2.3) shows a lipophilicity higher than INT-767, due to the presence of the methyl group in C23, but was still in a range of expected values according to the chemical structure.

#### **Synthetic carboxylated analogues of 6-Ethy-CA:**

The carboxylated analogue INT-777, with three hydroxyl groups in positions 3 $\alpha$ , 7 $\alpha$  and 12 $\alpha$ , and a C-23 Methyl shows a slightly higher lipophilicity with respect to the natural analogue CA. This is the result of the presence of an ethyl group in position C-6 and a methyl group in position C-23.

**Synthetic sulphonates and sulphate analogues of 6Ethyl-CA:**

The low Log P values of sulphonate and sulphate analogues of 6Ethyl-CA such as INT-1244 ,INT-2023,, and INT-2021 show a lower lipophilicity than the similar compound analogues of 6Ethyl-CA like INT-767 as a result of the presence of one additional hydroxyl group (three  $\alpha$ -OH groups in 3, 7 and 12) in the steroid rings.

**Synthetic carboxylates analogues of CDCA and CA containing a 16 $\beta$ - hydroxyl:**

The LogP of the carboxylated analogue INT-1212 (1.6), with three hydroxyl groups in positions 3 $\alpha$ , 7 $\alpha$  and 16 $\beta$  , indicates a slightly higher lipophilicity with respect to the natural analogue CA due to the presence of the ethyl in position C-6. This difference is likely due to the uncommon position of the 16 $\beta$  hydroxyl group, considering that position 12 $\alpha$  does not appear to play a major role in the detergency properties.

The carboxylated analogue which presents the highest hydrophilicity was INT-2024 (-0.05) which is a derivative of cholic but with an extra hydroxyl group in 16 $\beta$  .

**Taurine and glycine conjugated analogues:**

T-CDCA, T-INT-1212, T-INT-777 and G-INT-777 present LogP values of, respectively, 0.9, 0.3, -0.2 and 0.3. These values suggest that the taurine and glycine conjugated analogues preferentially stay in a water domain and the modification in the structure does not change their hydrophilicity.

In general, BA with a LogP <1 are hydrophilic and poorly absorbed by the intestine via a passive mechanism. Glycine and Taurine conjugated BA, despite having a low LogP(A-), are absorbed in the ileum not passively but via an active mechanism recognized by specific transporters independently from their physico-chemical properties.

Novel BA with uncommon side chain structure and a logP<1 are nor absorbed paasively and eventually must be subjected to an additional in vivo study to evaluate if they can be absorbed by an active mechanism. BA with a LogP(A-) >3 are highly lipophilic and thus potentially toxic even at low concentrations since they can accumulate in a lipid domain within target tissues and cells. All data of LogP(A-)<sub>A</sub><sup>-</sup> are summarized in the Table 3.5 below ((LogP = Log<sub>10</sub> ([BA]<sub>1-octanol</sub>/[BA]<sub>water</sub>)  $\pm$  SD).

BA	LogP <sub>A</sub> <sup>(d)</sup>	BA	LogP <sub>A</sub> <sup>(d)</sup>
CDCA	2.2 ± 0.2	CA	1.1 ± 0.2
INT747	2.5 ± 0.3	INT-777	1.4 ± 0.2
IN-T767	2.0 ± 0.1	T-CA	-0.5 ± 0.1
INT-1213	2.3 ± 0.2	T-INT-777	-0.2 ± 0.1
INT-855	2.9 ± 0.2	G-CA	-0.4 ± 0.1
INT-930	4.0 ± 0.3	G-INT-777	0.3 ± 0.1
INT-1212	1.6 ± 0.1	INT-1244	0.7 ± 0.1
T-INT-1212	0.3 ± 0.1	INT-2021	0.7 ± 0.1
T-CDCA	0.9 ± 0.1	INT-2023	0.6 ± 0.1
G-CDCA	0.4 ± 0.1	INT-2024	-0.05 ± 0.1
DCA	2.6 ± 0.2	UDCA	2.2 ± 0.1

*d* LogP<sub>A</sub><sup>(d)</sup>: 1-octanol-water partition coefficient of the studied BA as ionized species.

### 3.2.4. Albumin Binding

#### **Synthetic analogues of 6-Ethyl-CDCA:**

INT-747 (96%) presents a strong interaction with albumin quite similar to natural dihydroxy BA like CDCA and UDCA, suggesting similar kinetics in the hepatic uptake. INT-747 presents a relatively low unbound fraction and we expected that when absorbed by the intestine the compound will reach the liver via portal vein and a relatively high quantity will reach serum concentration via spill over as a result of a relatively low first pass clearance; however its behavior is similar to natural unconjugated analogs.

#### **Synthetic sulphate and sulphate analogues of 6-Ethyl-CDCA:**

The sulphate analogue INT-767 present a strong interaction with albumin quite similar to natural dihydroxy BA like CDCA and UDCA, suggesting similar kinetics in the hepatic uptake. INT-767 presents a low unbound fraction and its serum concentration is therefore higher as a result of a relatively low first pass clearance, and its behavior is similar to natural analogs.

The percent albumin binding of INT-1213 (97%) is slightly higher than that of INT-767 (85%) as a result of the addition of the methyl group in position C-23.

**Synthetic carboxylated analogues of 6-Ethy-CA:**

The percent albumin binding of INT-777 (62%) was comparable than CA (70%).

**Synthetic sulphonates and sulphate analogues of 6Ethyl-CA:**

The percent albumin binding of INT-1244, INT-2021, and INT-2023 sulphonate analogue) were similar to natural taurine conjugated BA analogues.

**Synthetic carboxylates analogues of CDCA and CA containing a 16 $\beta$ - hydroxyl:**

The percent albumin binding of INT-2024 and INT-1212 don't showed problem as the results obtained are comparable with the natural BA.

**Taurine and glycine conjugated analogues:**

For all taurine conjugate analogues studied, such as T-INT-777 and T-INT1212, the albumin binding is approximately 80% similarly to natural occurring BA . Similarly for G-INT-777.

All of these compounds presented an albumin binding compatible with a relatively fast hepatic uptake, similar to naturally occurring BA.

The structural modification in the sulphate and sulphonate analogues do not modify the albumin binding and therefore we expected that these compounds exhibit a PK similar to common BA. All data of albumin binding (%) are summarized in the Table 3.6 below (in %  $\pm$  SD).

BA	Albumin binding (%)	BA	Albumin binding (%)
CDCA	96 $\pm$ 2	CA	70 $\pm$ 1
INT-747	96 $\pm$ 3	INT-777	62 $\pm$ 2
INT-767	85 $\pm$ 2	T-CA	82 $\pm$ 3
INT-1213	97 $\pm$ 1	T-INT-777	81 $\pm$ 1
INT-855	97 $\pm$ 1	G-CA	65 $\pm$ 1
INT-930	99 $\pm$ 2	G-INT-777	71 $\pm$ 2
INT-1212	83 $\pm$ 3	INT-1244	81 $\pm$ 1
T- INT-1212	86 $\pm$ 1	INT-2021	74 $\pm$ 2
T-CDCA	70 $\pm$ 2	INT-2023	71 $\pm$ 2
G-CDCA	85 $\pm$ 1	INT-2024	47 $\pm$ 3
DCA	95 $\pm$ 1	UDCA	94 $\pm$ 2

### 3.2.5. Critical micellar pH

The CMpH value of INT-747 is similar to that of CDCA and lower than UDCA. According to this value, INT-747 does not present problems of intestinal solubility and requires a pH of 7.6 which is physiological to go in solution in a micellar phase. For example, UDCA with a CMpH of 8.4 requires a higher alkalization of the duodenal content and is solubilized in a micellar phase only in the post-prandial phase.

Analogues with three or four hydroxyl groups like INT-777, INT-2024 and INT-1212 have similar values to the CA so do not present problems of intestinal solubility.

INT-767, INT-1213, INT-2021, INT-2023 and taurine conjugated BA having a sulphate group do not present these problems since they are always soluble in the physiological pH from 2 to 9 as the pKa is very low and the compound is not protonated to form insoluble molecule.

The data show that, when administered in their acid form, the carboxylated analogues INT-2024, INT-855, INT-747, INT-777 and INT-1212 remain insoluble in the gastric content at a low pH and go into solution to form the salt (anion) once excreted into the duodenum due to the higher pH of the pancreatic and duodenal fluids. In the bile, they remain in solution, eventually forming micelles with other lipids.

To summarize, we avoid compounds characterized by a very low solubility in protonated form and with a high CMC if their pKa is 5. This is common for natural unconjugated BA while for sulphate or sulphonate analogues having a very low pKa and a high solubility in a wide range of pH, this is not a problem.

All The CMpH values are summarized in the table 3.7 below.

BA	CMpH	BA	CMpH	BA	CMpH
CDCA	7	CA	6.5	INT-2023	-
INT-747	7.2	INT-777	6.1	INT-2024	6.3
INT-767	-	T-CA	-	UDCA	8.4
INT-1213	-	T-INT-777	-	T-CDCA	-
INT-855	-	G-CA	6.3	G-CDCA	6.4
INT-930	-	G-INT-777	3.9	DCA	7.3
INT-1212	6.7	INT-1244	-		
T- INT-1212	-	INT-2021	-		

### 3.3. Conclusions

The previous extensive study of many naturally occurring BA and structurally modified BA allows us to understand that minor modifications in the BA molecule are able to modify their physico-chemical properties and on turn to target the molecule to a given organ and therefore playing a role in their pharmacokinetics, metabolism and activity.

For example, modifications in side chain structure (length, other modifications) determine the detergent-like properties while modifications in number, position, orientation of -OH and other groups play a role in the hydrophobic/hydrophilic balance.

We have selected the physico-chemical properties that properly define BA behaviour in aqueous solutions and in biological fluids and are appropriate to predict:

- a) Water solubility (protonated specie): Problems of formulation and solubility in the intestinal content (low pH).
- b) CMC (critical micellar concentration): Toxicity, membrane structure modification, surface tension lowering capacity, interaction and aggregation with lipids, proteins.
- c) Critical micellar pH: Solubility at different pH (gastric juice, intestinal content)
- d) Lipophilicity (LogP O/W partition coefficient): Predicts the efficiency of intestinal absorption, body fluid distribution and toxicity.
- e) Albumin binding: related to the blood transport and hepatic uptake.

The Table 3.8 below summarizes the functions of BA, the organic sector and important physico-chemical properties.

Table 3.8: Physico-chemical properties of the studied analogues and naturally occurring BA.

BA	Ws (a) ( $\mu\text{M}$ )	CMC(b) 0.15 M Na <sup>+</sup> (mM)	ST <sub>CMC</sub> Dyne/cm	CMpH	LogP <sub>A<sup>-</sup></sub> (d)	pKa	Albumin binding (%)
CDCA	32	3	45.5	7	2.2	5	96
GCDCA	7	2	45.2	6.4	0.4	3.9	85
TCDCA	hs	3	47	-	0.9	<1	70
DCA	28	3	50.2	7.3	2.6	5	95
UDCA	7	10	50.5	8.2	2.2	5	94
CA	273	9	49	6.5	1.1*	5	70
TCA	hs	4	51	-	-0.5	<1	82
GCA	32	8	48.8	6.3	-0.4	3.9	65
INT-767	hs	1.3	47.9	-	2.0	<1	85
INT-747	9	2.9	48.8	7.2	2.5	5	96
INT-1244	hs	2.8	43.4	-	0.7	<1	81
INT-1213	hs	Not available	Not available	-	2.3	5	97
INT-1212	120	5.9	52.4	6.7	1.6	<1	83
T- INT-1212	hs	2.7	43.6	-	0.3	<1	86
INT-855	15	-	-	-	2.9	5	97
INT-930	<0.02	Not determined	Not determined	-	4	<1	99
INT-2021	hs	5.6	38.3	-	0.7	-	74
INT-2023	hs	2.6	42.6	-	0.6	<1	71
INT-2024	290	6.3	43.2	6.3	-0.05	5	47
INT777	99	2	50.1	6.1	1.4	5	62
T-INT-777	hs	1.4	47.8	-	-0.2	<1	81
G-INT-777	1700	1.3	43.8	3.9	0.3	3.9	71

a Ws: water solubility refers to BA as protonated species

b CMC: Critical Micellar Concentration determined in 0,15 M NaCl water solution.

c ST<sub>CMC</sub>: Surface Tension at CMC in 0,15 M NaCl water solution.

d LogP<sub>A<sup>-</sup></sub>: 1-octanol-water partition coefficient of the studied BA as ionized species.



Summary of the chemical-physical parameters of BA in relation to the values obtained:

CMC	↓ Hydrophobic area ( $\beta$ face) ↑CMC (CDCA<CA<UDCA)
Transport and lipid solubilization (Bile)	↓Side chain length↑CMC
Intestinal absorption (Duodenal Juice)	↑Side chain length ↓ CMC Detergency of Taurine/Glycine BA (low CMC) > Free BA
Ws	Sulphonated/Sulphates/Taurine-BA soluble at all
Hepatic uptake (Serum)	physiological pH
Intestinal absorption (Duodenal Juice)	Glycine BA soluble at pH > 5.5 Free BA soluble at pH > 7.0
LogP	The LogP correlated with the rate and extent of ileal passive absorption :
Intestinal absorption (Duodenal Juice)	Taurine BA LogP $\leq 0$ impaired passive intestinal absorption.
Hepatic uptake (Serum)	Glycine BA LogP>0 compatible with a passive intestinal absorption.
Hepatic transport (Liver)	Free BA LogP > 1.0 passive intestinal absorption. BA LogP > 3.0 toxicity index
Albumin binding	The affinity of the BA for albumin is reduced by an increase in the polarity of the steroid ring. 3-OH BA<2-OH BA and Turo/Glyco BA < Free BA.
Hepatic uptake (Serum)	More BA will bind to albumin more the hepatic uptake will be high. More the affinity of the BA for albumin is high, more the hepatic uptake will be high.
CMpH	
Intestinal absorption (Duodenal Juice)	Required CMpH < 8.5

#### **4. PHARMACOKINETICS AND METABOLISM OF THE BA ANALOGUES: IV and ID single –dose administration to bile-fistula rat model.**

This study has been performed following the protocol and the animal model used in previous works for the study of a large amount of natural occurring BA and related synthetic analogues which allow us to define the relationship between physico-chemical properties and pharmacokinetics and metabolism in the rat (Aldini et al. 1996, 1996a, 1992a, 1992, 1990, 1989, 1982, 1981; Roda et al. 1993, 1988a, 1987, 1985; Montagnani et al. 1996). The role of side chain length and structure and the number, position and orientation of hydroxyls in determining the detergency, lipophilicity and in turn their intestinal absorption, hepatic uptake and metabolism has been previously well established and this facilitates the design of new organ specific analogues, with a PK adequate for their pharmacological activity (Pellicciari et al. 2009, 1989, 1985, 1984; Roda et al. 1995, 1995, 1994, 1990, 1989, 1988a, 1988, 1987; Clerici et al. 1992).

The first studied analogues INT-747 ( $EC_{50} = 0.1 \mu\text{M}$  determined by Alpha Screening FXR test), a potent FXR agonist now in phase 3 clinical trial in man, is an analogue of CDCA having an Ethyl group in six position. Thank to this modification the interaction with the FXR receptor was more potent than CDCA with a  $EC_{50} = 13 \mu\text{M}$  (Rizzo et al. 2010).

This structural modification does not play a role only in the receptor fitting but also in the BA physico-chemical properties and metabolism as previously described for other 6 substituted BA such as 6-Methyl-UDCA (Roda et al. 1995, 1995, 1994); the presence of a 6-Ethyl group sterically hinders the 7-dehydroxylation by dehydroxylases enzyme present in the intestinal bacterial, thus preventing the formation of potentially more toxic monohydroxy analogues. The 6-Ethyl group is shared by all the studied analogues since is important in determining the potency as agonist for FXR and also for TGR5 receptor, as more recently reported.

Modification in the side chain are also very important and profoundly modify the physico-chemical properties and the related PK as previously reported.

The presence of a 23-Methyl in the side chain prevents the first step in the conjugation with glycine and taurine in the liver i.e. the carboxyl CoA activation process by steric hindrance and in turn a Tauro-23-Methyl conjugate is highly stable toward cholyglycine hydrolases present in the intestinal bacteria again due to the lack of substrate specificity for these enzymes.

The role of conjugation with glycine and taurine is a metabolic prerequisite to reduce the lipophilicity of a BA to a critical value accounting for the possibility to be secreted into bile and conserved in the enterohepatic circulation.

If the amidation is prevented, a lipophilic BA could be excreted by the liver via formation of polar glucuronide not anymore preserved in the enterohepatic circulation.

To evaluate the PK and metabolism of synthetic BA, these BA analogues were administered both intra-duodenally (id) and intravenously(iv) at a dose of 1  $\mu\text{mol}/\text{min}/\text{kg}$  (1 hour infusion) and the choleric effect, biliary secretions rate and hepatic metabolism were evaluated in bile fistula rat model following the protocols previously used for natural BA and other synthetic analogues. These studies have been performed by Dott. Aldini group at the University Hospital S.Orsola, Bologna.

The quantitative determination of the compound in bile and its main metabolites after id administration allows to define the rate and extent of intestinal adsorption while after intravenous (iv) the hepatic uptake, metabolism can be defined. The two models are summarized in Figure 4.1 below.

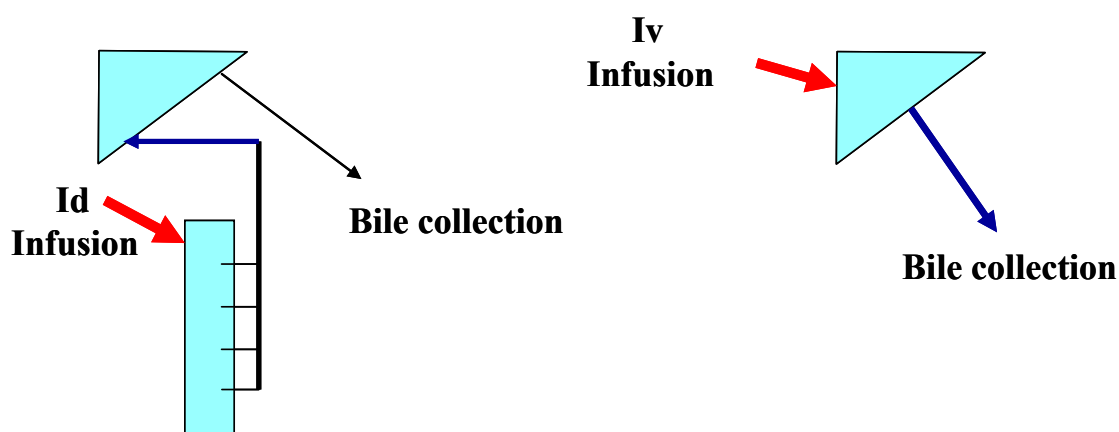


Figure 4.1: Bile fistula rat model after duodenal (id) and femoral (iv) administration

According to previously defined the administered compound will be secreted into bile unmodified and efficiently only if hydrophilic with a  $\text{LogP} < 1$  while, if lipophilic, it will be metabolized by the liver such as tauro and glyco conjugates.

Although the bile fistula model is the classical accepted model for the in vivo study of the intestinal absorption, the hepatic uptake, transport and biliary secretion are also involved and can somehow influence the absorption kinetics. Anyway the BA will be absorbed passively along the entire intestinal tract if the molecules are relatively lipophilic ( $\text{LogP}(\text{A}^-)$ ) similar to unconjugated natural analogues such as CDCA. An active carrier-mediated mechanism in the terminal ileum operates only for the corresponding taurine and glycine conjugates if they still have a structure similar to natural analogues such as TCDCA.

## **4.1. Material and methods**

### **4.1.1. Chemicals**

#### Natural BA:

Chenodeoxycholic acid (CDCA) and taurochenodeoxycholic acid (T-CDCA) were purchased from Sigma (St. Louis, MO).

All chemical structures are summarized in Table 3.1 in chapter 3.

#### Synthetic BA:

The present work has been carried out on the more recent BA analogues under study in the Bioanalytical laboratory that include: INT-2021, INT-2023, INT-2024, T-INT-1212, T-INT-777 and G-INT-777.

Data regarding INT-747, INT-767, INT-777, INT-1244, INT-1212, INT-855 and INT-1057 previously developed and fully characterized are also included for a more comprehensive interpretation of the structure-activity relationship.

All the molecules have been synthesized, purified in the laboratory of Prof. Pellicciari (Institute of Pharmaceutical Chemistry, University of Perugia, Italy). All the experiments were carried out using the sodium salts of the synthesized BA if containing a side chain carboxyl group. The sodium salts were prepared by adding an equimolar

amount of NaHCO<sub>3</sub> to the aqueous suspension of the free acid, which was heated to 80°C, mixed in an ultrasound bath, and then solubilized in a suitable aqueous solvent for the infusion. All chemical structures are summarized in Table 3.2 in chapter 3.

#### **4.1.2. Duodenal infusion**

The protocol of the animal model and the experimental studies have been carried out by Dott.R. Aldini group, as a part of the collaboration with the Bioanalytical Laboratory.

All the analogues were administered by intraduodenal infusion via a non flexible stainless steel curved button-ended needle (18G) at a dose of 1 µmol/min/kg (1 hour infusion) to male Wistars-Han rats (body weight 240 ± 10 g) .

Bile was collected by a drainage via a siliconated catheter implanted in the common bile duct in preweighted tubes and blood was also collected from the femoral vein at 30 m in time intervals. Duodenal infusion started after 75 minutes steady state and continued for 60 minutes. Bile samples were collected every 15 minutes for 3 hours. Samples were stored at -20°C until analysis. The bile samples were weighed and the bile secretion rate was calculated and expressed as a µL/min/Kg b.w. Biliary secretion of analogues and their metabolites were expressed as µmoles/min/Kg b.w.

In addition, 3 control rats were treated with saline solution under the same conditions for time and sampling (duodenal control rats) and additional 3 rats were treated with CDCA and TCDCA under the same conditions for time and sampling.

#### **4.1.3. Intravenous infusion**

The analogues were administered at a dose of 1 µmol/min/kg (1 hour infusion) in a saline solution containing BSA 3% (w/v) to a group of 3 male Wistar-Han rats (body weights 240 ±10 g) via femoral vein cannulation (iv).

Femoral infusion started after 75 minutes steady-state and continued for 60 minutes. Bile samples were collected every 15 minutes for 3 hours. The bile samples were weighed and the bile secretion rate was calculated and expressed as a µL/min/Kg b.w. Biliary secretion of analogues and their metabolites was expressed as µmoles/min/Kg b.w.

In addition, 3 rats were treated with saline solution with 3% (w/v)BSA under the same conditions for times and sampling (femoral control rats) and other 3 rats were treated with CDCA and TCDCA under the same conditions for time and sampling .

## **4.2. Results and discussion**

### **4.2.1. Choloretic effect after id and iv administration**

The choloretic effect of the administration of analogues was evaluated in comparison to untreated bile fistula rats by measuring the amount of bile secreted and the effect of id and iv administration was compared.

As a further controls the effect was also compared with that produced by the administration of CDCA and TCDCA at equimolar dose.

The mean (n=3) bile maximum secretion rates ( $\mu\text{l}/\text{min}/\text{Kg} \pm \text{SD}$ ) after iv and id administration of analogues, CDCA, TCDCA and untreated rats are reported in the Table 4.1 below.

Data obtained in previous works on INT-747, INT-767, INT-777, INT-1244, INT-1212, INT-855 and INT-1075 have been reported in order to allow a comparison with similar new analogues as INT-2021, INT-2023, INT-2024, T-INT-1212, T-INT-777 and G-INT-777 have been included in the table for comparative evaluation.

BA administered	Maximum secretion	
	Bile flow ( $\mu\text{l}/\text{min}/\text{Kg}$ )	
	I.V.	I.D.
Natural BA and control rat		
CDCA	$63 \pm 3$	$65 \pm 5$
CONTROL	$50 \pm 1$	$50 \pm 3$
Synthetic analogues of 6-Ethyl-CDCA		
INT-747*	$83 \pm 2$	$70 \pm 2$
INT-855*	$60 \pm 4$	$61 \pm 6$
Synthetic sulphonate and sulphate analogue of 6-Ethyl-CDCA		
INT-767*	$65 \pm 2$	$58 \pm 3$
Synthetic carboxylated analogues of 6-Ethy-CA		
INT-777*	$130 \pm 2$	$115 \pm 1$
INT-1075*	$85 \pm 7$	-
Synthetic sulphonates and sulphate analogues of 6Ethyl-CA		
INT-1244*	$65 \pm 6$	$87 \pm 1$
INT-2021	$73 \pm 1$	$40 \pm 2$
INT-2023	$63 \pm 3$	$53 \pm 4$
Synthetic carboxylates analogues of containing a $16\beta$ - hydroxyl		
INT-1212*	$60 \pm 2$	$57 \pm 1$
INT-2024	$52 \pm 2$	$47 \pm 2$
Taurine and glycine conjugated analogues		
T-INT-777	$60 \pm 5$	$57 \pm 4$
T-INT-1212	$56 \pm 1$	$40 \pm 2$
G-INT-777	$64 \pm 4$	$60 \pm 3$
T-CDCA	$41 \pm 2$	$44 \pm 2$

(\*)Data obtained in previous works

The effect on bile flow due to the duodenal administration of the reference compound CDCA is reported. The infusion of CDCA, in comparison to the control rat, slightly increased the bile flow during id and iv administration.

**Synthetic analogues of 6-Ethyl-CDCA:**

INT-747 and INT-855 have been previously studied.

After iv administration INT-747 increases the bile flow reaching maximum levels of approximately 80  $\mu\text{l}/\text{min}/\text{Kg}$ . The induced bile flow after id administration is slightly lower than iv administration

After id and iv infusion of INT-855 do not modify the bile flow in respect to control animal.

None of them is cholestatic at the administered dose.

**Synthetic sulphonate and sulphate analogue of 6-Ethyl-CDCA:**

A series of side sulphate and sulphonate analogues of CDCA have been previously studied including:

INT-767 analogue with a side chain sulphate ester head.

INT-1213 analogue with a side chain sulphate ester head and a C23-Methyl group (no further developed).

The id and iv infusion of INT-767 slightly increases the bile flow rate and the effect is slightly higher after iv infusion.

None of them is cholestatic at the administered dose.

**Synthetic carboxylated analogues of 6-Ethyl-CA:**

The following analogues have been previously studied:

INT-777 a C6-Ethyl analogues of CA with a C23-Methyl (S).

INT-1075 a C6-Ethyl analogues of CA with a C23-Methyl (R).

The iv and id infusions of INT-777 significantly increased the bile flow rate reaching the highest values found in all the studied analogues as reported in table X. The effect is also much higher than that obtained after infusion of CA at the same dose.

The iv infusion of INT-1075 also increased the bile flow rate but this effect was significantly lower than that observed for the isomer INT-777.

INT-777 presented the most potent choleric effect and this is related to its structure; a methyl group in the C-23 position partially prevents conjugation and this molecule can undergo a cholehepatic shunt pathway, like that observed for nor-BA and C-23-Methyl



analogues of UDCA (previously studied in our laboratory (Clerici et al. 1992; Pellicciari et al. 1989, 1985, 1984; Roda et al. 1988a, 1987, 1988; Gioiello et al. 2012).

None of them is cholestatic at the administered dose.

#### **Synthetic sulphonates and sulphate analogues of 6-Ethyl-CA:**

A series of side sulphate and sulphonate analogues of 6-Ethyl-CA have been previously studied such as INT-1244 .

More recently INT-2021 a C23-Methyl sulphate of 6-Ethyl-CA and INT-2023 a sulphate analogue of 6-Ethyl-CA have studied in this work.

During infusion experiments INT-1244 presents a choleric effect, that is more evident after id infusion; INT-2021 and INT-2023 induces a slight choleresis only after iv administration.

None of them is cholestatic at the administered dose.

#### **Synthetic carboxylates analogues of CDCA and CA containing a 16 $\beta$ - hydroxyl:**

INT-1212 is a synthetic analogue containing C6-Ethyl and two hydroxyl group in C-3 $\alpha$  and C-16 $\beta$  position and INT-2024 a similar structure with one more hydroxyl in C-12 $\alpha$  position.

The results of binding assays indicate that the BA with C-16 $\beta$  hydroxyl present 10 times more activity on FXR than on TGR5. Moreover the 16 hydroxyl group is present in many natural occurring BA in fish and reptiles [29].

INT-2024 does not modify the bile flow both after id and iv infusions. This phenomenon could be due to its high hydrophilicity (LogP(A<sup>-</sup>) = -0.05) which makes it more similar to the conjugated BA, instead of the derivatives of CA.

None of them is cholestatic at the administered dose.

#### **Taurine and glycine conjugated analogues:**

The following Glycine and Taurine analogue have been studied:

Tau-INT777, a Taurine conjugate of C6-Ethyl analogues of CA with a C23-Methyl (S)

Gly-INT777, a Glycine conjugate of C6-Ethyl analogues of CA with a C23-Methyl (S)

Tau-INT-1212, a Taurine conjugate of C6-Ethyl analogues of CDCA with two hydroxyl group in C-3 $\alpha$  and C-16 $\beta$  position.

The induced bile flow after id and iv administrations of the reference compound TCDCA is similar to the control rat being at the administered dose not toxic.

The infusion of T-INT-777 and G-INT-777 induces a slight choleresis in respect to TCDCA and the effect is slightly higher after iv administration.

The choleresis after iv administrations of Tau-INT-1212 is similar to TCDCA and control rats and higher after iv infusion.

None of them is cholestatic at the administered dose.

#### 4.2.2. BA secretion rates and hepatic metabolism after id and iv administration

##### Synthetic analogues of 6-Ethyl-CDCA:

In previous research we studied the biliary secretion after iv and id administration of CDCA. After iv administration the compound is efficiently secreted in bile, completely metabolized to its taurine conjugated form; the same is observed after id administration: the maximum secretion rate is slightly lower, but the total recovery calculated by the AUC is similar to that after iv administration.

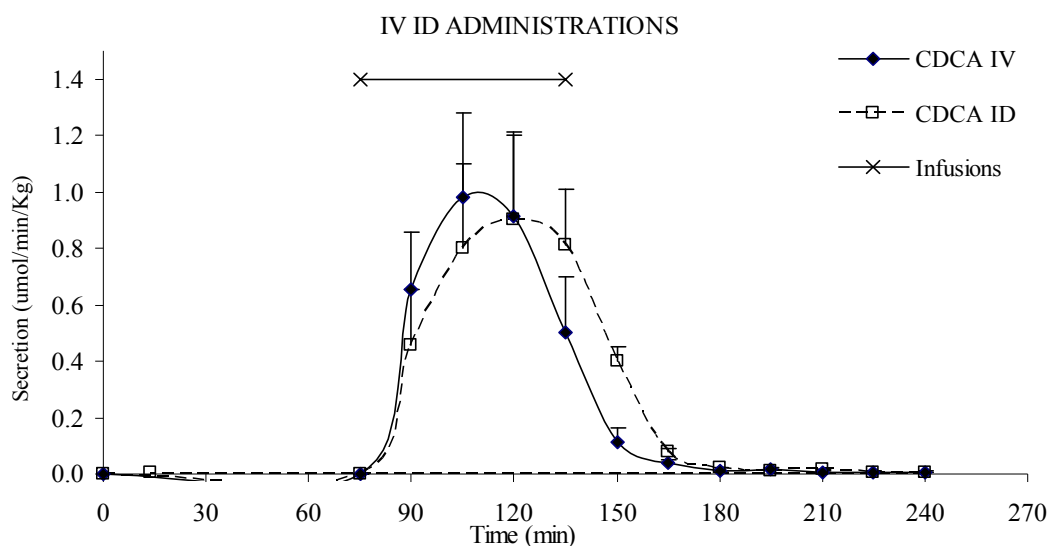
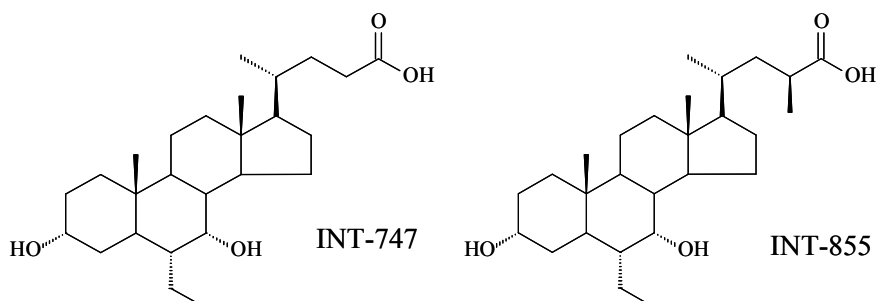


Figure 4.2: Mean secretion rates versus time of CDCA in femoral (n = 3) and duodenal (n = 3) experiments administered at a dose of 1  $\mu\text{mol/kg/min}$  for 1 hour. Standard deviations are also reported.

This compound is fully metabolized since it presents a relatively high lipophilicity and the conjugation with taurine renders the molecule much more hydrophilic and therefore able to be secreted into bile.



Similarly to CDCA it has been previously reported that INT-747 is efficiently secreted in bile after iv administration, primarily as taurine conjugate. The maximum secretion rate is achieved at 120-150 minutes, just at the end of the infusion period (the 60 minutes-infusion begins after 75 minutes of steady state). The maximum secretion rate is 0.96  $\mu\text{mol/kg/min}$ , close to the maximum achievable according to the administered dose of 1  $\mu\text{mol/kg/min}$  (an example of the profiles of INT-747 is shown in Figure 4.3 below).

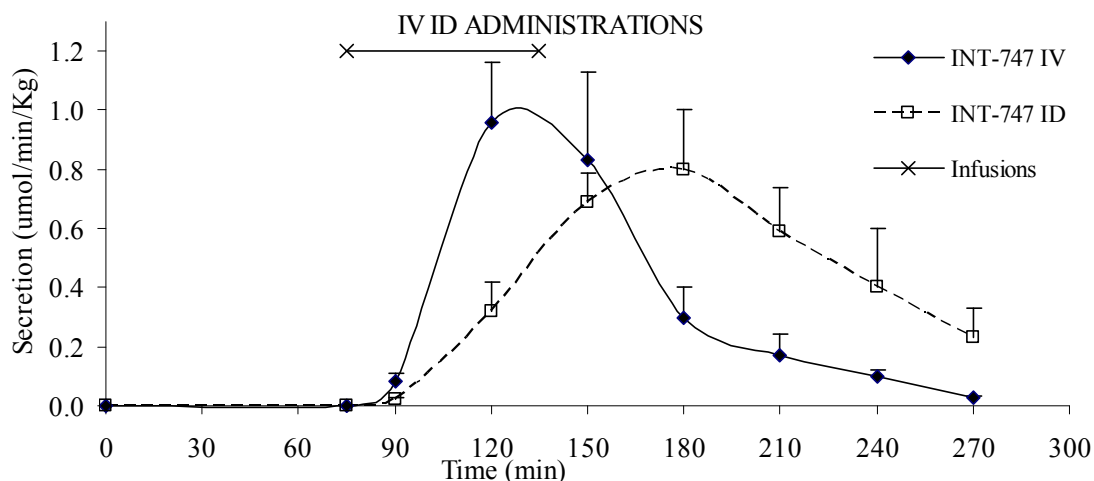


Figure 4.3: Mean secretion rates versus time of INT-747 in femoral ( $n = 3$ ) and duodenal ( $n = 3$ ) experiments administered at a dose of 1  $\mu\text{mol/kg/min}$  for 1 hour. Standard deviations are also reported.

It had previously reported that the behaviour of INT-747 is similar to that of natural dihydroxy BA such as CDCA or UDCA, which are efficiently secreted into bile only as

taurine conjugates since they have relatively high lipophilicity with LogP(A<sup>-</sup>) values similar to CDCA or even higher. Differently, trihydroxy BA such as cholic acid can be also partially secreted as such in unconjugated form thanks to the relatively lower LogP as a result of one more hydroxyl. Moreover the extent of BA secretion in the unmodified form is related to its lipophilicity and administered dose, and it is species-dependent.

In a previous studies the PK and metabolism has been carefully evaluated and the main achieved results are summarized.

The kinetics of the biliary secretion after iv administration and the extent of albumin binding suggest that the hepatic uptake and secretion of INT-747 is quite similar to that of natural analogues like CDCA and the rate of hepatic secretion is related to that of taurine conjugation mediated by a CoA activation and hepatic taurine availability. As previously shown the preferential conjugation with taurine is peculiar for the rat; in other animal species (pig, hamster, rabbit) and in man this compound is preferentially conjugated with glycine and only to a less extent with taurine .

According to these data, liver uptake and secretion of INT-747 are efficient and its recovery in bile as a taurine conjugated is almost complete.

The hepatic metabolism of INT-747 produces mainly the taurine conjugated form similarly to CDCA having a similar side chain structure The taurine conjugation process appears efficient at the administered dose. Traces (less than 0.02%) of glycine conjugate are also present, and a small amount of INT-747 (in the order of 0.1-0.3%) is secreted in bile in unconjugated form.

After id infusion INT-747 like CDCA is secreted into bile as taurine conjugate and its recovery is almost complete, similarly to that observed after iv infusion. The maximum secretion rate is achieved at 180 minutes (i.e., 60 minutes after the end of infusion). The maximum secretion rate is 0.80  $\mu\text{mol/kg/min}$ , slightly lower than that measured after iv infusion as a results of the dilution effect in the intestine due to the administration by duodenal infusion. The taurine conjugation appears efficient at the administered dose. Trace amounts (less than 0.2%) of the compound are also conjugated with glycine and a similar amount is secreted as such in bile.

It has been previously reported that the biliary secretion kinetics of the analogue INT855, a lipophilic molecule having a C-23 Methyl was quite different to CDCA and INT-747.

After iv and id administrations, INT-855 is secreted poorly or not secreted as such (0.0007 and 0.0003  $\mu\text{mol/kg/min}$ , respectively after iv and id administration) in bile and the only metabolite identified so far in bile is a glucuronide derivative (0.01 or 0.009  $\mu\text{mol/kg/min}$ , respectively after iv and id administration) and to a much less extent as a taurine conjugate (0.0025 and 0.0020  $\mu\text{mol/kg/min}$ , respectively after iv and id administration).

The glucuronide formation is the rate limiting step allowing the partial recovery of the compound in bile with presumably high intrahepatic concentration.

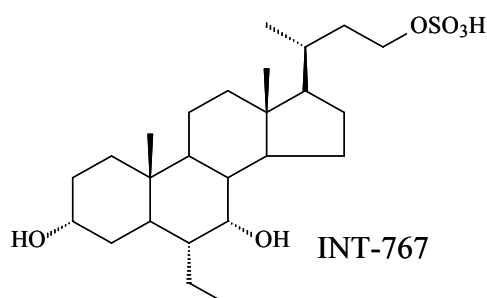
INT855 presents peculiar ADME and PK differences from other CDCA analogues. This molecule is highly lipophilic ( $\text{LogP(A-)} = 2.9$ ) and cannot be secreted in bile as such. Similarly CDCA and INT-747 were not recovered as such in bile but the efficient side chain taurine conjugation allowed to recover these compounds into bile almost completely as taurine conjugated in rat.

The 23-Methyl group almost completely prevents the conjugation pathway and the INT-855 needs to be conjugated by an alternative pathway in order to be excreted into bile. The glucuronide conjugation is the main metabolite recovered in bile. Moreover the recovery of this compound is very low suggesting that the compound will be retained by the liver and slowly secreted into bile.

We expected that at higher doses or under sub-chronic administration this compound could be slightly toxic to liver cells.

These basic studies together with previously carried out in Prof. Roda's Lab allows to design new analogues with a suitable pharmacokinetic and metabolism to distribute in the target organ as required to act on the molecular target so far identified.

**Synthetic sulphonate and sulphate analogues of 6-Ethyl-CDCA:**



Other CDCA analogues have been previously designed with the rationale to modify the side chain structure replacing the carboxyl group with a sulphate ester or a sulphonate group trying to mimic the structure of a taurine conjugate in term of acidic character of the molecule, having these derivative a very low pKa similarly to the taurine conjugated analogues.

After iv infusion of INT-767 a fast appearance in bile is observed accounting for a rapid hepatic uptake and secretion of the compound as such but the maximum secretion rate is lower that CDCA and INT-747.

In the id experiments the secretion rate is slower as a result of the poor intestinal absorption resulting by the relatively low LogP(A<sup>-</sup>).

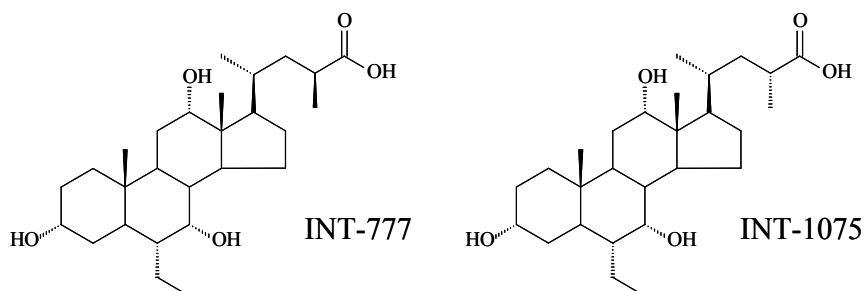
These data show that INT-767 is still absorbed by the intestine, efficiently taken up by the liver and promptly secreted into bile partially unmodified and partially metabolized to a glucuronide conjugate.

In the id infusion the glucuronide derivative formation is much less than the iv experiments in which the glucuronide is present in a concentration similar to intact INT-767. In the iv experiment a higher intrahepatic concentration of INT-767 is reached as a result of an efficient hepatic uptake of INT-767. The higher intrahepatic concentration requires an increased glucuronidation process to facilitate the secretion of the compound in bile as a mechanism of toxicity prevention. Under this condition a larger amount of INT-767 is present as a glucuronide.

In conclusion the presence of the sulphate group in the side chain facilitates the biliary secretion of the molecule as such, unmodified, in respect to CDCA which is fully taurine conjugated. As a consequence, INT-767 could accumulate in the liver cells

causing toxicity since its hepatic residence time depends upon the rate of amidation with taurine and glycine or the elimination as such or by alternative metabolic pathways.

**Synthetic carboxylated analogues of 6-Ethy-CA:**



As a part of the previous structure-activity relationship program developed in the laboratory, analogues of CA all containing the 6-Ethyl were synthesized and admitted to the complete physico-chemical and biological screening.

The first analogue developed in 2008 was INT-777.

The biliary secretion of INT-777 after iv administration was efficient and the compound was recovered in bile unmodified at a relatively high percentage (80-90%) of the administered dose.

The kinetic secretion profile indicates that INT-777 was efficiently taken up by the liver and secreted in bile largely unmodified and to a lesser extent (10%) as 23 Methyl isomer conjugated with taurine (T-INT-1075).

The discovery of the INT-777 isomerization was very important in the structure-activity relationship studies and the metabolite (INT-1075) was synthesized and admitted to this study (Pellicciari et al. 2009).

After id administration the recovery of INT-777 in bile was lower than after iv administration suggesting that the compound is not efficiently absorbed by the intestine. Taking into account the physico-chemical properties of INT-777, we expected that this compound would be moderately absorbed by a passive diffusion mechanism ( $\text{LogP}(A^-) = 1.44$ ) and that an active mechanism was not involved.

When the isomer INT-1075 was administered, the kinetic profile of the compound showed that it was metabolized by the liver more extensively than INT-777. The compound is secreted in bile as such and as taurine conjugate. With respect to its

diastereoisomer INT-777, the percentage of conjugation is higher (30-40%) and the maximum secretion rate of the unconjugated form is lower (60-70%).

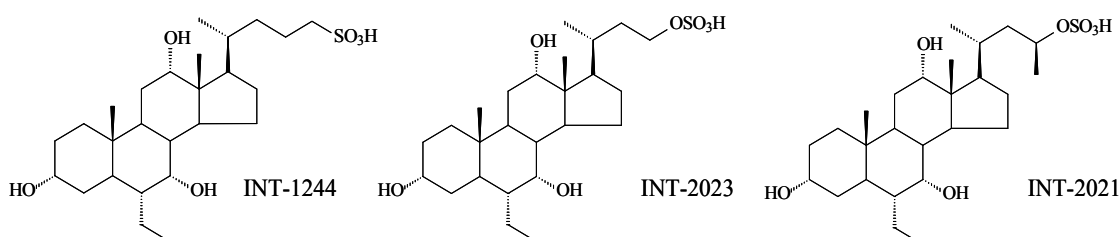
The authors of the study suggest that the C-23(R) isomer (INT-1075) presents a side chain geometry and Methyl orientation more suitable for the amidation process compared to the isomer (S) which is secreted as the unconjugated (INT-777) form at a higher percentage (80-90%). The conjugation with taurine contributes to the improved INT-1075 recovery in bile which is approximately 70% to 80% of the administered dose. Other minor metabolites, including glucuronides, have been identified in bile in trace amount but the formation of glucuronides could become relevant if the molecule is administered at higher doses.

From these previous studies the role of side chain structure and hydroxyl substituents has been further clarified and it has proved very useful to design the more recent molecules studied in the present work.

The presence of the methyl group in the C-23 position hinders the physiological conjugation process with taurine and glycine which is relevant for efficient secretion of almost all naturally occurring carboxylated BA. This is crucial for lipophilic dihydroxy-BA and to a lesser extent for trihydroxy-BA.

The presence of three hydroxyl groups allows the molecule to be efficiently taken up by the liver and secreted into bile. In addition, the 6-Ethyl group prevents the intestinal bacteria 7-dehydroxylation as observed previously for 6-Methyl substituted BA [17].

#### **Synthetic sulphonates and sulphate analogues of 6Ethyl-CA:**



The biliary secretion of INT-1244, has been previously studied. More recently INT-2023 and INT-2021 have been studied.

INT-2023 and INT-2021 after iv administration were efficiently taken up by the liver and almost completely secreted and recovered in bile as shown for INT-2023 and INT-2021 (Figure 4.4 and 4.5 below).



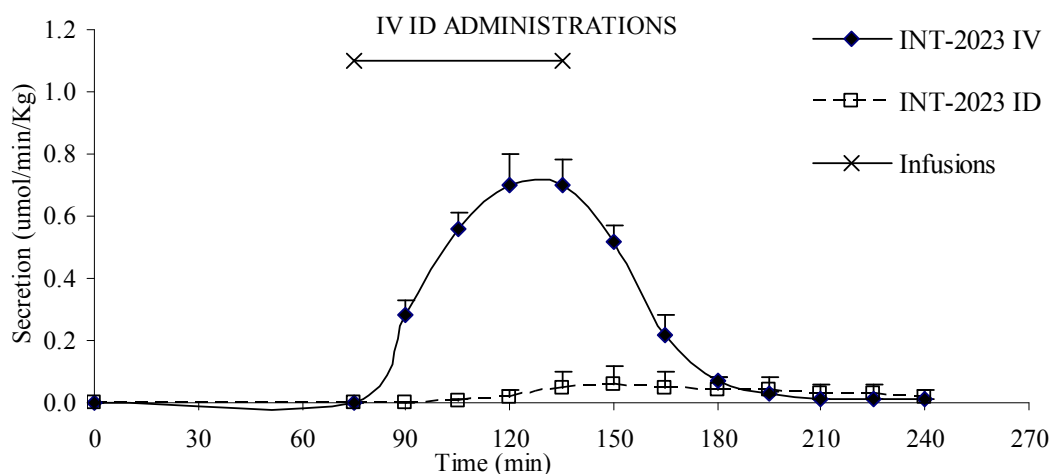


Figure 4.4: Mean secretion rates versus time of INT-2023 in femoral ( $n = 3$ ) and duodenal ( $n = 3$ ) experiments administered at a dose of  $1 \mu\text{mol/kg/min}$  for 1 hour. Standard deviations are also reported.

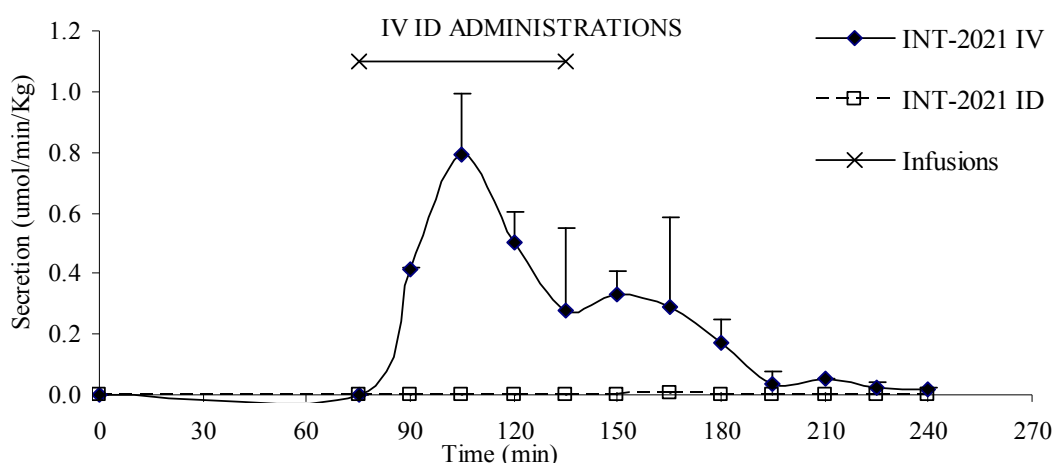


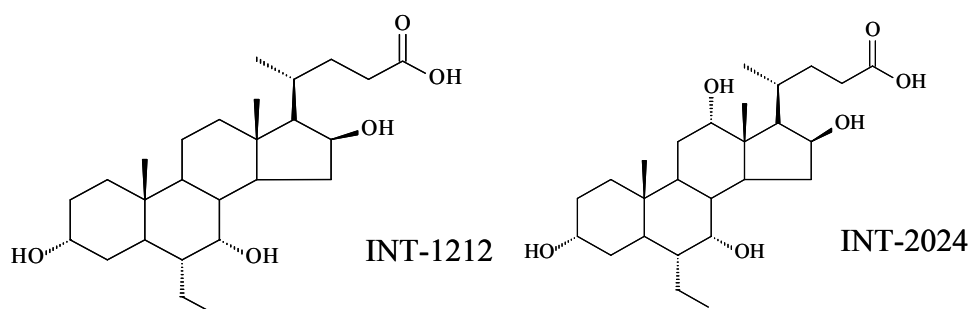
Figure 4.5: Mean secretion rates versus time of INT-2021 in femoral ( $n = 3$ ) and duodenal ( $n = 3$ ) experiments administered at a dose of  $1 \mu\text{mol/kg/min}$  for 1 hour. Standard deviations are also reported.

The kinetic profiles indicate that the analogues were efficiently taken up by the liver and secreted in bile as such without hepatic metabolism. On the contrary, after id administration (orally) the recovery in bile was much lower suggesting that the compounds are poorly absorbed by the intestine.

The compounds are secreted in bile unmodified both after iv and id administration. According to the physico-chemical properties, we expected that these compounds would be poorly absorbed by the intestine through a passive diffusion mechanism. Their low

partition coefficient in octanol/water  $\text{LogP}(A^-)$  (0.7 for INT-1244 and INT-2021 and 0.6 for INT-2023) accounts for these results, since these values should be higher than 1 for reasonable passive diffusion possibility. Moreover, an active mechanism mediated by intestinal transporters like that occurring for the hydrophilic taurine conjugated BA did not seem to be involved.

**Synthetic carboxylates analogues of containing a 16 $\beta$ -hydroxyl:**



It has been reported that INT-1212, after iv infusion, was extensively metabolized by the liver to form the taurine conjugate and was secreted into bile partially in this form and also unmodified. The conjugation with taurine improved its recovery in bile which is approximately 70% of the administered dose. The INT-1212 molecule behaved similarly to CA, as it can be secreted as such (CDCA can be secreted into bile only conjugated with taurine) and, despite the methyl group in the C-23 position, INT-1212 can be partially amidated.

The INT-1212 biliary secretion after id administration was lower than after the iv experiments, suggesting that the intestinal absorption of the molecule is not efficient like other BA. This molecule undergoes hepatic metabolism like naturally occurring BA with similar physico-chemical properties such as lipophilicity ( $\text{LogP}(A^-) = 1.6$ ).

After both iv and id administration experiments the main metabolite found was INT-1212 conjugated with taurine but in different percentages in fact after iv administration INT-1212 is present in bile 70% as tauro and 30% as free bile acid while after id administration we find it 70% and 30% respectively as free and tauro-conjugated form.

The biliary secretion of INT-2024 (an example of the profiles of INT-2024 is shown in Figure 4.6 below) after iv administration was efficient and the compound was recovered in bile at a relatively high percentage (80-90%) of the administered dose.

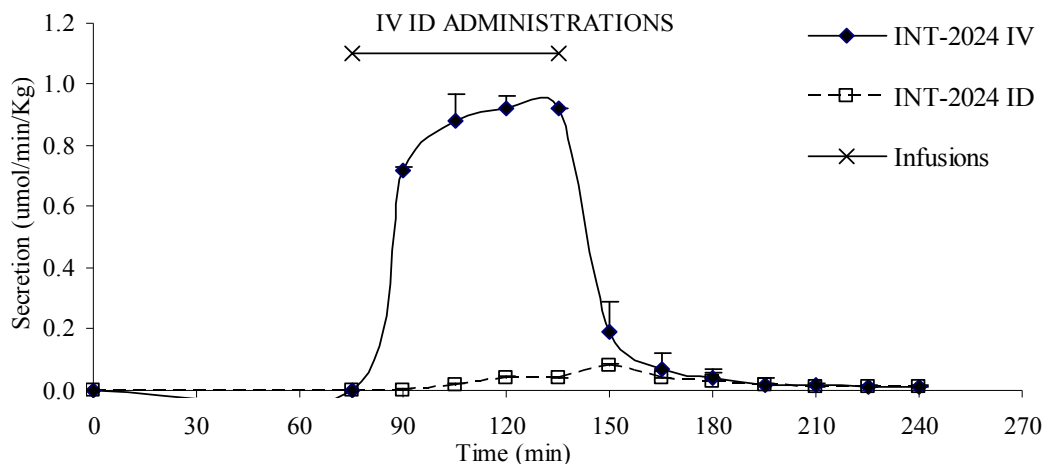
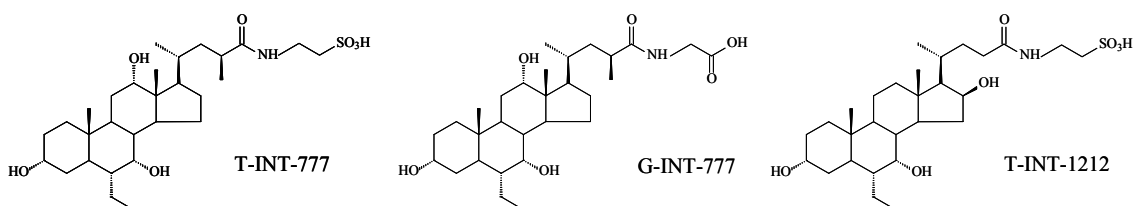


Figure 4.6: Mean secretion rates versus time of INT-2024 in femoral ( $n = 3$ ) and duodenal ( $n = 3$ ) experiments administered at a dose of  $1 \mu\text{mol/kg/min}$  for 1 hour. Standard deviations are also reported.

The kinetic profile indicates that INT-2024 was efficiently taken up by the liver and secreted in bile mainly unmodified and also, to a lesser extent (10%) conjugated with taurine (data are reported in section 2.2.4.). No other metabolites have been identified in bile maybe because of the high hydrophilicity of this compound compared with INT-1212.

After id administration the recovery in bile for INT-2024 was lower than the recovery after iv administration suggesting that the compound is not efficiently absorbed by the intestine. We expected that INT-2024 would be absorbed by active mechanism ( $\text{LogP(A-)} = -0.05$ ) which is a derivative of CA but with an additional hydroxyl group in  $16\beta$  which breaks the lipophilicity of BA  $\beta$  face.

#### Taurine and glycine conjugated analogues:



When the natural BA (T-CDCA) and related analogues (T-INT-777, G-INT-777 and T-INT-1212) were iv administered as taurine or glycine conjugates, the recovery in bile was almost complete and similar to that of trihydroxy BA and no additional metabolites have been found. (Profiles of T-INT-777 and G-INT-777 are shown in Figure 4.7 and 4.8 below).

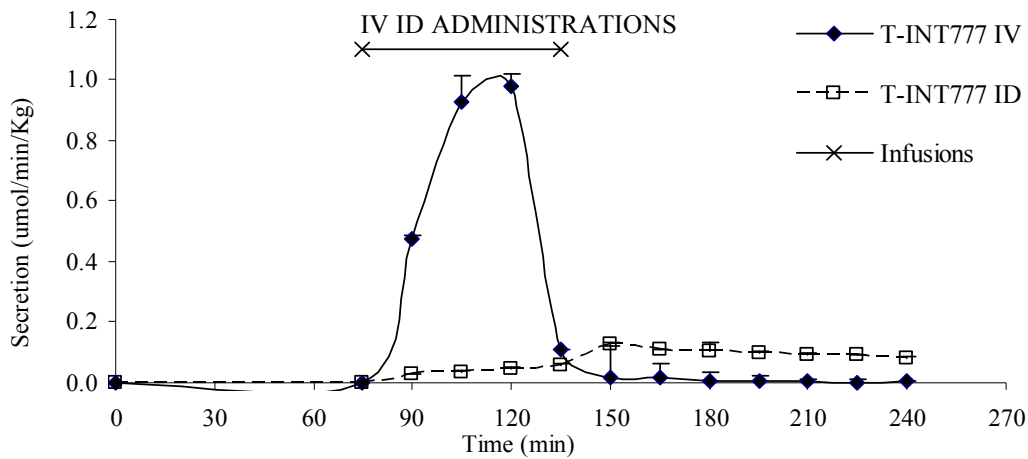


Figure 4.7: Mean secretion rates versus time of T-INT-777 in femoral ( $n = 3$ ) and duodenal ( $n = 3$ ) experiments administered at a dose of  $1 \mu\text{mol/kg/min}$  for 1 hour. Standard deviations are also reported.

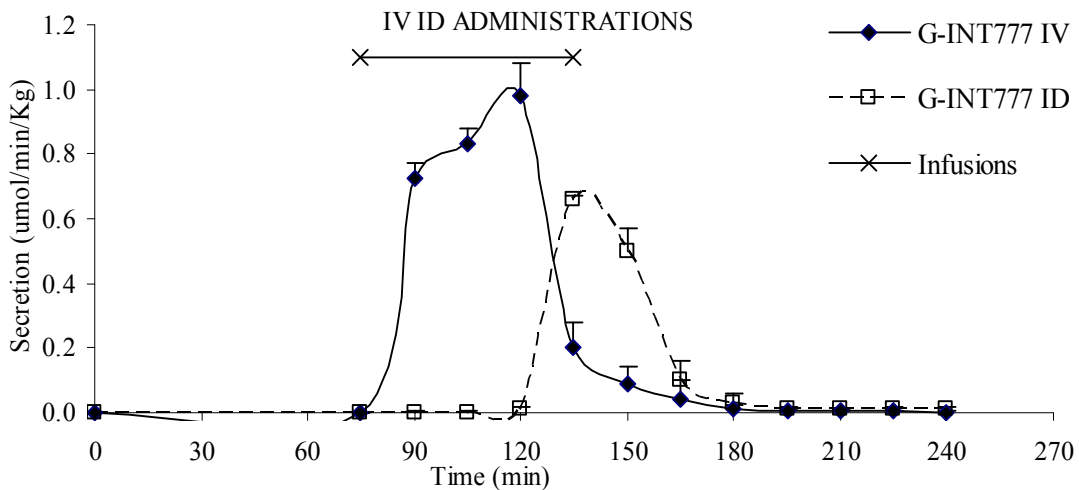


Figure 4.8: Mean secretion rates versus time of G-INT-777 in femoral ( $n = 3$ ) and duodenal ( $n = 3$ ) experiments administered at a dose of  $1 \mu\text{mol/kg/min}$  for 1 hour. Standard deviations are also reported.

T-CDCA, T-INT-777, G-INT-777 and T-INT-1212 are secreted into bile unmodified

both after iv and id administration..

The relatively low recovery after id infusions, for T-CDCA, T-INT-777 and T-INT-1212, is due to the mode of absorption : only in the ileum by an active mechanism peculiar to the taurine/glycine conjugated BA.

The good recovery after id infusion for G-INT-777 is due to the mode of absorption. The glycine conjugates have a rather efficient active absorption in the ileum but they are liable also of passive diffusion in all the intestine.

Table 4.3. summarize the main metabolites so far identified for the studied BA.

Administered BA	Hepatic metabolism in rat	
	I.V.	I.D.
Natural BA		
CDCA	T-CDCA(95%)>> CDCA(5%)	T-CDCA(95%)>> CDCA(5%)
Synthetic analogues of 6-Ethyl-CDCA		
INT-747*	T-INT-747(99.7%) >> INT-747(0.3%)	T-INT-747(99.7%) >> INT-747(0.3%)
INT-855*	GLUC-INT-855(75%) >> T-INT-855(18%) > INT-855(7%)	GLUC-INT-855(75%) >> T-INT-855(18%) > INT-855(7%)
Synthetic sulphonate and sulphate analogue of 6-Ethyl-CDCA		
INT-767*	INT-767(60%) > GLUC-INT-767(40%)	INT-767(75%) > GLUC-INT-767(25%)
Synthetic carboxylated analogues of 6-Ethy-CA		
INT-777*	INT-777(90%) >> T-INT-1075(10%)	INT-777(70%) > T-INT-1075 (30%)
INT-1075*	INT-1075(70%) > T-INT-1075(30%)	-
Synthetic sulphonates and sulphate analogues of 6Ethyl-CA		
INT-1244*	NONE	NONE
INT-2021	NONE	NONE
INT-2023	NONE	NONE
Synthetic carboxylates analogues of containing a 16 $\beta$ - hydroxyl		
INT-1212*	T-INT-1212(70%) >> INT-1212(30%)	T-INT-1212(30%) < INT-1212(70%)
INT-2024	INT-2024(90%) >> T-INT-2024(10%)	INT-2024(50%)=T-INT-2024 (50%)
Taurine and glycine conjugated analogues		
T-INT-777	NONE	NONE
T-INT-1212	NONE	NONE
G-INT-777	NONE	NONE
T-CDCA	NONE	NONE

(\*)Data obtained in previous works

### 4.3. Conclusions

Bile secretion increases during infusion of all BA studied as a result of BA-dependent flow. The modulation of bile flow depends on the amount of BA secreted into bile and on the qualitative composition of bile induced by their secretion and metabolism.

Synthetic sulphonates and sulphate analogues of CA (INT-2023, INT-2021 and INT-1244) and CDCA (INT-767) showed a moderate or absent choleric effect. Only INT-2021 shows a choleric effect maybe due to the presence of the methyl group at C<sub>23</sub>, that, preventing the amidation, facilitates the ductular absorption and recycling via the chole-hepatic shunt pathway pumping bicarbonate and water into bile.

This phenomenon is shared by all the carboxylated BA with a C-23 Methyl group such as INT-2021, INT-777 and INT-1075.

When administered as taurine or glycine conjugates, they show a weaker choleric effect; this is particularly evident for dihydroxy BA (T-CDCA and T-INT-1212) and, to a lesser extent, for trihydroxy BA (T-INT-777 and G-INT-777). Their hydrophilicity is much higher than that of the respective unconjugated BA due to the polar characteristics of the amide bond and the sulphonic acid terminal group (fully ionized and more hydrated) which is not balanced by the increased length of the side chain. As a result, they do not follow a cholehepatic shunt pathway and their retention in the liver cell is shorter than the corresponding unconjugates showing a very fast hepatic transit time.

Considering these findings, the induced bile flow of unconjugated BA seems highly related to the amount of unconjugated forms reabsorbed via a cholehepatic shunt. This is reasonable for the dihydroxy BA which can diffuse passively and for the 23-Methyl analogues.

The structural modification profoundly modify the pharmacokinetics and metabolism in respect to the natural analogues CDCA and CA. We can summarize some important features observed in these studies for these bile acid analogs:

- Higher stability toward bacteria metabolism since the bacterial 7-dehydroxylation process is almost absent due to the steric hindrance of the ethyl group in six position.

- The presence of the methyl group in the C-23 (S) position of INT-777 partially prevents conjugation with taurine in respect to his isomer INT-1075; due to its low lipophilicity however the molecule can be efficiently secreted unmodified.
- Unconjugated trihydroxy BA analogues are more hydrophilic than dihydroxy BA analogues and this accounts for their lower recovery in bile after id administration due to lower intestinal absorption as documented by the lower LogP values.
- For lipophilic dihydroxy BA analogues the hepatic conjugation step appears essential for biliary secretion. Carboxylated BA with a conventional side chain length and structure are amidated with taurine and glycine and secreted in bile. Modification in the side chain length and the introduction of a 23-Methyl group prevent conjugation with a retention of the molecule in the liver and activation of alternative conjugation pathways to allow their secretion into bile and preventing their potential hepatic toxicity.
- Taurine/Glycine conjugated analogues are secreted in bile as such with a fast kinetic profile . These analogues are not metabolized either in the live or in the intestine. Glycine conjugates analogues could be absorbed via active and passive (if relatively lipophilic) mechanisms while taurine conjugated bile acid analogues only by active mechanism in the ileum. The use of these analogues could be limited by the potential poor intestinal absorption also possibly due to a competition in the transport with the natural BA.
- The presence of the sulphonate group in the side chain facilitates the biliary secretion in respect to the same synthetic carboxylated analogues. The synthetic sulphonated analogues can be secreted as such and additionally as glucuronide derivates. Moreover their intestinal absorption by passive diffusion is limited by the relatively high hydrophilicity.



## 5. REFERENCES

- Aldini R., Barbara L., Benelli A., Borzatta V., Geminiani S., Mascellani G., Morselli A.M., Roda A., Roda E., Effects of a salt of cholestiramine and 2-[4-(p-chlorobenzoyl)phenoxy]2-methyl propionic acid (alpha-1081) on biliary lipid secretion in rats, *British Journal Of Pharmacology*, 74, 3, 611-617, **1981**.
- Aldini R., Montagnani M., Roda A., Hrelia S., Biagi P.L., Roda E., Intestinal absorption of bile acids in the rabbit, different transport rates in jejunum and ileum, *Gastroenterology*, 110, 459-468, **1996a**.
- Aldini R., Roda A., Lenzi P., Ussia G., Vaccari C., Bile acid active and passive ileal transport in the rabbit, effect of luminal stirring, *European Journal Of Clinical Investigation*, 22, 744-750, **1992a**.
- Aldini R., Roda A., Lenzi P.L., Calcaterra D., Vaccari C., Calzolari M., Festi D., Mazzella G., Roda E., Cantelli Forti G., Hepatic uptake and biliary secretion of bile acids in the perfused rat liver, *Pharmacological Research*, 25, 51-61, **1992**.
- Aldini R., Roda A., Montagnani M., Cerrè C., Pellicciari R., Roda E., Relationship between structure and intestinal absorption of bile acids with a steroid or side chain modification, *Steroids*, 61, 590-597, **1996b**.
- Aldini R., Roda A., Montagnani M., Cerrè C., Pellicciari R., Roda E., Relationship between structure and intestinal absorption of bile acids with a steroid or side chain modification, *Steroids*, 61, 590-597, **1996**.
- Aldini R., Roda A., Labate A.M., Cappelleri G, Roda E., Barbara L., Hepatic bile acid uptake: effect of conjugation, hydroxyl and keto groups, and albumin binding, *Journal Lipid Research*, 23, 1167-1173, **1982**.
- Aldini R., Roda A., Labate A.M., Grigolo B., Simoni P., Roda E., Barbara L., Species differences of the hepatic uptake of bile acids, *Italian Journal of Gastroenterology*, 19, 1-4, **1986**.
- Aldini R., Roda A., Simoni P., Lenzi P., Roda E., Uptake of Bile Acids by perfused Rat liver, evidence of a structure-activity relationship, *Hepatology*, 16, 10, 840-845, **1989**.
- Aldini R., Ussia G., Roda A., Grilli Cilioni C., Rizzoli R., Calcaterra D., Roda E., Casanova S., Lenzi P., Festi D., Mazzella G., Bazzoli F., Vaccari M.C.,

- Galletti G., Evaluation of the ileal absorption capacity for bile acids in the rabbit, *European Surgical Research*, 22, 93-100, **1990**.
- Aldini R., Roda A., Grigolo B., Paselli L., Morselli A. M., Roda E., Barbara L., Species differences in the hepatic uptake of bile acids, *American Journal Of Physiology*, **1984**.
  - Almè B., Bremmelgaard A., Sjøvall J., Thomassen P., Analysis of metabolic profiles of bile acids in urine using a lipophilic anion exchanger and computerized GC-MS, *Journal Of Lipid Research*, 18, 339-362, **1977**.
  - Ananthanarayanan M., Von Dyppe P., Levy D., Identification of the hepatocyte Na<sup>+</sup> dependent bile acid transport protein using monoclonal antibodies, *Journal Of Biological Chemistry*, 263, 8338-8343, **1988**.
  - Angelin B., Einarsson K., Hellstrom K., Evidence for the absorption of bile acids in the proximal small intestine of norma- and hyperlipidaemic subjects, *Gut*, 17, 420-425, **1976**.
  - Batta A.K., Salen G., Arora R., Shefer S., Batta M., Person A., Side chain conjugation prevents bacterial 7-dehydroxylation of bile acids, *Journal Of Biological Chemistry*, 265, 10925-10928, **1990**.
  - Batta A.K., Salen G., Shefer S., Substrate specificity of cholyglycine hydrolysis of bile acid conjugates, *Journal Of Biological Chemistry*, 259, 15035-15039, **1984**.
  - Cabral. D.J. Small D.M., Lilly H.S., Hamilton J.A., Transbiliary movement of bile acids in model membranes, *Biochemistry*, 26, 1801-1804, **1987**.
  - Carey M.C., Measurement of the physico-chemical properties of bile salt solutions. In *Bile Acids in Gastroenterology*, **1983**.
  - Carey M. C., Igimi H., Physico-chemical basis for dissimilar intraluminal solubilities and intestinal absorption efficiencies of chenodeoxycholic and ursodeoxycholic acids. In *Bile Acids and Lipids*. G. Paumgartner A. Stiehl, and W. Gerok, editors. MTP Press Limited, Lancaster, England. 123-132, **1981**.
  - Cavrini V., Gatti R., Roda A., Cerrè C., Roveri P., HPLC-fluorescence determination of bile acids in pharmaceuticals and bile after derivatization with 2-bromoacetyl-6-methoxynaphthalene, *Journal Of Pharmaceutical And Biomedical Analysis*, 11, 761-770, **1993**.

- Chawla, A., Repa, J. J., Evans, R. M., Mangelsdorf, D. J., Nuclear receptors and lipid physiology, opening the X-files, *Science*, 294, 1866-1870, **2001**.
- Chen, W., Owsley, E., Yang, Y., Stroup, D., Chiang, J. Y., Nuclear receptor-mediated repression of human cholesterol 7 $\alpha$ -hydroxylase gene transcription by bile acids, *Journal of Lipid Research*, 42, 402-412, **2001**.
- Clerici C., Dozzini G., Distrutti E., Gentili G., Sadeghpour B.M., Natalini B., Pellicciari R., Rizzoli R., Roda A., Pelli M.A., Morelli A., Effect of intraduodenal administration of 23-methyl-UDCA diastereoisomers on bile flow in hamsters. *Digestive Diseases and Sciences*, 37 (5), 791-798, **1992**.
- Costantino G., Macchiarulo A., Entrena-Guadix A., Camaioni E., Pellicciari R., Binding mode of 6ECDCA, a potent bile acid agonist of the farnesoid X receptor (FXR), *Bioorganic & Medicinal Chemistry Letters*, 13, 1865–1868, **2003**.
- Cowen A. E., Korman M. G., Hofmann A. F., Thomas P. J., Plasma disappearance of radioactivity, after intravenous injection of labeled bile acids in man, *Gastroenterology*, 68, 1567-1573, **1975**.
- Cui J., Huang L., Zhao A., Lew J.L., Yu J., Sahoo S., Meinke P.T., Royo I., Pelaez F., Wright S.D., Guggulsterone is a farnesoid X receptor antagonist in coactivator association assays but acts to enhance transcription of bile salt export pump, *Journal Of Biological Chemistry*, 278, 10214–10220, **2003**.
- Czuba B., Vessey D.A., Structural characterization of choly-CoA, glycine/taurine N-acyl-transferase and a covalent substrate intermediate, *Journal Of Biological Chemistry*, 261, 6260-6263, **1986**.
- Czuba B., Vessey D.A., The effect of bile acid structure on the activity of bile acid-CoA, glycine/taurine N-acyl-transferase, *Journal Of Biological Chemistry*, 257, 8761-8765, **1982**.
- Dietschy J.M., Mechanisms for the intestinal absorption of bile acids, *Journal of Lipid Research*, 9, 297-309, **1968**.
- Downes M., Verdecia M.A., Roecker A.J., Hughes R., Hogenesch J.B., Kast-woelbern H.R., Bowman M.E., Ferrer J.L., Anisfeld A.M., Edwards P.A., Rosenfeld J.M., Alvarez J.G., Noel J.P., Nicolaou K.C., Evans R.M., A

- chemical, genetic, and structural analysis of the nuclear bile acid receptor FXR, *Molecular Cell*, 11, 1079–1092, **2003**.
- Dussault I., Beard R., Lin M., Hollister K., Chen J., Xiao J.H., Chandraratna R., Forman B.M., Identification of gene-selective modulators of the bile acid receptor FXR, *Journal Of Biological Chemistry*, 278, 7027–7033, **2003**.
  - Evans, R. M., The steroid and thyroid hormone receptor superfamily, *Science*, 240, 889, **1988**.
  - Evans M.J. et al. A synthetic farnesoid X receptor (FXR) agonist promotes cholesterol lowering in models of dyslipidemia, *American Journal Of Physiology-Gastrointestinal And Liver Physiology*, 296, G543–552, **2009**.
  - Fini A., Roda A., Fugazza R., Grigolo B., Chemical properties of bile acids. III. Bile acid structure and their solubility in water, *Journal of Solution Chemistry*, 8, 595-603, **1985**.
  - Fini A., Roda A., Chemical properties of bile acids. IV. Acidity constants of glycine-conjugated bile acids, *Journal of Lipid Research*, 28, 755-759, **1987**.
  - Fini A., De Maria P., Roda A., Chemical properties of bile acids. Part II, pKa values in water and methanol of some hydroxy bile acids, *European Journal Of Medicinal Chemistry*, 5, 467-470, **1982**.
  - Fiorucci S., Baldelli F., Farnesoid X receptor agonists in biliary tract disease, *Current Opinion In Gastroenterology*, 25, 252–259, **2009a**.
  - Fiorucci S., Mencarelli A., Palladino G., Cipriani S., Bile-acid-activated receptors, targeting TGR5 and farnesoid-X-receptor in lipid and glucose disorders, *Trends in Pharmacological Sciences*, 30, 570–580, **2009**.
  - Fitzgerald M. L., Moore K. J., Freeman M. W., Nuclear hormone receptors and cholesterol trafficking, the orphans find a new home, *Journal Of Molecular Medicine*, 80, 271-281, **2002**.
  - Francis G. A., Fayard E., Picard F., Auwerx J., Nuclear receptors and the control of metabolism., *Annual Review Physiology*, 65, 261-311, **2003**.
  - Gioiello A., Rosatelli E., Nuti R., Macchiarulo A., Pellicciari R., Gioiello A., Rosatelli E., Nuti R., Macchiarulo A., Pellicciari R., *Expert Opinion on Therapeutic Patents*, 22, 12, 1399-414, **2012**.

- Goole J., Lindley D.J, Roth W, Carl SM, Amighi K, Kauffmann JM, Knipp GT., The effects of excipients on transporter mediated absorption, *International Journal of Pharmaceutics*, 30, 393, 17-31, **2010**.
- Griffiths WJ, Crick PJ, Wang Y., Methods for Oxysterol Analysis, Past, Present and Future, *Biochemical Pharmacology*, 13, 81-6, **2013**.
- Gurantz, D., Hofmann A. F., Influence of bile acid structure on bile flow and biliary lipid secretion in the hamster, *American Journal of Physiology*, **1984**.
- Hagenbuch B., Stieger B., Foguet M., Lubbert H., Meier P.J., Functional expression cloning and characterization of the hepatocyte Na<sup>+</sup>/bile acid cotransport system, *Proceedings of the National Academy of Sciences of the United States of America*, 88, 10629-10633, **1991**.
- Hagey L.R., Bile acid biodiversity in vertebrates, chemistry and evolutionary implications., *Ph.D. Thesis*, University of California, San Diego, **1992**.
- Hagey L.R., Hofmann A.F., 5 $\alpha$ /5 $\beta$  isomerization during enterohepatic cycling, bile acids of 5 dragons (Amigdae), *Hepatology*, 22, A425, **1995**.
- Hagey L.R., Schteingart C.D., Ton-Nu H.-T., Hofmann A.F., Biliary bile acids of fruit pigeons and doves (Columbiformes), presence of 1 $\beta$ -hydroxy-chenodeoxycholic acid and conjugation with glycine as well as taurine, *Journal of Lipid Research*, 35, 2041-2048, **1994**.
- Haslewood G.A.D., The biological utility of bile salts., North Holland Publishing Co., Amsterdam, **1978**.
- Hedenborg G., Norman A., Ritzen A., Lipoprotein-bound bile acids in serum from healthy men, postprandially and during fasting. *Scandinavian Journal of Clinical Laboratory Investigation*, 48, 817-824, **1988**.
- Hofmann A. Mysels K., *Colloids Surf.*, 30,145–173, **1988**.
- Hofmann A.F., Bile acids, in *The Liver, Biology and Pathobiology*, Third edition, Arias I.M., Boyer J.L., Fausto N., Jakoby W.B., Schachter D.A., Shafritz D.A. Eds., Raven Press Ltd, New York, p. 677-718, **1994**.
- Hofmann A.F., Enterohepatic circulation of bile acids, in *Handbook of Physiology. The Gastrointestinal System* , vol 111, Schultz S.G., Forte J.G., Rauner B.B. Eds., Bethesda, 567-596, **1989**.

- Hofmann A.F., Roda A., Physico-chemical properties of bile acids and their relationship to biological properties, an overview of the problem, *Journal Lipid Research*, 25,1477-89, **1984**.
- Houck K.A. et al. T0901317 is a dual LXR/FXR agonist., *Molecular Genetics and Metabolism*, 83, 184–187, **2004**.
- Houten S. M., Watanabe, M., Auwerx J., Endocrine functions of bile acids, *The EMBO journal*, 25, 1419–25, **2006**.
- Huijghebaert S.M., Hofmann A.F., Influence of amino acid moiety on deconjugation of bile acid amidates by cholyglycine hydrolase or human fecal cultures, *Journal of Lipid Research*,, 27, 742-752, **1986**.
- Kamada S., Maeda M., Tsuji A., Umezawa Y., Kurahashi F., Separation and determination of bile acids by high-performance liquid chromatography using immobilized 3 $\alpha$ -hydroxysteroid dehydrogenase and an electrochemical detector, *Journal of Chromatography*, 239, 773-783, **1982**.
- Karlaganis, G., Schwarzenbach R.P., Paumgartner G., Analysis of serum bile acids by capillary gas-liquid chromatography-mass spectrometry, *Journal of Lipid Research*, 21, 377, **1980**.
- Kast H.R. et al. Farnesoid X-activated receptor induces apolipoprotein C-II transcription, a molecular mechanism linking plasma triglyceride levels to bile acids, *Molecular Endocrinology*, 15, 1720–1728, **2001**.
- Katsuma S. et al. Bile acids promote glucagon like peptide-1 secretion through TGR5 in a murine enteroendocrine cell line STC-1, *Biochemical and Biophysical Research Communications*, 329, 386–390, **2005**.
- Kawamata Y. et al. A G protein-coupled receptor responsive to bile acids, *Journal Of Biological Chemistry*, 278, 9435–9440, **2003**.
- Killenberg P.G., Measurement and subcellular distribution of choloyl-CoA synthetase and bile acid-CoA,amino acid N-acyltransferase activities in rat liver, *Journal of Lipid Research*, 19,24-31, **1978**.
- Kirsi A. et al. Functional brown adipose tissue in healthy adults, *The New England Journal of Medicine*, 360, 1518–1525, **2009**.

- Kramer W., Bickerl U., Busher H.P., Gerok W., Kurtz G., Bile salt binding polypeptides in plasma membranes of hepatocytes revealed by photoaffinity labeling, *European Journal of Biochemistry.*, 129, 13-24, **1982**.
- Lange V., Picotti P., Domon B., Aebersold R., Selected reaction monitoring for quantitative proteomics, a tutorial, *Molecular Systems Biology.*, 4, 222, **2008**.
- Lin M.C., Mullady E., Wilson F.A., Timed photoaffinity labeling and characterization of bile acid binding and transport proteins in rat ileum, *American Journal of Physiology*, 265, **1993**.
- Lin M.C., Weinberg S.L., Kramer W., Burckhardt G., Wilson F.A., Identification and comparison of bile acid binding polypeptides in ileal BAolateral membrane, *Journal of Membrane Biology*, 106, 1-11, **1988**.
- Ikononou M.G., Blades A.T., Kebarle P., Investigations of the electrospray interface for liquid chromatography mass spectrometry, *Analytical Chemistry*, 62, 957, **1990**.
- Ishii D., Murata S., Takeuchi T., Analysis of bile acids by micro high-performance liquid chromatography with post-column enzyme reaction and fluorimetric detection, *Journal of Chromatography*, 282, 569-577, **1983**.
- Lu T.T., Makishima M., Repa J.J., Schoonjans K., Kerr T.A., Auwerx J., Mangelsdorf D.J., Molecular Basis for feedback regulation of bile acid synthesis by nuclear receptors, *Molecular Cell*, 6, 507-515, **2000**.
- Mac Donald I.A., Bokkenheuser V.D., Winter J., Mc Leron A.M., Mosbach E.H., Degradation of steroids in the human gut, *Journal of Lipid Research*, 24, 675-700, **1983**.
- Macchiarulo A. et al. Molecular field analysis and 3D-quantitative structure-activity relationship study (MFA 3D-QSAR) unveil novel features of bile acid recognition at TGR5, *Journal of Chemical Information and Modeling.*, 48, 1792-1801, **2008**.
- Maloney P.R. et al. Identification of a chemical tool for the orphan nuclear receptor FXR, *Journal of Medicinal Chemistry*, 43, 2971-2974, **2000**.
- Marschall H.U., Egestad B., Matern H., Maern S., Sjdvall J., N-acetylglucosaminides. A new type of bile acid conjugate in man, *Journal Of Biological Chemistry*, 264, 12989-12993, **1989**.

- Maruyama T. et al. Identification of membrane-type receptor for bile acids (M-BAR), *Biochemical and Biophysical Research Communications*, 298, 714–719, **2002**.
- Matern H., Matern S., Formation of bile acids glucosides and dolichyl phosphoglucose by microsomal glucosyltransferase in liver, kidney and intestine of man, *Biochimica et Biophysica Acta*, 921, 1-6, **1987**.
- Mi L.Z. et al. Structural basis for bile acid binding and activation of the nuclear receptor FXR, *Molecular Cell*, 11, 1093–1100, **2003**.
- Montagnani M., Aldini A., Roda A., Caruso M.L., Gioacchini A.M., Lenzi P.L., Roda E., Species differences in hepatic bile acid uptake, Comparative evaluation of taurocholate and tauroursodeoxycholate extraction in rat and rabbit, *Comparative Biochemistry and Physiology* 113A, 157-164, **1996**.
- Mukerjee P., Mysels K. J., Critical micelle concentration of aqueous surfactant systems, NSRDS-NB-36 U.S. Government Printing Office, Washington, DC **1971**.
- Mukerjee P., Moroi Y., Murata M., Yang A. Y. S., Bile salts as a typical surfactants and solubilizers, *Hepatology*, 4, 61-65, **1984**..
- Mysels K. J., Florence A. T., The effect of impurities on dynamic surface tension- for a valid surface purity criterion. *Colloid. Interface Science*, 43, 557-582. **1973**.
- Parks D.J., Blanchard S.G., Bledsoe R.K., Chandra G., Consler T.G., Kliewer S. A., Stimmel J.B., Willson T.M., Zavacki A.M., Moore D.D., Lehmann J. M., *Science*, 284, 1365, **1999**.
- Pellicciari R., Cecchetti S., Natalini B., Roda A., Grigolo B., Fini A., Bile Acids with Cyclopropane containing Side Chain, I, Preparation and Properties of 3 $\alpha$ ,7 $\beta$ -Dihydroxy-22,23-Methylene-5 $\beta$ -cholan-24-oic acid, *Journal of Medicinal Chemistry*, 27, 746, **1984**.
- Pellicciari R., Cecchetti S., Natalini B., Roda A., Grigolo B., Fini A., Bile Acids with Cyclopropane containing side chain. II Synthesis and Properties of 3 $\alpha$ ,7 $\beta$ -Dihydroxy-22,23-Methylene 5 $\beta$ -cholan-24-oic acid-N-12- sulfoethyl Amide, *Journal of Medicinal Chemistry*, 28, 239-242, **1985**.



- Pellicciari R., Gioiello A., Macchiarulo A., Thomas C., Rosatelli E., Natalini B., Sardella R., Pruzanski M., Roda A., Pastorini E., Schoonjans K., Auwerx J., Discovery of 6 $\alpha$ -Ethyl-23(S)-methylcholic acid (S-EMCA, INT-777) as a potent and selective agonist for the TGR5 receptor, a novel target for diabetes, *Journal of Medicinal Chemistry*, 52, 7958-7961, **2009**.
- Pellicciari R., Natalini B., Roda A., Machado M.I.L., Marinozzi M., Preparation and Physico-chemical Properties of natural (23R) 3 $\alpha$ ,7 $\beta$ ,23- and (23R) 3 $\alpha$ 12 $\alpha$ ,23-trihydroxylated Bile Acids and their (23S)-Epimers, *Journal of the Chemical Society, Perkin Transactions 1*, 1289-1296, **1989**.
- Pellicciari R. et al. 6 $\alpha$ -Ethyl-chenodeoxycholic acid (6-ECDCA), a potent and selective FXR agonist endowed with anticholestatic activity, *Journal of Medicinal Chemistry*, 45, 3569–3572, **2002**.
- Pellicciari R. et al. Farnesoid X receptor, from structure to potential clinical applications, *Journal of Medicinal Chemistry*, 48, 5383–5403, **2005a**.
- Pellicciari R. et al. Nongenomic actions of bile acids. Synthesis and preliminary characterization of 23- and 6,23-alkyl-substituted bile acid derivatives as selective modulators for the G-protein coupled receptor TGR5, *Journal of Medicinal Chemistry*, 50, 4265–4268, **2007a**.
- Pellicciari R., Costantino G., Camaioni E., Sadeghpour B. M., Entrena A., Willson T. M., Fiorucci S., Bile acid derivatives as ligands of the farnesoid X receptor. Synthesis, evaluation, and structure-activity relationship of a series of body and side chain modified analogues of chenodeoxycholic acid, *Journal of medicinal chemistry*, 47(18), **2004a**.
- Pinkerton A.B. et al. Kalypsys, Inc. Heterocyclic modulators of TGR5, WO2008067222A1.
- Pinkerton, A.B. et al. Kalypsys, Inc. Heterocyclic modulators of TGR5, for treatment of disease, WO2008097976A1.
- Pinkerton, A.B. et al. Kalypsys, Inc. Quinazoline modulators of TGR5, WO2008067219A2.
- Pols T. W. H., Noriega L. G., Nomura M., Auwerx J., Schoonjans K., The bile acid membrane receptor TGR5 as an emerging target in metabolism and inflammation, *Journal of hepatology*, 54, 1263–72, **2011**.

- Porez G., Prawitt J., Gross B., Staels B., Bile acid receptors as targets for the treatment of dyslipidemia and cardiovascular disease, *Journal Of Lipid Research*, 53, 1–45, **2012**.
- Radomska-Pyrek A., Zimniak P., Irshaid Y.M., Lester R., Tephly T.R., St. Pyrek J., Glucuronidation of 6 $\alpha$ -hydroxy bile acids by human liver microsomes, *Journal of Clinical Investigation*, 80, 234-241, **1987**.
- Rizzo G., Passeri D., De Franco F., Ciaccioli G., Donadio L., Rizzo G., Orlandi S., Sadeghpour B., Wang XX, Jiang T., Levi M., Pruzanski M., Adorini L. Functional characterization of the semisynthetic bile acid derivative INT-767, a dual farnesoid X receptor and TGR5 agonist, *Molecular Pharmacology*, 78, 4, 617-30, **2010**.
- Roda A., Cappelleri G., Aldini R., Roda E., Barbara L., Quantitative aspects of the interaction of bile acids with human serum albumin, *Journal of Lipid Research*, 23,490-5, **1982**.
- Roda A., Pellicciari R., Cerrè C., Polimeni C., Sadeghpour B., Marinozzi M., Forti G.C., Sapigni E., New 6-substituted bile acids, physico-chemical and biological properties of 6 $\alpha$ -methyl ursodeoxycholic acid and 6 $\alpha$ -methyl-7-epicholic acid, *Journal of Lipid Research*, 35,2268-79, **1994**.
- Roda A., Aldini R., Grigolo B., Simoni P., Roda E., Pellicciari R., Lenzi P., Natalini B., 23-Methyl-3 $\alpha$ ,7 $\beta$ -dihydroxy-5 $\beta$ -cholan-24-oic acid, Dose-Response study of Biliary Secretion in Rat, *Hepatology*, 8, 1571-1576, **1988a**.
- Roda A., Aldini R., Grigolo B., Simoni P., Effect of Bile Acid structure on liver uptake and secretion in the Rat. In, "Recent Advances in Bile Acid Research", Ed. L. Barbara, R.H. Dowling, A.F. Hofmann, E. Roda, Raven Press, 49-57, **1985**.
- Roda A., Biliary secretion and metabolism of INT1103 in bile-fistula rat after duodenal (id) and jugular (iv) administration, *Report for Intercept pharmaceuticals*, **2008a**.
- Roda A., Biliary secretion and metabolism of INT-747 in bile-fistula rat after duodenal (id) and femoral (iv) administration, *Report for Intercept pharmaceuticals*, **2011**.

- Roda A., Cappelleri G., Aldini R., Roda E., Barbara L., Quantitative aspects of the interaction of bile acids with human serum albumin, *Journal of Lipid Research*, 23, 490-495, **1982**.
- Roda A., Cerrè C., Simoni P., Polimeni C., Vaccari C., Pistillo A., Determination of free and amidated bile acids by high-performance liquid chromatography with evaporative light scattering mass detection, *Journal of Lipid Research*, 33, 1393-1402, **1992**.
- Roda A., Fini A., Effect of Nuclear Hydroxy substituents on Aqueous Solubility and Acidic Strength of Bile Acids, *Hepatology*, 4, 72-76, **1984**.
- Roda A., Grigolo B., Aldini R., Simoni P., Pellicciari R., Natalini B., Balducci R., Bile Acids with a Cyclopropyl-containing Side Chain. IV. Physico-chemical and Biological Properties of the four Diastereoisomers of 3 $\alpha$ ,7 $\beta$ -dihydroxy-22,23-methylene-5 $\beta$ -cholan-24-oic Acid, *Journal of Lipid Research*, 28, 1384-1397, **1987**.
- Roda A., Grigolo B., Minutello A., Pellicciari R., Natalini B., Physico-chemical and biological properties of natural and synthetic C-22 and C-23 hydroxylated bile acids, *Journal of Lipid Research*, 31, 289-298, **1990**.
- Roda A., Grigolo B., Pellicciari R., Natalini B., Structure-activity relationship studies on natural and synthetic bile acid analogs, *Digestive Diseases And Sciences*, 34, 1-12, **1989**.
- Roda A., Grigolo B., Roda E., Simoni P., Pellicciari R., Natalini B., Fini A., Morselli Labate A.M., Quantitative Relationship between Bile Acid Structure and Biliary Lipid Secretion in Rat, *Journal of Pharmaceutical Science*, 77, 596-605, **1988**.
- Roda A., Hofmann A.F., Mysels K.J., The influence of bile salt structure on self-association in aqueous solutions, *Journal Of Biological Chemistry*, 258, 6362-6370, **1983**.
- Roda A., Pastorini E., Biliary secretion and metabolism of INT855 in bile-fistula rat after duodenal (id) and femoral (iv) administration, *Report for Intercept pharmaceuticals*, **2010**.

- Roda A., Pastorini E., Vecchiotti S., UPF1067, UPF1075. Pharmacokinetics and Metabolism in Bile-Fistula Rat after IV Administration Administrations, *Report for Intercept pharmaceuticals*, **2009a**.
- Roda A., Pastorini E., Vecchiotti S., UPF930, UPF1067, UPF1212, UPF1213, UPF1244. Physico-chemical Properties, In Vitro Metabolism, and Pharmacokinetics and Metabolism in Bile-Fistula Rat after IV and ID Administrations, *Report for Intercept pharmaceuticals*, **2009**.
- Roda A., Pellicciari R., Cerré C., Polimeni C., Sadeghpour B., Marinozzi M., Cantelli-Forti G., Sapigni E., New 6-substituted Bile Acids. Physico-chemical and biological properties of 6 $\alpha$ -Methyl-Ursodeoxycholic acid and 6 $\alpha$ -Methyl-7-Epicholic acid, *Journal of Lipid Research*, 12, 108-120, **1994**.
- Roda A., Pellicciari R., Polimeni, C., Cerré C., Cantelli-Forti G., Sadeghpour B., Sapigni E., Gioacchini A.M., Natalini B., Metabolism, Pharmacokinetics and activity of a new 6-fluoro analog of ursodeoxycholic acid in rat and hamster, *Gastroenterology*, 108, 1204-1214, **1995**.
- Roda A., Physico-chemical properties of 6-Ethyl Chenodeoxycholic Acid (INT 747) And 6-Ethyl 23-sulphate Chenodeoxycholic Acid (INT 1103), *Report for Intercept pharmaceuticals*, **2008**.
- Roda A., Simoni P., Cerré C., Polimeni C., Cipolla A., Analysis of bile, Method in biliary research., Muraca M. Ed., CRC Press, London, 123-139, **1995**.
- Roda E., Aldini R., Mazzella G., Festi D., Bazzoli F., Roda A., Hepatic secretion of bile acid. In, Hepatic transport and bile secretion, physiology and pathophysiology, Chap. 37, Raven Press Ltd., New York, 553-569, **1993**.
- Roda, A. Minutello, M. A. Angellotti, Fini. A., Bile acid structure-activity relationship, evaluation of bile acid lipophilicity using I-octanol/water partition coefficient and reverse phase HPLC, *Journal of Lipid Research*, 31, 1433-1443, **1990a**.
- Russell D.W., Setchell K.D.R., Bile acids biosynthesis, *Biochemistry*, 31, 4737-4749, **1992**.
- Sato H. et al. Novel potent and selective bile acid derivatives as TGR5 agonists, Biological screening, structure–activity relationships, and molecular modeling studies, *Journal of Medicinal Chemistry*, 51, 1831–1841, **2008**.

- Scagnolari F., Roda A., Fini A., Grigolo B., Thermodynamic feature of the interaction of bile acid with albumin, *Biochimica et Biophysica Acta*, 791, 274-277 **1984**.
- Scalia S., Group separation of free and conjugated bile acids by pre-packed anion-exchange cartridges, *Journal of Pharmaceutical and Biomedical Analysis*, 3, 235-241, **1990**.
- Scalia S., Pazzi P., Group separation of non-sulphated and 3-sulphated bile acids by disposable anion-exchange cartridges., *Chromatographia*, 30, 377-381, **1990a**.
- Schiff E.R., Small N.C., Dietschy J.M., Characterization of the kinetics of the passive and active transport mechanisms for bile acid absorption in the small Intestine and colon of the rat, *Journal of Clinical Investigation*, 51, 1351-1362, **1972**.
- Sinal C.J. et al. Targeted disruption of the nuclear receptor FXR/BAR impairs bile acid and lipid homeostasis, *Cell*, 102, 731–744, **2000**.
- Soisson S.M. et al. Identification of a potent synthetic FXR agonist with an unexpected mode of binding and activation, *Proceedings of the National Academy of Sciences of the United States of America*. 105, 5337–5342, **2008**.
- Suzuki T. et al. The novel compounds that activate farnesoid X receptor, the diversity of their effects on gene expression, *Journal Pharmacology Science*, 107, 285–294, **2008**.
- Takikawa H., Beppu T., Seyama Y., Profiles of bile acids and their glucuronide and sulphate conjugates in the serum, urine and bile from patient undergoing bile drainage, *Gut*, 26, 38-42, **1985**.
- Tan K.P. et al. Activation of nuclear factor (erythroid-2 like) factor 2 by toxic bile acids provokes adaptive defense responses to enhance cell survival at the emergence of oxidative stress, *Molecular Pharmacology*, 72, 1380–1390, **2007**.
- Tiwari A, Maiti P., TGR5, an emerging bile acid G-protein-coupled receptor target for the potential treatment of metabolic disorders, *Drug Discovery Today*, 14, 9-10, 523-30, **2009**.
- Urizar N.L. et al. A natural product that lowers cholesterol as an antagonist ligand for the FXR, *Science*, 296, 1703–1706, **2002**.

- Van De Waterbeemd, H., Testa B., The parametrization of lipophilicity and other structural properties in drug design, *Advances in drug research*, 16, 85-225, 1987.
- Vessey D.A., Crissey M.H., Zakim D., Kinetic studies on the enzymes conjugating bile acids with taurine and glycine in bovine liver, *Biochemical Journal*, 163, 181-183, **1977**.
- Vlahcevic Z.R., Heuman D.M., Hileman P.B., Physiology and pathophysiology of enterohepatic circulation of bile acids. In *Hepatology*, Zakim D.Z., Boyer J.L., Eds., Saunders WB, Philadelphia, PA, 341-377, **1990**.
- Von Dyppe P., Drain P., Levy D., Synthesis and transport characteristics of photoaffinity probes for the hepatocyte bile acid transport system. *Journal Of Biological Chemistry*, 258, 8896-8901, **1983**.
- Waxman D.J., Lapenson D.P., Aoyama T., Gelboin H.V., Gonzalez F.J., Korsekwa K., Steroid hormone hydroxylase specificities of eleven cDNA-expressed human cytochrome P450s, *Arch. Biochem. Biophys.*, 290, 160-166, **1991**.
- Weisiger R., Gollan J., Ochendr R., Receptor for albumin on the liver cell surface may mediate uptake of fatty acids and other albumin-bound substances, *Science*, 211, 1048-1051, **1981**.
- White B.A., Fricke R.J., Hylemon P.B., 7-hydroxylation of ursodeoxycholic acid by whole cells and cell extracts of the intestinal anaerobic bacterium *Eubacterium* species V.P.I. 12708, *Journal of Lipid Research*, 22, 891-898, **1982**.
- Willson T. M., Jones S. A., Moore J. T., Kliewer S. A., Chemical genomics, functional analysis of orphan nuclear receptors in the regulation of bile acid metabolism., *Medicinal Research Reviews*, 21, 513-522, **2001**.